Master's thesis

2021

Shreejay Shrestha

NTNU
Norwegian University of
Science and Technology
Faculty of Humanities
Department of Music

Shreejay Shrestha

Study of Low Frequency Impact Sound Transmission For Auralization

Master's Thesis in
Music Communication & Technology
Supervisors: Peter Svennson & Andreas Bergsland
from NTNU and Anders Buen, Brekke & Strand AS

June 2021

NTNU
Norwegian University of
Science and Technology

NTNU
Norwegian University of
Science and Technology

Study of Low Frequency Impact Sound Transmission For Auralization

A thesis presented for the degree of

Master of Philosophy in Music Communication & Technology

Shreejay Shrestha

June, 2021

Department of Music,
Norwegian University of Science & Technology

Department of Musicology,
University of Oslo

Abstract

Footfall induced noise in buildings is traditionally assessed with Impact Sound Transmission (IST) measurements following diffuse field model of the receiving room which is not valid below Schröeder frequency neither it facilitates auralization. This master thesis aims to create a method to estimate low frequency (LF) sound pressure in the receiving room below Schröeder frequency based on modal sum theory in room acoustics followed by measurement of IST, impulse response of the receiving room and acceleration of the main floor at two fixed position in two vertically adjacent laboratories. The study also aims to create monoaural auralization of the sound pressure with a hypothesis that the impulse response of the combined system of floor and receiving room can be used to synthesize the acoustic sound pressure at listening positions in the receiving room.

The method to create the LF sound pressure in the receiving room was found to be working to some degree with the main floor showing comparatively higher modal density. More accurate results can be achieved by measuring acceleration of the floor at multiple points. Similarly, the auralization method worked between $20 - 200Hz$ with some errors and more accurate results can be accomplished by measuring force signals at higher sampling rate and a more precise calculation of impulse response of the coupled system.

Acknowledgement

I extend my sincere gratitude towards my supervisors from NTNU; Peter Svennson and Andreas Bergsland as well as Anders Buen from Brekke & Strand AS whom we collaborated the project with.

I would also like to thank Tim Cato Netland for helping me set up the equipment, physical inspection of the laboratories and providing me documents and valuable informations about the two laboratories used in this project.

My heartfelt gratitude to my dear wife Anita, and my lovely daughter Sriaanswi for their love and support.

Many thanks to my family friends Samita Giri, Candra Mandil Yogal and sweet Venesha for helping me out with some of my lab works.

Thanking Peter Svennson once is not enough. I want to thank him again for the numerous meetings, invaluable teachings and answering all of my questions.

Thank you!

Blog-post link

This master thesis has a blog post which contains a short description of the thesis along with video of the measurement as well as auralizations. The blog post will be active from sometime around 2021/06/30 and the link is as follows;

https://mct-master.github.io/masters-thesis/2021/06/30/ImSoTra.html

Contents

1 Introduction

This master thesis deals with the study of *Low Frequency* (LF) noise induced by footsteps in buildings via *Impact Sound Transmission* (IST). There is no particular standard of LF-range but a range of $20 - 200/250Hz$ are usually considered as low frequencies (p.240 Persson Waye, 2011; Berglund, Hassmén, and Job, 1996, p.2986). As shown in figure (1.1), footsteps relate to sound source/human activities of walking or jumping on a floor in the sending room. Similarly, IST relates to the noise induced in the receiving room due to impact between a sound source and an intermediate layer/floor in the sending room.

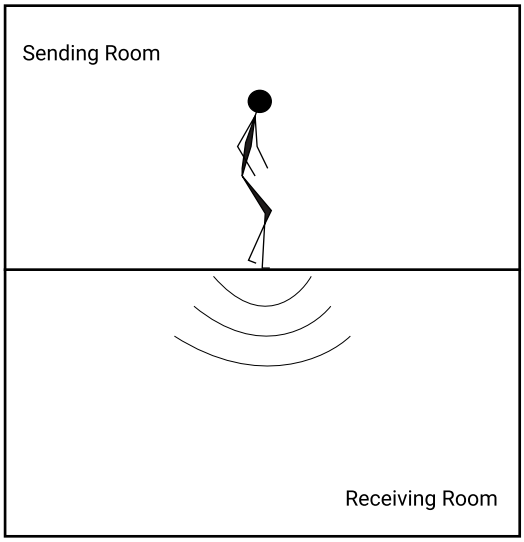

Figure 1.1: Visualising IST

The study involves quantifying LF-noise below *Schröeder* frequency (described in chapter 3.3) while measuring the IST followed by *aurallization* of the measured sound pressure. The measurement of IST in buildings is traditionally done with one-third octave band level resolution and following the *diffuse- field* (described in chapter 3.3) model of the receiving room. ISO 10140-3:2021 (ISO, 2021) is used for the measurements of IST in laboratory while ISO 16283-2:2020 (ISO, 2020a) is used for field measurements. The standard practice for the measurements of IST involves calculat-

ing a single representative value for the objective measure of impact sound insulation known as *Single Number Quantity (SNQ)* defined in ISO 717-2 (ISO, 2020b). The *SNQ* only counts from $100Hz - 3150Hz$, however, by applying the spectrum adaptation term C_I (also defined in ISO 717-2), the frequency range can be extended from $50Hz - 5000Hz$ in one third octave band (ISO, 2020a). Still, it is uncertain if the traditional practice of measuring IST gives accurate sound pressure level at such low frequencies, simply because the sound field below such low frequencies leave the domain of diffuse-field i.e. the conventional measurement approach is no longer valid in such low frequencies. This is a well known phenomenon marked by the Schröeder frequency.

But even after applying the correction term, the traditional approach does not give any information below $50Hz$, neither it shows the frequency spectrum. Moreover, the traditional approach of studying IST does not facilitate *auralization*. Auralization can be understood as a form of acoustic virtual reality. It makes it possible for example to perceive the *SNQ* which would further highlight the surrounding environment including nature of the sound, localization of the sound source and so on. As such, auralization can add another dimension in assessing annoyance or any other health affects from noise.

The study will therefore research on following questions;

1. How to predict sound pressure level and sound pressure spectrum of IST in the receiving room in the LF-range (with simpler methods than the Finite Element Method (FEM)[(i)]?"
    (a) As there are standard ways to predict sound pressure level above the *Schröeder* frequency, with diffuse-field methods, can the quite simple *modal sum* method[(ii)] be used for the estimation at low frequencies?
    (b) How can the results be verified?
2. How to auralize IST at a desired listening position in the receiving room?

[(i)] FEM is a mathematical model that solve complex problems and requires a significant amount of computing

[(ii)] Modal sum method is described in chapter 3.4

(a) Can this method be used to replace various sound source and flooring/ceiling system?

(b) How to verify the results?

Based on the research questions, this master thesis envisage to create a method for estimating sound pressure in the receiving room at LF-resolution below *Schröeder* frequency induced via IST for a selected sound sources in two vertically adjacent rooms. The study can be done in ordinary buildings or laboratories. The sound field in the receiving room will be studied with modal analysis which could represent the room resonance phenomena.

Similarly, impulse response of the receiving room will be measured which can verify the theoretical room resonances. Acceleration of the floor will also be measured which can highlight dynamic response of the floor in terms of mode shapes and natural frequencies of the floor and support in the estimation of sound pressure amplitude in the receiving room. Finally, force signals of various sound sources will also be measured which will be used to create a method to auralize the estimated/measured sound pressure.

Auralization will be based on a hypothesis that the measured or simulated transfer function of combined system of the floor and receiving room can be used to synthesize the sound pressure in the listening position. The accuracy by which this can be done will be investigated in the project, and the influence of various factors such as excitation position, number of measurement points, characteristics of the interface surface, influence of flanking transmission might be investigated. Primarily, a monaural approach can be used for this low-frequency study, but an expansion which could handle the directionality of the sound might be explored.

This master thesis report has been divided into six chapters and two annexes. The first chapter gives a brief introduction of the thesis project. A thorough literature review is presented in the next chapter titled *Background*. The review consists of findings that provides a basis/ a foundation for this master thesis. The *Theory* chapter contains necessary mathematical equations and established theoretical methods that provide support for the thesis. The *Methodology* chapter explains the methods derived from

theory to accomplish the goals of this master thesis. It describes the models used in this study and clarifies various steps that were taken to meet the objective of this study. The *Results & Discussion* lays out the major findings from the study. It also presents a thorough discussion about the achieved goals and limitations and reflect on what went right, what was wrong, and how could the work be improved. Similarly, the *Conclusion* chapter presents all findings from the study. Finally, annex *A Various* includes some pictures and data supporting the study while annex *B Matlab Scripts* contains a few Matlab scripts used to process and analyse the raw data.

2 Background

Acoustics is a very broad discipline, an amalgam of physics, engineering, music and psychology. Its soul is sound, a vibration that propagates through a medium in the form of acoustic wave. Sound can be pleasing music, or a disturbing noise which can also be hazardous to human health. European Environment Agency (2010, p.5) describes noise as an *audible sound that causes disturbance, impairment or health damage*. On the other hand, human health has been defined as *a state of complete physical, mental, and social well-being and not merely the absence of disease or infirmity* (WHO, 1946). This broader definition of human health is used in providing practical and validated tools to calculate health impacts of noise (European Environment Agency, 2010).

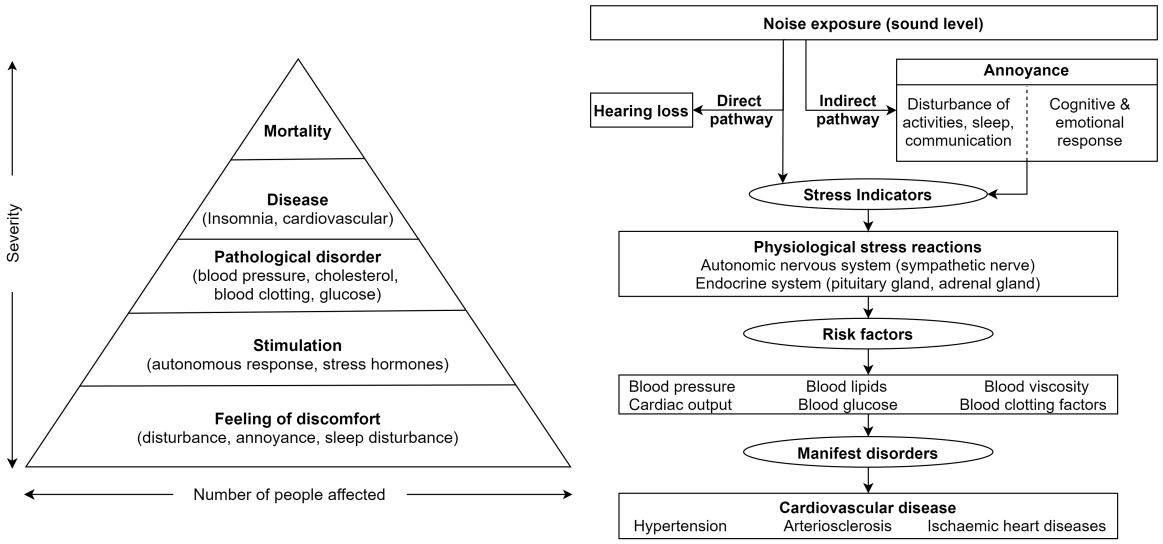

(a) Pyramid of effects from noise exposure[iii]

(b) Noise effects reaction scheme[iv]

Figure 2.1: Effects of noise on human health

(Source: European Environment Agency (2010) and Babisch (2002))

In a study of relation between noise-stress and risk assessment of adverse health effects of noise, Babisch (2002) presents a hierarchical order of events that effect health from noise exposure which are; changes in physiological stress indicators, increase in

[i] redrawn from (European Environment Agency, 2010, p.6)

[ii] redrawn from (European Environment Agency, 2010, p.15)

biological risk factors, increase of the prevalence or incidence of diseases and premature death (figure 2.1). The development of adverse health effects on the population has been depicted through a shape of a pyramid that reflects a decrease in population for an increase in acuteness of the effects (figure 2.1a). Similarly, the author has presented two possible pathways that noise exposure can traverse in affecting the human health (figure 2.1b). The direct pathway can either lead to *hearing loss* or activate the *sympathetic nerve* & *endocrine system* via *acoustic nerves*, while the indirect pathway reacts with subjective perception of sound, its cognitive interpretation and the coping ability of the subject in developing physiological reaction (European Environment Agency, 2010).

Babisch (2002) also highlight that *acute noise effects also occur at relatively low environmental sound levels especially when certain activities like concentration, relaxation or sleep are disturbed beside occurring at high sound levels in occupational settings*. European Environment Agency (2010) also states that, assessments of adverse health effects from noise exposure comprises of complex models for the relations between noise-stress and noise-sleep disturbance, and most models are verified either experimentally or qualitatively and are accepted as describing the relations between noise and human health (European Environment Agency, 2010, p.5-6).

Noise has always been one of the major environmental problems for humans. Goldsmith (n.d) has presented several interesting historic incidents of noise exposure in his website [(v)]. For instance he writes, potters, tinsmiths, and other tradesmen had to live outside the city walls because of the noise they made in a Greek colony in 6^{th} century *BCE*. Similarly, he mentions, wagons were not allowed in the streets of Rome during the night in 44 *BCE* (also endorsed by Berglund, Lindvall, et al., 1999, p.iii). He also writes, *Hippocrates* in 5^{th} century *BCE*, identified *tinnitus* to be caused by prolonged exposure to noise, and so on. The world has changed a lot with time and it is highly likely that it is way too noisier today than it was in the past. Beside development, industrialization and urbanization have introduced a lot of noise in the cities around the world along with bringing other environmental problems.

Noise in the urban environment spreads across all frequencies and it has been rec-

[(v)] https://mikegoldsmith.weebly.com/history-of-noise.html

ognized as a global problem of reduced human well-being (WHO, 1980; Berglund, Hassmén, and Job, 1996, p.2985). The average human population can hear noise in the range of $\mathbf{20 - 20kHz}$ and as shown in figure (2.2) the sensitivity of hearing is significantly low below $\mathbf{20Hz}$, maximum around $\mathbf{3 - 4kHz}$ and slightly low towards higher frequencies (for old estimates see p.91 Fletcher and Munson, 1933; ISO, 2003). As such, the low frequencies were considered to be less annoying, but now the effects from low frequencies on human health has been well understood (Berglund, Hassmén, and Job, 1996; Leventhall, 2004; Persson Waye, 2011).

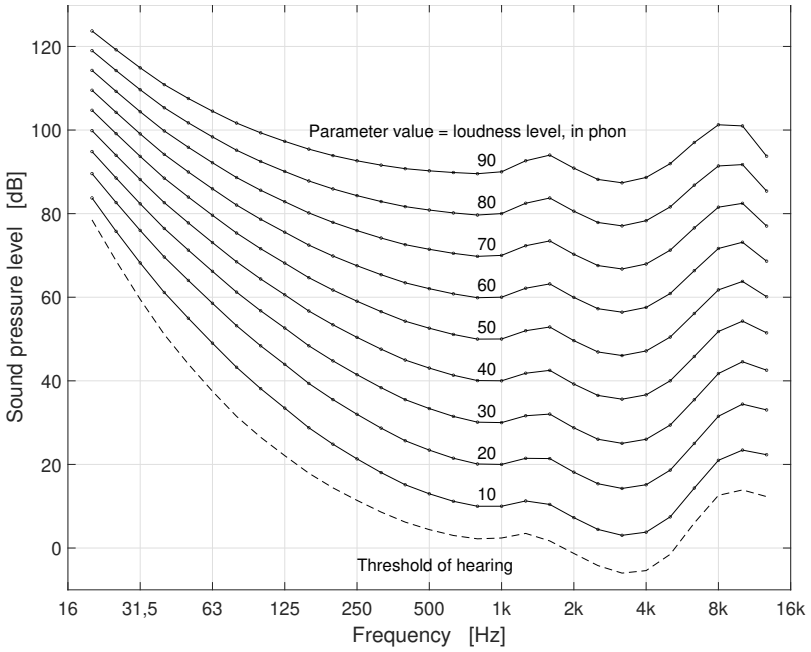

Figure 2.2: Loudness level contours [(vi)]

(Source: ISO (2003))

While studying sources and effects of LF- noise, Berglund, Hassmén, and Job (1996, p.2987) report that, effects from LF-noise are more concerning than other noise in urban environment as the LF-noise is pervasive, efficient in propagation and has a low tendency of being attenuated by building structures. The authors further add that intense LF-noise appears to produce clear symptoms including respiratory impairment and aural pain and that LF-noise can cause a person to feel vibration. The sensation of vibration in human bodies induced by LF-noise is reported by several authors (see Yamada et al., 1983; Inukai et al., 1986; Møller and Lydolf, 2002) and Takahashi (2013) suggests that the effects of LF-noise can be appropriately assessed by clarifying the

[(iv)] Figure drawn using matlab script by P.Svennson that calls a function by Tackett (2021)

characteristics of vibratory sensation.

In a report, Persson Waye (2011, p.244) states that LF-noise do not usually have an immediate distraction in comparison to high frequency noise. She also writes, symptoms like lack of concentration, sleepiness, tiredness, irritation, pressure on eardrums and pressure in the head have been found to be related to noise annoyance in experimental and field experimental studies which tend to increase with higher levels of low frequencies. She highlights that in workplaces and living environments, LF-noise may occur in combination with vibrations. She further states that although airborne noise has been found to be greater in combination with vibrations, there is a lack of knowledge about the combined effects of LF-noise and vibration. She finally concludes that adverse effects from the widely spread LF-noise in the current *urban societies* may occur at very low sound pressure levels and there is an increasing acceptance that LF-noise needs to be specially attended to (Persson Waye, 2011).

Urban cities in 2018 were inhabitated by nearly 55% of the global population which is expected to reach 68% by 2050 (UN, 2019, p.xix). A typical urban city is densely populated and comprises of multi-storey apartments and condominiums, business complexes, numerous services and infrastructures including different modes of transportation and so on. The future cities perhaps may require constructing of more infrastructures for its growing urban population. Thus it is important to assess issues with noise exposure in the urban environment that could provide support in designing sustainable solutions in the future pertaining to the effects from noise exposure on human health.

In a study to measure noise exposure in Norway, *Statistics Norway (SSB)* has calculated the number of people exposed to noise from traffic (road, rail and air), as well as manufacturing and other business activities (SSB, 2016). The study found that road noise was the largest noise source in 2014 and number of people exposed to it increased from 1.2 million in 1999 to 1.87 million in 2014. In another study based on both field measurements of sound insulation and questionnaire survey in *multi-unit dwellings* in Norway, Løvstad et al. (2017) assessed general annoyance and restrictive behaviour of the residents due to different sound sources. They found that impact sound from footsteps was reported as slightly more annoying than traffic noise as shown in figure (2.3a). Likewise, they found that people tend to restrict themselves to

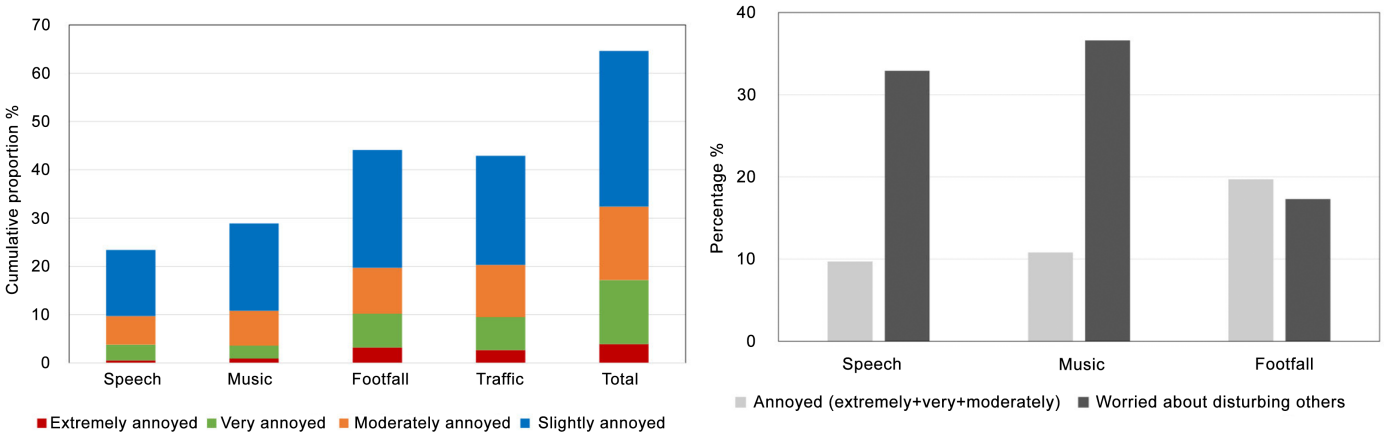

(a) Annoyance due to different sound sources

(b) Restrictive behaviour to annoyance due to different sound sources

Figure 2.3: Annoyance and restrictive behaviour of residents in multi-unit dwellings
(Source: Løvstad et al. (2017))

some extent from disturbing others in case of speech and music. Whereas for the footsteps noise, as shown in figure(2.3b), the percentage of the people who are worried about disturbing others seem to be slightly less than the percentage annoyed by it.

Apartments, condominiums or multi-unit dwellings are all similar kind of housing solutions that solve many problems of an urban ecology. For instance, they save space and share common resources, infrastructures and services. By doing that, they contribute to a sustainable and economically viable solution that puts less pressure on the environment. However, such buildings often *share* common walls, floors and corridors that increase the probability of noise complaints from dwellers due to their neighbours' activities inducing either airborne (speech, music etc) or structure-borne noise (footsteps, dropping objects, dragging furniture and others). Impact noise in buildings are mainly associated with two adjoining rooms in two levels, separated by a common floor. In addition to concrete floors, many authors appreciate that the problem is even worse in case of buildings with light weight constructions (Shi, 1995; Homb, 2006; Martins et al., 2015). Therefore, there is a general practice of providing sound insulation in such buildings, e.g constructing a *floating floor*[(vii)] in case of impact sound insulation.

However, many authors have reported footsteps noise complaints even with floating floors (see Park, Lee, and Yang, 2016; Park, Lee, Yang, and Kim, 2016; Burkhart and

[(vii)] see chapter(3.2) for more information on floating floor

Wolf, 2016; Park and Lee, 2017; Na et al., 2019). The complaints are mostly related to the LF-*boomy* noise produced by the footsteps (Burkhart and Wolf, 2016). Many of the investigations of such complaints addressed by the measurement of impact sound insulation in the field, revealed that the complained noise levels met with the legal requirements when the regulation did not require to implement the spectrum adaptation term C_I (Schneider and Fischer, 2013).

A survey from Direktoratet for byggkvalitet (2016) reported a similar finding in Norway which formed the basis for revision of the *Norwegian standard NS 8175:2019* (Norwegian Standard, 2020). Beside informing about the importance of inclusion of the C_I in the noise regulation in Norway, the report also highlights that, both the actual frequency range of the noise complaints and the methods to determine it, are however unclear (Direktoratet for byggkvalitet, 2016, p.10). An overview of the former and the updated impact sound regulation in Norway is shown in table (2.1) and table (2.2).

Table 2.1: Former standard for impact sound insulation in Norway
Source: (Direktoratet for byggkvalitet, 2016, p.7)

Forskrift årstall	**Trinnlydnivå**	**Kommentar**
1987 (forskrift)	L'n,w $\leq 53dB$	Rekkehus og andre sammenbygde småhus (boenheter med vertikal skillekonstruksjon)
	L'n,w $\leq 58dB$	Flerfamiliehus (boligblokker, terrassehus,hybelhus osv)
1997 (standard)	L'n,w $\leq 53dB$	Gjelder alle typer boliger, mellom boenheter og mellom boenheter og korridor, fellesgang osv.
2010 (standard)	L'n,w $\leq 53dB$	Gjelder alle typer boliger, mellom boenheter og mellom boenheter og korridor, fellesgang osv.

Thus, there are complexities in measuring sound pressure level below the Schröder frequency and the conventional approach of measuring impact sound transmission in buildings below the Schröder frequency may not be accurate. Therefore, it is also possible that the impact noise acceptance levels defined by the conventional method may not be accurate either.

A method for assessing the LF- sound pressure level from impact sound transmission could contribute in the field of acoustics, psychology, health sciences, architecture, urban planning, building construction and other relevant fields to fill some of the gaps discussed earlier.

Table 2.2: Updated standard (NS8175:2019) for impact sound insulation in Norway
Source: (Norwegian Standard, 2019)

Type brukeområde	**Målestørrelse**	**Klasse A**	**Klasse B**	**Klasse C**	**Klasse D**
		dB	dB	dB	dB
Between dwellings$^{(a)}$	$L'_{n,w} + C_{I,50-2500} \leq$	46	50	54	-
In a dwelling from common areas	$L'_{n,w} \leq$	-	-	-	56
/communication routes such as common					
corridors, galleries$^{(b)}$, stairwells etc.					
In a dwelling from business service,	$L'_{n,w} + C_{I,50-2500} \leq$	40	44	48	-
premises, parking facilities,	$L'_{n,w} \leq$	-	-	-	52
shared roof terraces, etc.					
In a dwelling from the toilet, bathroom,	$L'_{n,w} + C_{I,50-2500} \leq$	40	44	48	-
storage shed etc. and from the	$L'_{n,w} \leq$	-	-	-	52
balcony, etc. in another dwelling					
Between living rooms(including	$L'_{n,w} \leq$	54	58	-	-
bedrooms) without direct					
connecting doors in the same dwelling					

$^{(a)}$ This also applies to roof terraces in adjacent dwellings and from internal staircases in different dwelling

$^{(b)}$ For galleries, the limit value applies without the adaptation term $C_{I,50-2500}$

3 Theory

This chapter provides brief definitions, mathematical equations and core concepts to accomplish this master thesis. The topics include natural frequency of finite-size plate and floating floor, Schröeder frequency, basic principles of digital signal processing (in terms of impulse response and convolution) and Auralization.

3.1 Natural frequency of vibrating finite-size plate

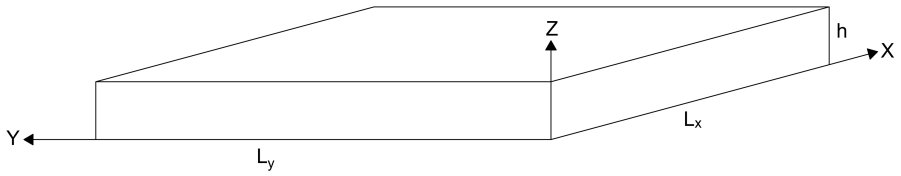

Figure 3.1: Finite size thin plate

For a given rectangular thin plate as shown in figure (3.1) with dimensions L_x, L_y and h in meters, the natural frequency of a mode of vibration of the plate under simply supported boundary condition is given by equation (3.1) (Vigran, 2008)

$$f_{m,n} = \frac{\pi}{2}\sqrt{\frac{D}{\rho h}}\left[\left(\frac{m}{L_x}\right)^2 + \left(\frac{n}{L_y}\right)^2\right] \tag{3.1}$$

Here, $\{m, n\} \in \mathbb{N}^*$[(viii)] are two indices that define specific mode number/mode shape of the vibration and ρ is the density of the plate in kg/m^3. Similarly, D is the bending stiffness of the plate with its unit in $Pa \cdot m^4$ which is given by;

$$D = \frac{Eh^3}{12(1-\nu^2)} \tag{3.2}$$

Likewise, in equation (3.2) E is Young's modulus in GPa and ν is Poisson's ratio.

[(viii)] $\mathbb{N}^* = \{1, 2, 3.....\}$i.e. natural numbers excluding 0

3.2 Resonance frequency of a floating floor

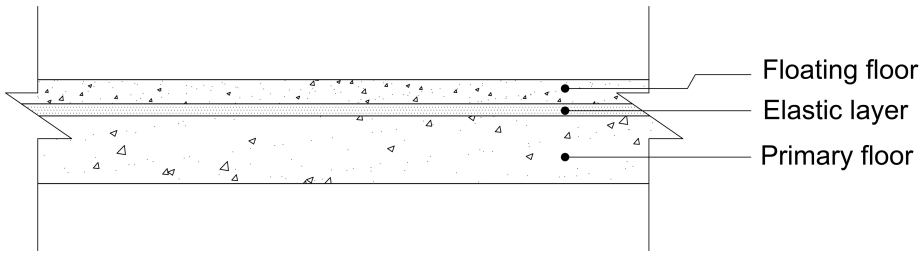

Figure 3.2: A basic floating floor system on a continuous elastic layer (redrawn from Vigran, 2008, see pg.306)

A floating floor system is a solution for reducing airborne and impact sound transmission exceeding 1.5 times its resonance frequency (Hongisto et al., 2020, p. 425 line90-94). It can be considered as a mass-spring system where the elastic layer acts as the spring while the top layer and the main floor act as mass of the system. Figure (3.2) shows a principle floating floor system for a heavyweight concrete construction with a continuous elastic layer. The resonance frequency of such a system according to ISO 9052-1:1989 (ISO, 1989) is given by;

$$f_r = \frac{1}{2\pi}\sqrt{\frac{s'}{m'_t}} \tag{3.3}$$

$$s' = s'_t + s'_a \tag{3.4}$$

$$s'_a = \frac{111}{d} \tag{3.5}$$

where m'_t is the total mass per unit area of the mass-spring system in kg/m^2 and s' is the dynamic stiffness of the spring or elastic layer of the mass-spring system given by equation (3.4). Similarly, s'_t is the apparent dynamic stiffness per unit area of the resilient layer in N/m^3 and s'_a is the dynamic stiffness of the air. For an atmospheric pressure of $0.1Mpa$ and porosity of 0.9, the dynamic stiffness per unit area of the enclosed gas/air is given by equation (3.5) where d is the thickness of the resilient layer in mm (ISO, 1989). A mass-spring system can have different forms depending on the type of coupling between given number of mass and springs. Therefore, the equation (3.3) can take different forms where the effective stiffness and effective mass would replace the term s' and m'_t respectively.

3.3 Schröeder Frequency ($f_{Schröder}$)

Diffuse sound field is based on statistics and probability of sound energy being same at any position in a room, (Vigran, 2008, p.117). However, in a reverberant room, the sound field acts differently at low frequencies. According to Manfred Schröeder (Schroeder, 1996), there occurs well separated room resonances below a certain frequency, called Schröeder Frequency and above that frequency, there exists many overlapping normal modes. For airborne sound in a reverberant room, the Schröeder frequency is given by;

$$f_{Schröder} = 2000\sqrt{\frac{T_{60}}{V}} \tag{3.6}$$

where T_{60} is the reverberation time of the room, measured in seconds, V is volume of the room in m^3 and 2000 is an empirical constant with unit = $m^{3/2} \times s^{-3/2}$.

As such, the peaks seen in a frequency response of a room below the Schröeder Frequency are the actual resonance frequencies of the room while those above the Schröeder Frequency are not the actual resonances of the room but they are random interference peaks.

3.4 Modal Sum (Wave Theoretical Room Acoustics)

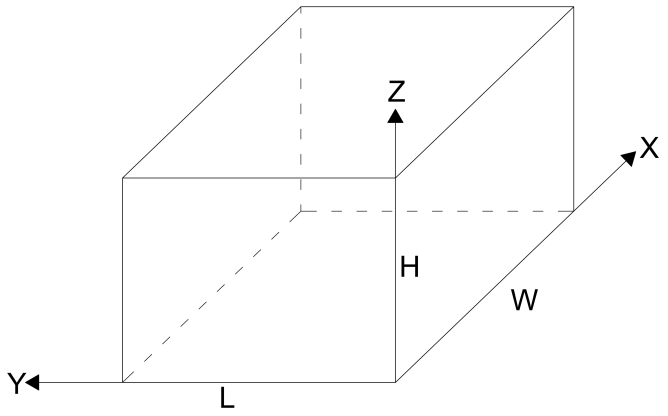

Figure 3.3: Shoe-box shaped reference room with rigid walls

For a shoe-box shaped room with perfectly rigid walls, the modal sum (Cremer and Muller, 1982) describes the sound pressure, magnitude and phase in every position (x, y, z) in the room for a given position of a sound source in the room. This study follows a mode sum model which accounts for damping in a similar room presented by Sjösten et al. (2016). According to the model, if a sound source is located at position r_P with volume velocity of U_P and speed of sound c_0, a general solution at frequency ω for the sound pressure at position r within an enclosure of volume V, is given by the modal sum expressed as a transfer function $H(r, r_P)$ in equation (3.7). The transfer function of the room would remain unchanged even if the position of receiver and the source are interchanged, this phenomenon is known as reciprocity (see eg. Samarasinghe, Abhayapala, and Kellermann, 2017)

$$p(r, \omega) = \frac{j\omega\rho_0 U_P(\omega){c_0}^2}{V} \times \sum_N \frac{1}{\varepsilon_N} \frac{\psi_N(r)\psi_N(r_P)}{\omega_N^2 - \omega^2 + 2j\delta_N\omega_N} = U_P H(r, r_P) \tag{3.7}$$

$$\psi_N(r) = \psi_{lmn}(x, y, z) = cos\frac{l\pi x}{W} cos\frac{m\pi y}{L} cos\frac{n\pi z}{H} \;\; \& \;\; 0 \leq |\psi_N(r)| \leq \tag{3.8}$$

The eigenfunction for the mode index N, denoted by ψ_N, in such room is given by equation (3.8). The mode index $N = [l, m, n]$ which correspond to the x, y, and z axis respectively. The room volume $V = W \times L \times H$ with room dimensions W, L and height H, as shown in figure (3.3). The factor ε_N in equation (3.7) is a mode normalization factor such that for axial modes (one index is nonzero), $\varepsilon_N = 1/2$. Similarly, for tangential modes (two indices are nonzero), $\varepsilon_N = 1/4$ and for oblique modes (all indices are nonzero), $\varepsilon_N = 1/8$. Likewise, the expression ω_N in equation (3.7) is the resonance frequency (or eigenfrequency) that corresponds to mode N and is given by equation (3.9)

$$\omega_N = \omega_{lmn} = \pi c_0 \sqrt{\left(\frac{l}{W}\right)^2 + \left(\frac{m}{L}\right)^2 + \left(\frac{n}{H}\right)^2} \tag{3.9}$$

Further, the model states that, when $\omega \rightarrow \omega_N$, the relative amplitude in equation (3.7) for mode N becomes large and when excited exactly at the resonance frequency, the modal amplitude is only limited by the modal damping denoted by δ_N given by;

$$\delta_N = 3 \cdot \frac{log10}{T_{60}} \tag{3.10}$$

Similaly, when the modes are well-separated at a certain resonance frequency, this particular mode with a shape defined by equation (3.8) will be the dominating term for the sound pressure amplitude at all positions within the enclosure (Sjösten et al., 2016).

At very low frequencies, the wavelength of the sound waves are very large and therefore the walls or any other component in a room (furniture, curtains etc) cannot influence the wave. Hence the modal sum method is very practical for low frequencies. However, for the higher frequencies, the case will be quite opposite and the room components can highly influence the sound waves by reflecting, absorbing or diffracting the waves. So, the method may not be accurate for higher frequencies.

The modal sum method can not be used if the room shape is substantially different from a shoe-box shape. Small deviations do not matter much, for the same reason that small objects do not affect the sound field at low frequencies, or if some wall(s) has substantial absorption.

3.5 Impulse Response (IR) and Convolution

A Linear Time Invariant (LTI) system e.g sounds in a room, as shown in figure (3.4), can be characterized by the *impulse response* (IR) of the system $h(n)$ whose input-output relation for the discrete-time signals is given by the *Convolution* (Smith, 1997, see chap.6). Convolution (denoted by $*$) is analogous to mathematical operations like multiplication, addition, and integration and while addition takes two numbers and produces a third number, convolution takes two signals and produces a third signal (Smith, 1997).

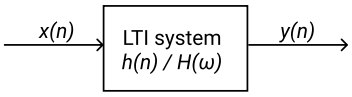

Figure 3.4: A basic single input single output LTI system

$$\boldsymbol{y(n) = x(n) * h(n)} \tag{3.11}$$

$$\boldsymbol{Y(\omega) = H(\omega) \times X(\omega)} \tag{3.12}$$

Equation (3.11) gives the input-output relationship of the LTI system in figure (3.4) in time domain. The same input-out relationship in the frequency-domain is given by equation (3.12) where $\boldsymbol{Y(\omega)}$, $\boldsymbol{H(\omega)}\&\boldsymbol{X(\omega)}$ are the output, transfer function and input of the LTI system respectively.

As IR of a LTI system is unique, it allows to generate any output signal from the system by convolving the input singnal with IR as given by equation (3.11). IR of a LTI system can be measured by various methods and some of the methods are listed in table (3.1)

Table 3.1: Few methods to determine IR of a LTI system
Source: (Svennson, 2020)

Index	Method	Excitation signal
1	DFT based deconvolution	
	to find $\lvert H(\omega_k)\rvert$	a finite length exponential chirp or log-sweep
2	Direct measurement of $h(n)$	Pulse signal
3	Time-domain deconvolution to find $h(n)$	A signal which has an inverse signal

3.6 Auralization

Auralization can be defined as a technique of creating audible signals from numerical data which could be in the form of simulated, measured or synthesized data (Vorländer, 2008). Auralization of an LTI system can be done by convolving the input signal with the impulse response of the system as given by equation (3.11). Auralization can be done in many levels, for instance monoaural, binaural, ambisonics etc.

4 Methododology

This master thesis is based on measurements of IST between two vertically adjacent rooms. The measurements were followed by analytical estimation of the sound pressure level and sound pressure spectrum as well as auralization of the transmitted sound in the receiving room. Laboratories were considered for the measurements for a controlled environment and to avoid various acoustics concerns in the field like noise from the external environment, construction techniques of buildings, flanking transmission and others. Objective analyses were performed based on various algorithms presented in (annex.....) while subjective analysis of the auralization was performed by listening the measured and auralized signals through headset. A sketch of the measurement and analysis method opted in this study is presented in figure (4.1). Similarly, the list of all equipments used in the study is presented in table (4.1) and the details of the measurement procedure are given in chapter (4.2).

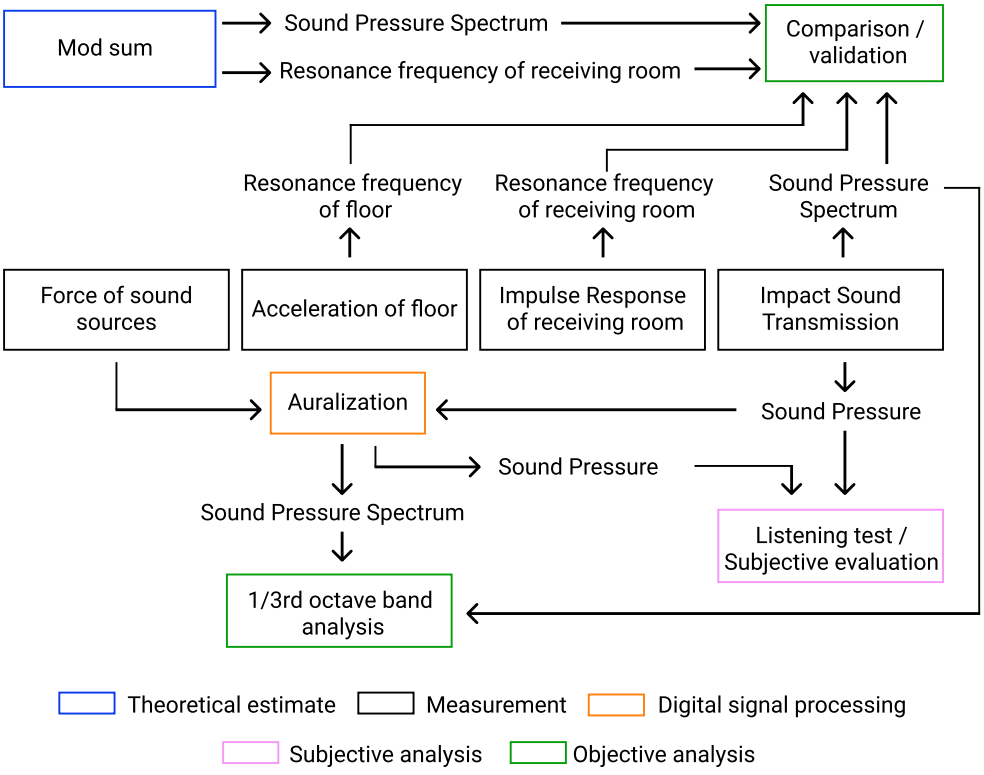

Figure 4.1: Methodological scheme

4.1 List of equipment

The following table lists all the equipment used in the measurement of IST between the two laboratories. Besides, the list also consists of equipment used in the measurement of impulse response in the receiving room including the measurement of ground force of various sound sources and acceleration of the main floor. Information about most of the equipment can be easily found by looking at the name of the equipment with corresponding manufacturer and its type/number that is provided in the table.

Table 4.1: List of Equipment
(Various cables, connectors, and stands were used but are not listed)

Index	Manufacturer	Type/ number	Equipment	Quantity
1	Brüel & Kjaer	4375	Accelerometer	2
2	MMF	VC20	Vibration Calibrator	1
3	Endevco	2721	Charger amplifier	1
4	Vernier	FP-BTA	Forrce Plate	1
5	Vernier	-	LabQuest Mini interface for the Force plate	1
6	Vernier	-	Logger Pro 3.16.1 software for the Force plate	1
7	NTi Audio	M4261	Microphone with inbuilt preamp	1
8	Norsonic	Nor1256	microphone calibrator	1
9	ZOOM	H5	Handy recorder with SD memory card	2
10	FLUKE	77	Multimeter	1
11	PURE	-	Medisin ball 4kg (solid, new & 20cm in diameter)	1
12	NIKE	Air Max Tavas white	Soft sole, size EU 42.5 (used over 2.5 years)	1
13	AFMG		EASERA software	1
14	X	X	Homemade corner speaker without stand	1
15	Roland	UA-1610	Audio interface	1
16	Leica	Accessories	laser measure	1
17	-		concrete slab (1.25 x 0.72 x 0.05 m^3)	1
18	Rockwool		mineral wool (1.2 x 0.6 x 0.02 m^3)	2
19	Canes	Schutz Quadro Takk	Expanded polystyrene(EPS) (1.2 x 0.6 x 0.025 m^3)	1
20	Canes	Schutz Quadro Takk Pro	Expanded polystyrene(EPS) (1.2 x 0.6 x 0.05 m^3)	1
21	Plantronics, Inc.	BlackBeat Go 600	Bluetooth Headphone	1

4.2 Measurement Procedure

4.2.1 Physical inspection of laboratories

In the acoustics facilities at NTNU, Trondheim, two laboratories called *Lydrom 2* and *Lydrom 3* were used for the measurements as sending room and receiving room respectively. As seen in figure (4.2a) and figure (4.2b), the sending room is adjoined with another laboratory (Lydrom 1 with similar size as Lydrom 2) where the central divid-

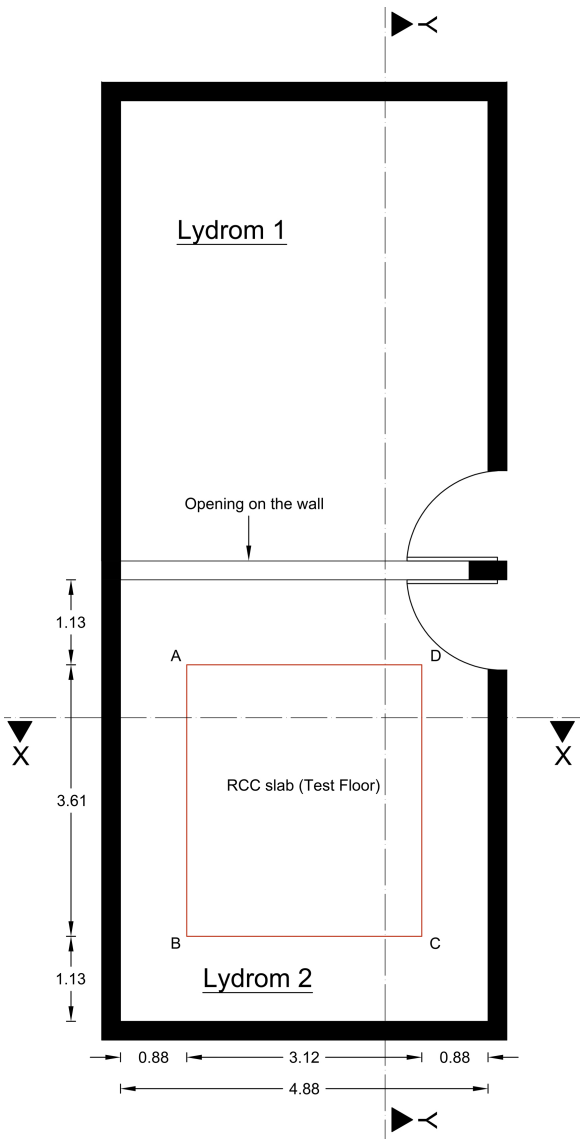

(a) Lydrom 2 (Sending room)

(b) View of Lydrom 2 with Lydrom 1 on background

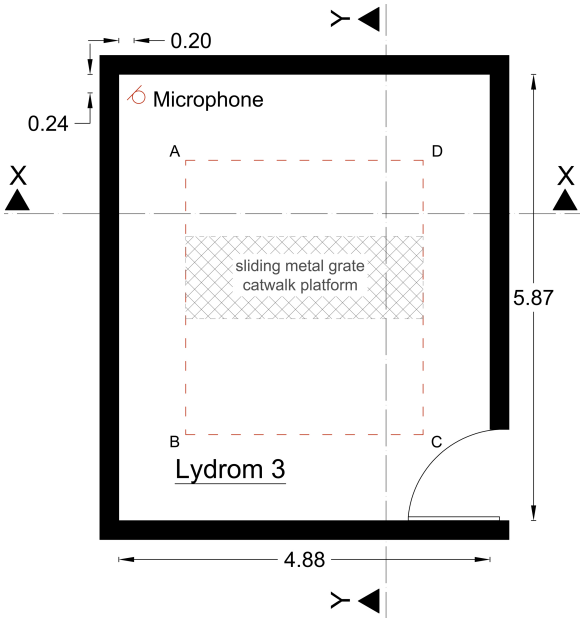

(c) Lydrom 3 (Receiving room)

Figure 4.2: Floor plan and images of Lydrom2 and Lydrom 3

(Measured and drawn by the author with reference to original drawing. Drawings are not to scale.)

ing wall has a big void for placement of test walls. The void was left completely open during the measurements in this project. Similarly, the test floor in the sending room is sunken and screwed to the structure around its edges. From visual inspection, the test floor seemed to be well-separated from the lower structure. Metal frames/rims were also seen throughout the perimeter of the floor along with two layers of resilient materials like felt. Besides, a box containing scaled model weighing roughly $30 - 40kg$ transferred its load through a leg, near the edge on the test floor as seen in figure 4.3b). Similarly, a metal platform is installed in the receiving room including two corner speakers. Apart from this, both the rooms were empty with hard concrete finishing on all the interior surfaces. Moreover, existing drawings (see chapter ....) were only available for the laboratories and no documentation was found for the test floor. But, the floor was informed to be installed in the late 60's. It was also noted that the test facilities no longer followed any international standards after reflectors/diffusers were removed from the two rooms many years ago.

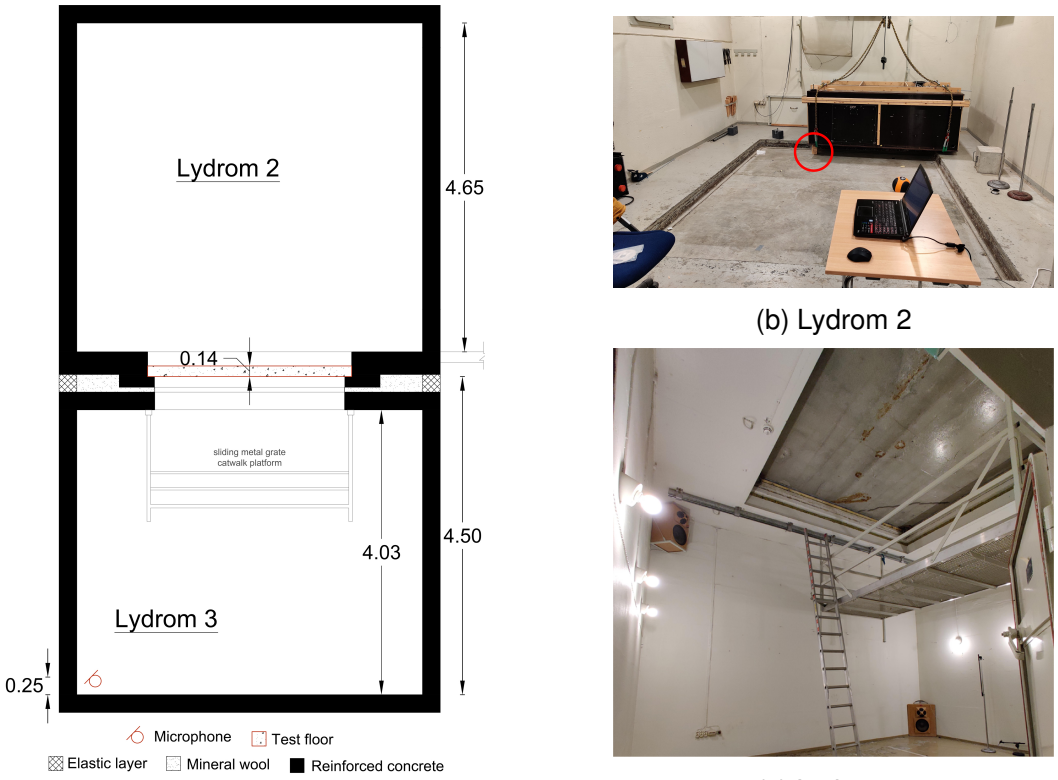

(a) Section through X-X

(b) Lydrom 2

(c) Lydrom 3

Figure 4.3: Section and images of Lydrom2 and Lydrom 3

(Measured and drawn by the author with reference to original drawing. Drawings are not to scale.)

4.2.2 IST Model (ImSoTra)

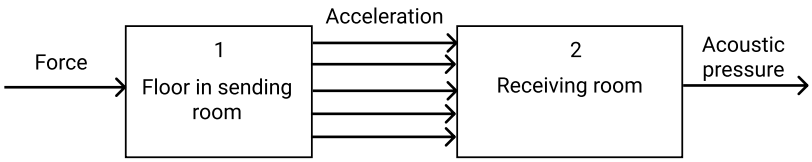

Figure 4.4: Schematic layout of ImSoTra model

To measure the IST as well as acceleration of the floor, this study has developed the *ImSoTra* model, as shown in figure (4.4). Coined as an acronym to IST, the model has two sub-systems. Here, *Force* implies to the amount of force exerted by a sound source while exciting the floor (sub-system 1) at a point which sets the floor into vibration, as signified by *Acceleration*. However, the vibration of the floor gets distributed throughout the surface area of the floor. This phenomenon is quite complex and is depicted in the figure with several arrows instead of one. Similarly, the transmitted sound disturbs the atmospheric pressure and induces acoustic pressure in the receiving room (sub-system 2).

In principle, the sound waves generated from the impact between a sound source and the floor will transmit into the receiving room as well as reflect back to the sending room. However, this method only considered the former case to simplify the problem. Likewise, the transmitted sound in the sending room will have both structure-borne sound and airborne sound induced by the impact. This study did not differentiate between the two components of the transmitted sound. Further, as the experiment was performed in acoustic test facilities meant for similar assessments, flanking transmission was also assumed to be negligible. In simple terms, flanking transmission can be understood as sounds transmitting through adjoining walls, ceiling, ducts, void in floor section, openings and other structural/ building component that envelope the sound source in a building.

4.2.3 Preparation for measurements

For the measurements of IST in the receiving room, the main floor was divided into four equal quadrants to define excitation points. Based on the symmetry of the quadrants,

five excitation points were selected on the top left quadrant as shown in figure (4.5a). For simplicity, two positions were marked on the floor to measure the acceleration of the floor as shown in the figure (4.5a). For more accurate modeling, vibrations of the entire floor should be sampled, but a basic idea was that the simplified approach might work if vibration modes are well separated.

Similarly, beside the main floor, a small section of a floating floor system was created as shown in figure (4.5b) with different layers listed in table (4.2). The choice of four layers under the concrete plate are not used that way in reality. It was an improvisation in the study while hoping to get as low resonance as possible.

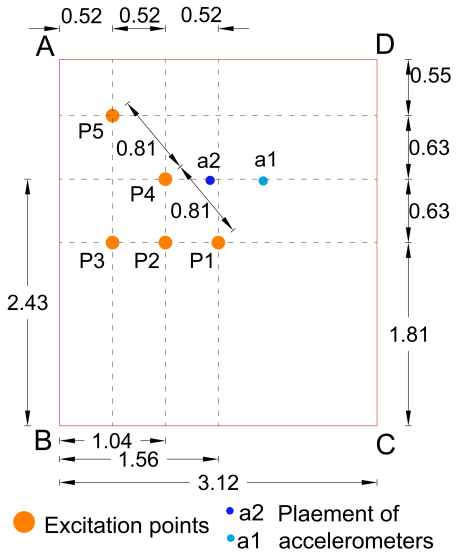

(a) Excitation points on main floor / Source position on ceiling

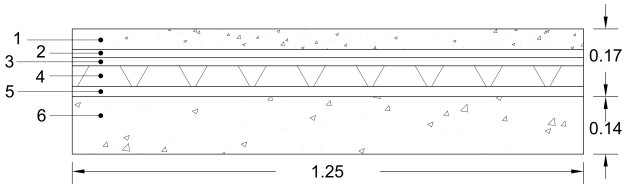

(b) Floating floor used in the measurement (detail of the layers are listed in table 4.2)

Figure 4.5: Excitation points in sending room, sample of floating floor and source position in receiving room

Table 4.2: List of the floating floor layers and physical properties of materials considered for calculations of natural frequency of the floors

Index	Element	Length (m)	Width (m)	Thickness (m)	ρ (kg/m^3)	k (MN/m^3)	E (GPa)	ν
1	Concrete plate	1.25	0.72	0.05	2300	-	2.77*	0.18
2	Mineral wool	1.2	0.6	0.02	-	12.8	-	-
3	Mineral wool	1.2	0.6	0.02	-	12.8	-	-
4	EPS	1.2	0.6	0.05	-	10	-	-
5	EPS	1.2	0.6	0.025	-	20	-	-
6	Main floor	3.12	3.61	0.14	2300	-	2.77*	0.18

* For concrete $E = 25GPa$ but it varies from $12 - 45GPa$ depending upon age and quality

Rubber is used as a standard sound source in the measurements of LF- IST (Japanese Standard Association, 2000; ISO, 2021). In this study, a type of rubber ball known as *medisin ball* along with actual footstep with shoes and without shoes were used as sound sources[(ix)] for the measurement of LF-IST. The measurements were taken in three phases. Force signals were measured in the first phase and IST as well as acceleration of the floor were measured in the second phase. Similarly, impulse response (IR) of the receiving room was measured in the third phase. Details of the measurements are explained in following sections.

4.2.4 Measurement of force signals

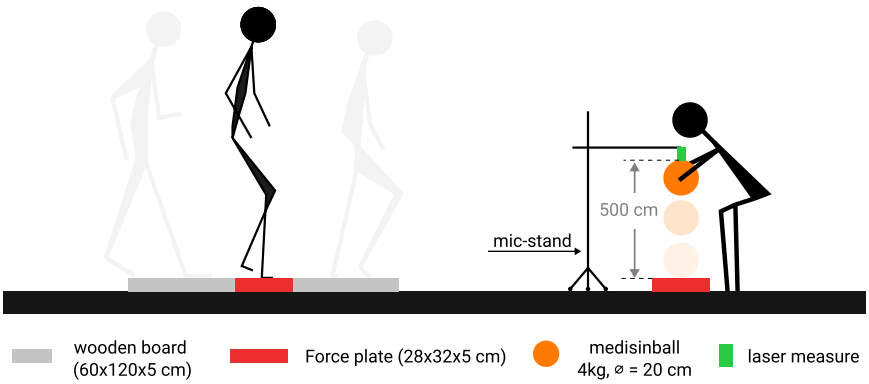

Figure 4.6: Measuring force signals with Vernier force plate

Force of the sound sources were measured using *Vernier Force Plate* (specification given in table 4.1 index 4-6). The force plate was raised about 5 cm above the main floor. Two wooden boards of similar thickness were placed on either sides of the force plate to make a flat plane as shown in figure (4.6). A number of *Ground Reaction Force* (GRF) of an adult (male, weight 80 kg & height 175 cm) were measured while waking with and without shoes. The subject tried to walk on the board through the force plate naturally with the same pace in all of the measurements.

Similarly, a series of impact forces of the medisin ball was measured while releasing the ball manually from a height of 500 cm to make a free fall impact with the force plate and catching it on the rebound. A laser device fixed to a microphone stand was used as a reference point to mark the height and dropping position of the ball, as shown in

[(ix)] Specification of the medisin ball and shoes are given in table (4.1), index 11 & 12 respectively)

figure (4.6). The force signals were saved as '.txt' files for further processing. The force plate had a fairly low sampling frequency rate of 1 kHz so the measured force signals were up-sampled to 48 kHz in the post-processing to make it easier to combine with other measured signals sampled at 48 kHz.

4.2.5 Measurement of IST

The IST in the receiving room was recorded using a microphone[(x)] fixed at (0.2,0.24,0.25) in meters towards (x, y, z) axis respectively as shown in figure (4.2c) and figure (4.3a). The measurements were taken/recorded in three sessions, one for each sound source, while two layered metal doors were left closed in the receiving room. In the first session, the medisin ball was used to excite the floor at the five excitation points in the sending room (P1-P5 in ascending order as shown in figure 4.5a). The dropping mechanism of the ball (as shown in figure 4.7) was manual and similar to the measurement of force signal as explained earlier in chapter (4.2.4). The measurement procedure at each excitation point in the sending room was as follows;

- The microphone stand was positioned in such a way that the laser pointer fell at the center of the excitation point.
- The medisin ball was held in a squat position and it was made sure that the tip of the ball just touched the laser pointer.
- The ball was released freely from a height of 500 cm and was caught in the rebound. It was also made sure that no other noise was produced except impact between the ball and the floor.
- After standing still for about 12-15 seconds, the process was repeated for 9 more times at the same excitation point.
- The whole process was repeated at the next excitation point.

In the next two sessions, a similar process was followed for the measurement of IST in the receiving room using footstep with shoes and without shoes respectively. In these two sessions, one stride of a foot made an impact with the floor. After the impact, the foot was laid still and flat on the floor and released after about 12-15 seconds. A total

[(x)] see table 4.1 index 7 & 9 for specification of the microphone and recorder

of 10 repetitions at each of the five excitation points were recorded following the same procedure.

During the whole measurement session of the IST, two sets of accelerometers were also fixed at the two designated positions on the main floor in the sending room as shown in the figure (4.5a). Similar to the recordings of the IST, the acceleration of the floor corresponding to each of the impacts in each of the sessions were recorded in total of 3 sessions. In the end, there were three sessions of the microphone signal recordings and other three sessions of the acceleration signal recordings. All of the microphone and acceleration signals were pre-programmed to be recorded with a sampling frequency of 48kHz in the recorder.

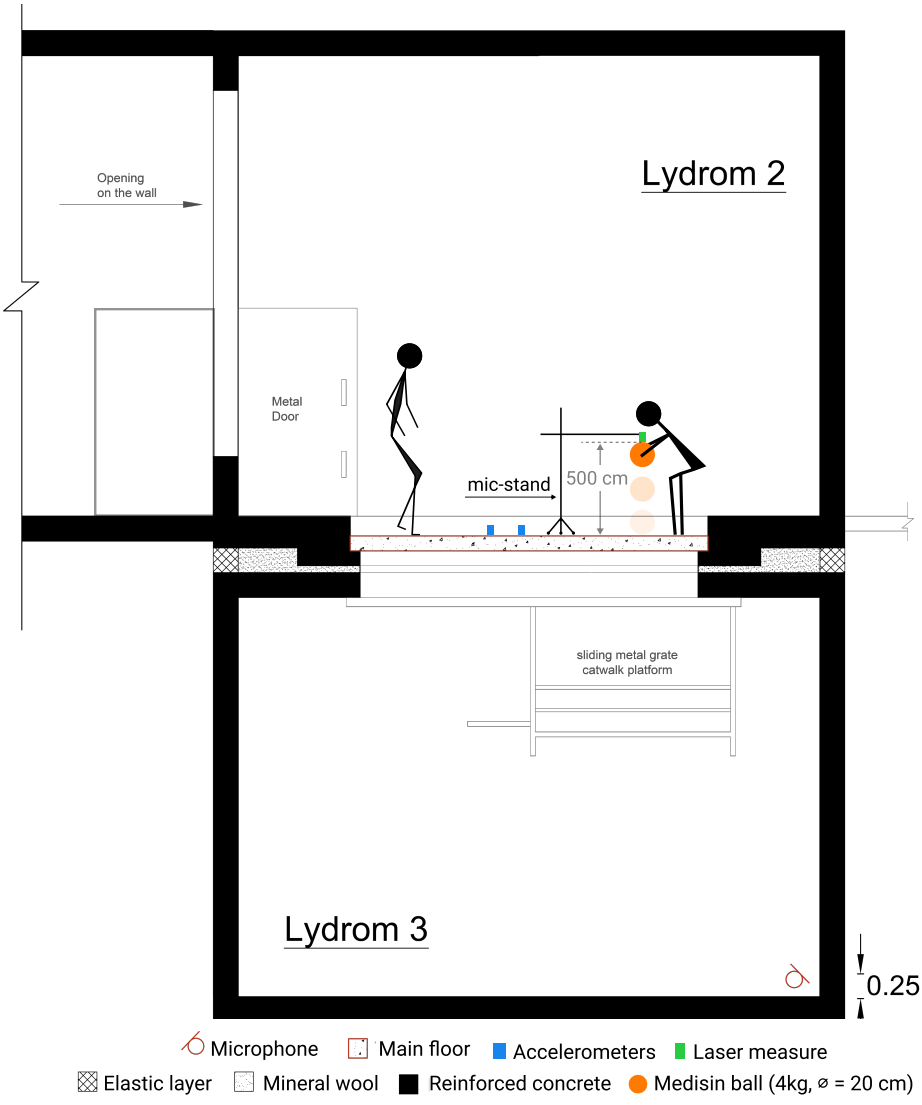

Figure 4.7: Measurement of ImSoTra: Section through Y-Y

A similar approach was applied for the measurement of IST in the receiving room via the sample of floating floor as shown in figure (4.5). All of the measurement process remained the same except that all the excitations were now made on the floating floor. For the measurements on the floating floor, the laser measure fixed to a microphone stand was used to trace the excitation points marked on the main floor onto the floating floor. It involved dragging the heavy floating floor to align its center with the laser pointer pointing towards the corresponding excitation point marker on the main floor. Finally, three sessions of IST measurements were made on the floating floor for the corresponding three sound sources. Besides, the idea of fixing the accelerometers at the designated two positions on the main floor did not match with the floating floor. To address this issue, accelerometers would have to be placed at many different locations on the main floor near to the floating floor. Thus, this process would add more complexity in the measurement process. Hence the measurement of acceleration of the floating floor was not implemented in this study.

4.2.6 Dynamic response of the floor

Equation (3.1) and (3.3) were used to calculate the natural frequencies of the main floor and the floating floor respectively based on the physical properties of relevant materials listed in table (4.2). The theoretical estimate of the natural frequencies were compared to the measured natural frequencies and the mode shapes of the main floor were speculated while assuming a simply supported boundary condition. A thorough structural modal analysis was not performed in the study.

4.2.7 Theoretical estimate of sound pressure spectrum

The *Modal Sum* method in room acoustics, as described in chapter 3.4, was used to estimate the sound pressure spectrum in the receiving room. The method was executed by using a Matlab function called modalsum_rigidroom.m, created by P. Svennson (see Annex .... for the script). Equations 3.7, 3.8 and 3.9 are incorporated in the script that calculates sound pressure, modal amplitude and resonance frequencies in the receiv-

ing room. Five source positions on the ceiling in the sending room (figure 4.5a) and one listening position at a corner in the receiving room (figure 4.2a) were considered for the calculations. Besides, the reverberation time ($T_{60} = 5s$) and speed of sound ($c_0 = 344m/s$) was considered for the calculations. Besides, the shortest distance between each source position (P1-P5) to the listening position were also measured as shown in table 4.3).

Table 4.3: Shortest disance between source and receiver position

Description	P1	P2	P3	P4	P5
Horizontal distance to mic (m)	3.50	3.20	2.95	2.69	1.88
Vertical distance to mic (m)	4.00	4.00	4.00	4.00	4.00
Shortest / direct distance to mic (m)	5.31	5.12	4.97	4.82	4.41

4.2.8 Measurement of IR of the receiving room

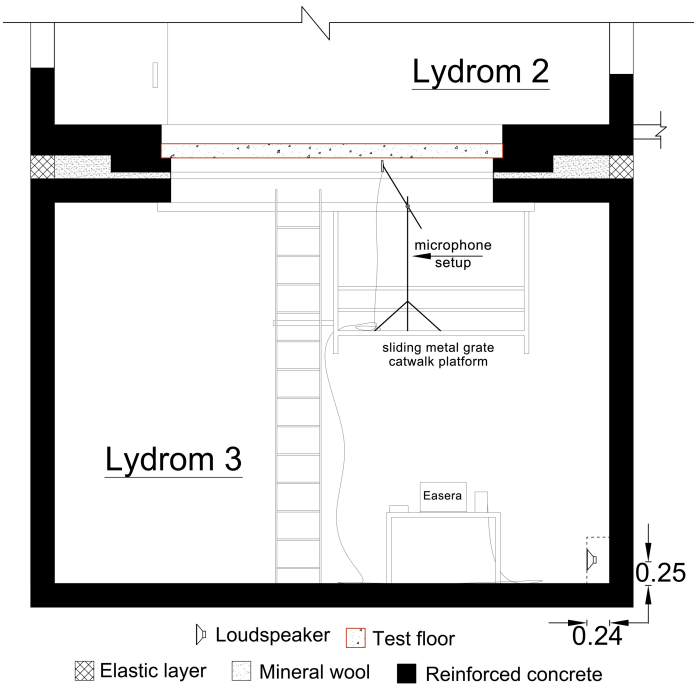

Figure 4.8: Measuring IR of the receiving room

The IR was measured at 5 different source positions on the ceiling and one listening position at a corner in the receiving room. The source and the listening positions were replicated from the corresponding positions in the IST measurements. The idea was to measure the frequency response of the receiving room at the five sets of source and

listening positions and obtain the resonance frequency of the receiving room. IR of the room was measured/calculated by following the method of DFT-based deconvolution while using a log-sweep as an excitation signal as stated in table (3.1, index 1). This method was implemented by using EASERA software (see table 4.1index 13). To avoid the complexity of fixing/placing loudspeakers as the point sources on the ceiling, the reciprocity principle in the mode-sum method, as explained in chapter (3.4) was applied to switch the placement of source and receiver positions as shown in figure (4.8).

The measurement setup in EASERA was prepared by selecting a dual channel FFT while establishing various connections as follows; The microphone(see table 4.1, index 7) was connected to *input channel 1* in the audio interface (see table 4.1, index 15) while selecting *HW input channel 1* in the software. For reference sound, *HW input channel 2* and *HW output channel 4* was selected in the software and a *TSR* cable was connected to the audio interface from *input channel 2* to *output channel 4*.

Similarly *HW output channel 3* was selected in the software and the *homemade-speaker* was connected to the *output channel 3* in the audio interface. Further, about 40 seconds long log sweep at 48kHz sampling rate with pink frequency weighting was chosen as the stimulus for the impulse response. Likewise, choosing the create button, starting and ending frequency was selected as 10Hz and 24000Hz respectively. Further, a test signal was played and the software was ready for measurements. Finally five measurements were taken by placing the microphone 5 cm below the ceiling at the 5 positions one at a time while fixing the loudspeaker at a corner as shown in figure (4.8), throughout the measurement.

‘

4.2.9 Creating Auralization signals

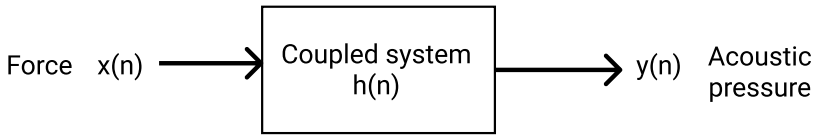

Figure 4.9: Creating auralization signals from the coupled system

To create auralization signals in the study, the two subsystems in the ImSoTra model as shown in figure (4.4), were combined into a coupled system as shown in the figure (4.9). Following three monoaural auralization signals were created;

- Medisin ball on main floor
- Footstep with shoes on main floor
- Footstep without shoes on main floor

The auralized signals were calculated by using the equation (3.11) where $\boldsymbol{x(n)}$ is the input force signals of the seleted sound source, $\boldsymbol{h(n)}$ is the impulse response of the coupled system and $\boldsymbol{y(n)}$ denotes the auralized acoustic pressure of the corresponding sound source. On the other hand, the impulse response of the coupled system was determined by considering the medisin ball as the reference sound source. IR was then calculated by convolving the measured sound pressure of the medisin ball with an *equilization filter*. IR of the coupled system could have been naively calculated by convolving the measured sound pressure of the medisin ball with an inverse filter of the measured force signal of the medisin ball based on the equation (3.11). But this naive approach would enhance the noise at very low and very high frequencies. To address this issue, the force signals could have been carefully filtered with an inverse filter removing the noise. However, for simplicity, a model of the force signal was created and the *equilization filter* was calculated based on the model of the force signal. The process of developing the model of the force signal and calculation of the *equilization filter* can be seen in the script: *analyse_forsig.mat* (see annex....) originally created by P. Svennson.

4.2.10 Subjective evaluation of auralization

The auralized signals were scaled down by a factor of 2.4 to prevent the signals from clipping while exporting the signals as wave audio files in Matlab [(xi)]. The scaling factor was defined by checking the maximum absolute value of all the signals and setting the maximum absolute value as 0.9 before exporting the signals. All of the auralized signals and their corresponding original signals were carefully listened by the author for a number of times, on full volume (on both PC. and headphones), through bluetooth headphones (see table 4.1 index 21, for specification). Three parameters were defined to characterize the original and auralized signals based on boominess, loudness and ringing tones. Besides the signals were also evaluated based on the presence of different artifacts and or additional noise between the original and the auralized signals. No standard was followed to perform the evaluation.

[(xi)] While using audiowrite function to export .wav files in Matlab, the signals with max(abs(signal))> 1 are clipped.

5 Results & Discussion

5.1 Dynamic response of the main floor

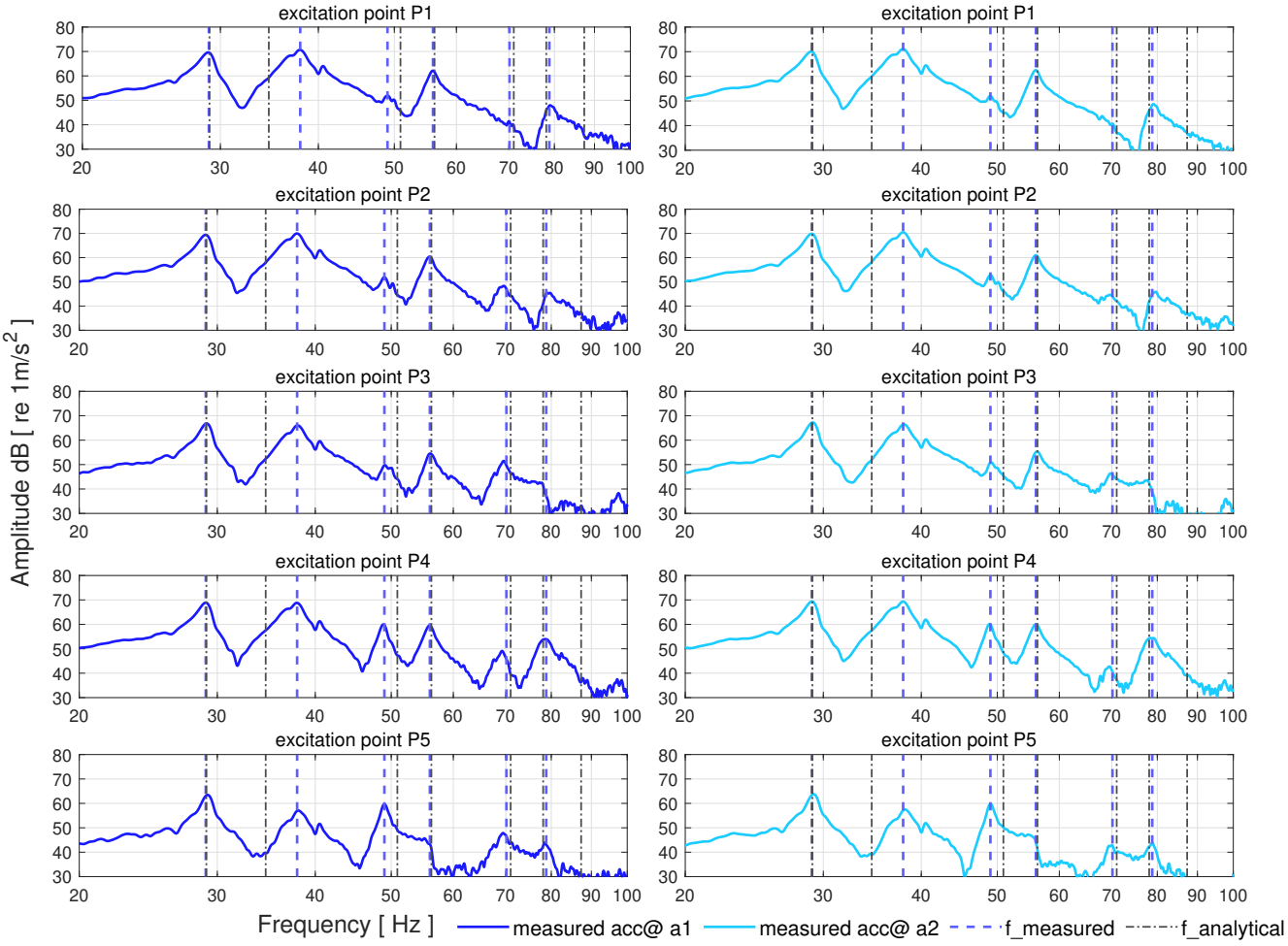

Figure 5.1: Measured acceleration spectrum with Medisin ball excitation at the five points (P1-P5) on main floor with accelerometers placed at a1 (left) and a2 (right)

Table 5.1: Theoretical and measured natural frequencies of the main floor

Modes	1	2	3	4	5	6	7	8
Theoretical natural frequency (Hz)	f_0	f_1	f_2	f_3	f_4	f_5	f_6	f_7
(assuming simply supported boundary condition)	12.7	29.0	34.5	50.8	56.2	70.9	78.0	87.2
Measured natural frequency (Hz)	28.9	37.9	49.0	56.0	70.1	78.8	-	-

From the measurements of acceleration of the main floor measured at points (a1 and a2) induced by the medisin ball excitation at points (P1-P5) as shown in figure (4.5a), six modes of vibration of the floor were observed at the corresponding natural frequencies below $100Hz$ as listed in table (5.1). Both of the accelerometers' readings corresponded well with the observed natural frequencies as seen in figure (5.1). However, the theoretical estimate of the natural frequencies of the main floor was found to be largely deviated from the observed ones. Under the assumption of simply supported boundary condition while using equation (3.1), the value for $\boldsymbol{E = 2.77GPa}$ had to be considered to get the theoretical estimates of the natural frequencies close to the measured values as shown in the table (5.1). This raised a big question on the theoretical estimate and perhaps the assumption of the simply supported boundary condition may not be true in this case.

There was insufficient information regarding construction details of the main floor. A basis drawing of the laboratories was available as shown in annex (A.1). The floor was found to be screwed to the structure during visual inspection which led to assume the simply supported boundary condition. Moreover, two resilient layers were also found below the main floor along with metal frames which may have been fastened with some gaskets. Therefore the natural frequency of the main floor was reviewed while considering the main floor as a floating floor, as shown in table (5.2),

Table 5.2: Reviewing natural frequencies of the main floor

Element	**Thickness** (m)	**Length** (m)	**Width** (m)	**Mass** (kg)	**Area** (m^2)	k (MN/m^3)	**Natural frequencies (Hz)** f_0	f_1	f_2
Main floor	0.14	3.61	3.12	3863	-	-	29.2	36.0	41.0
Rim	0.2	5.87	4.88	10173.0	-	-	-	-	-
Gasket	-	-	-	-	-	94.22	-	-	-
felt	0.07	7.22	6.24	-	0.94	-	-	-	-

The first two reviewed natural frequencies of the main floor were somewhat near to the observed values as shown in table (5.2). The first mode ($\boldsymbol{f_0}$) was calculated by following the equation (3.3, and neglecting stiffness of air) while the other two modes were assumptions based on excluding moments in the main floor. Thickness of the rim was assumed to be 0.2m and its length and width were calculated as 5.87m and 4.88m respectively. Similarly, the effective dynamic stiffness of gasket k was calculated as $94.22MN/m^3$. Detail of the calculations are provided in annex (A.2).

As shown in figure 5.2, amplitude of the measured acceleration spectrum of the main floor were found to be dominated by the first two modes followed by the fourth mode. The mode shapes of the vibrations are speculated in figure (5.3) based on the measured acceleration spectrum. The first natural modes in simply supported boundary condition are usually the piston mode, thus it was assumed the same here. Likewise in general, the amplitudes at P3 and P5 would be relatively low from the amplitudes at other points since the two points lie quite close to the nearest edge of the floor (side AB and AD in the figure 5.3). However, when other excitation points lie on a nodal line, amplitudes at P3 and P5 could be larger than the amplitudes at those points.

In principle, the amplitudes at all points in mode 1 should be larger than all other modes. But in this case, the amplitudes at P1 and P2 were found to be slightly larger in mode 2 than that in mode 1. And at P4, the amplitude were almost the same for both the first two modes. Hence, the behaviour was found slightly unusual.

In the third mode $(f_2 = 49.0Hz)$, the amplitudes at P1, P2 and P3 were about 8-10dB lower than that at P4 and P5. It implied that there could be a nodal line running through the points P1, P2 and P3 as shown in figure (5.3).

Similarly, at the fourth mode $(f_3 = 56.0Hz)$, the amplitude seemed to drop abruptly. So P5 could either lie on or very close to a nodal line as shown in the figure (5.3).

Likewise, at the fifth mode $(f_4 = 70.1Hz)$, a quick rise in amplitude was seen from P1 to P2. It implied that a nodal line could run vertically through point P1. Besides, the amplitudes at all points measured at a1 were larger than the amplitudes measured at a2. A nodal line running vertically through or very close to P1 supported the difference in amplitudes measured at a1 and a2 as a2 was placed almost in a vertical line running over P1 as shown in the figure (5.3).

Lastly, at the sixth mode $(f_5 = 78.8Hz)$, the amplitude at P1 and P2 were about 8-10dB lower than that at P4, somewhat similar to mode 3. But in mode three there seemed to be only one nodal line whereas in this case, due to the shape of the amplitude curve, P3 and P5 could be influenced by another modal line running close to them shown in the figure (5.3).

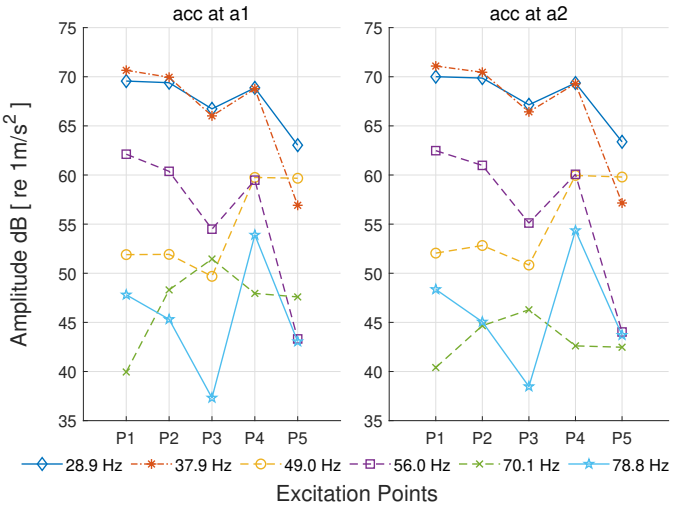

Figure 5.2: Amplitude of acceleration spectrum of the main floor as a function of excitation points

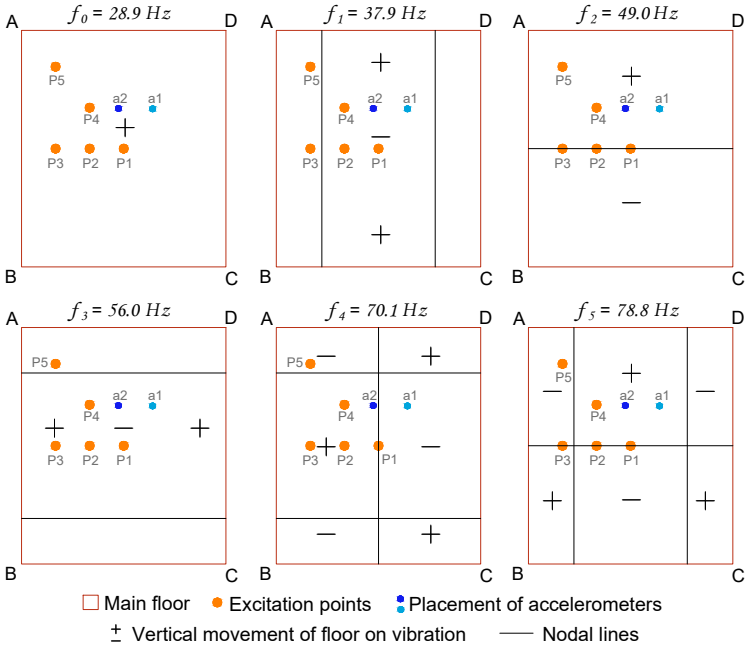

Figure 5.3: Speculating mode shapes of the main concrete floor

This study followed a simplified approach to investigate the dynamic response of the floor. The acceleration of the floor was only measured at two fixed positions on the floor for all the excitation points. It limited further analysis of the dynamic response of the floor. It could not find the unusual behaviour of the floor or shed light on the boundary condition of the floor. In contrast, measurement of acceleration of the floor at many points could reveal the modes more efficiently. This approach could carry more potential in answering the mystery of the boundary condition and diagnose the dynamic response of the floor more prominently.

5.2 Frequency Response of the receiving room

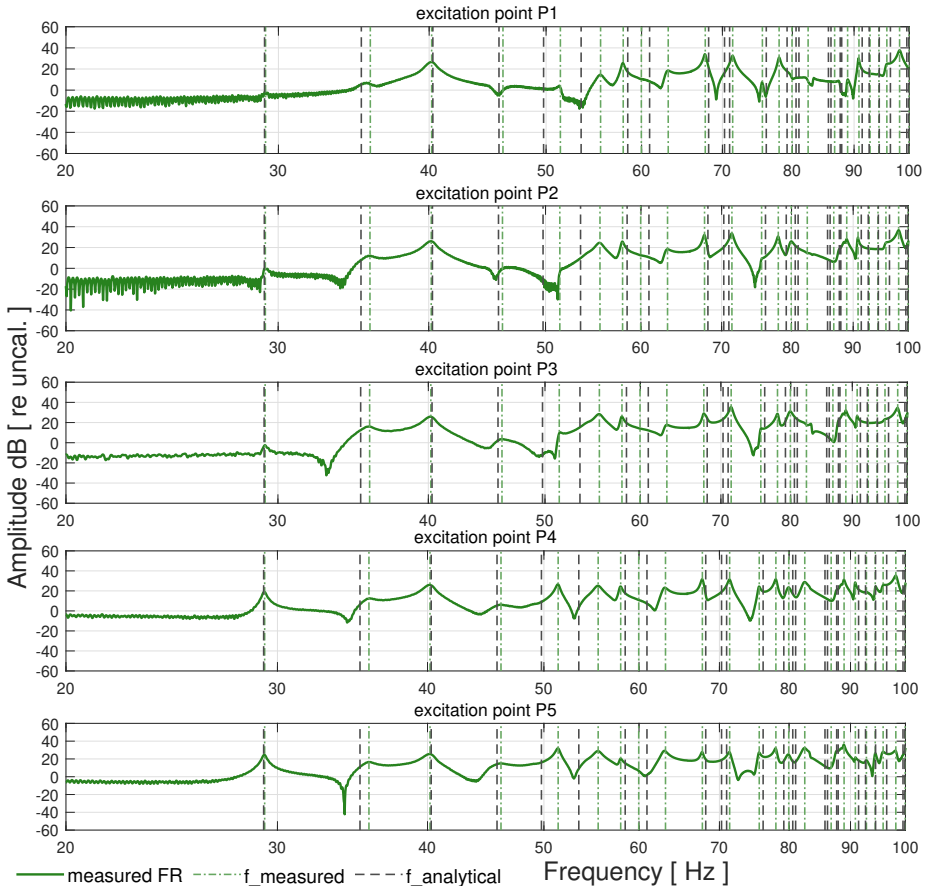

Figure 5.4: Measured Frequency Response of the receiving room

(f_measured & f_analytical mark the measured & analytical room resonance frequencies respectively.)

Many well separated peaks were formed in the frequency response between $20 - 100Hz$ which revealed the resonance frequencies of the receiving room (figure 5.4). The identified room resonances include 24 modes with 7 axial modes, 13 tangential modes and 4 oblique modes as shown in table (5.3). 3D-visualization of few of the room modes are presented in figure (5.5) where the coloured area represent the region of maximum sound pressure amplitude. The measured room resonances were validated by analytical approach by using the equation (3.9) as shown in figure (5.4) and table (5.3). All of the room resonances were found to be very close to the analytical estimate below a difference of $1Hz$, except mode number 13 and 16 with a difference of 1.2 and $1.5Hz$ respectively. Similarly, mode number 13 was not found in the measurement. The deviation in the measurements could be due to several factors. First, the assumption of $T_{60} = 5s$ could have influenced the analytical estimate as T_{60} varies

with frequencies. Besides the calculation of T_{60} revealed an average of $5.2s$ from the T_{20} estimate as shown in table (5.4). Secondly, the difference in the co-ordinates of the listening and source positions considered in the analytical calculation could also influence the deviation. Although the loudspeaker was fixed at a corner position throughout the measurement, the microphone was manually positioned at each of the five points for successive measurements of the IR.

Mode number	Measured (Hz)	Analytical (Hz)	Mode index N (l)	(m)	(n)
1	29.3	29.2	0	1	0
2	35.8	35.1	1	0	0
3	40.2	40.3	0	0	1
4	46.1	45.7	1	1	0
5	49.0	49.8	0	1	1
6	53.0	53.5	1	0	1
7	57.9	58.4	0	2	0
8	61.3	60.9	1	1	1
9	67.7	68.2	1	2	0
10	69.5	70.3	2	0	0
11	71.4	71.0	0	2	1
12	75.6	76.1	2	1	0
13	78.0	79.2	1	2	1
14	79.9	80.6	0	0	2
15	82.0	81.0	2	0	1
16	84.2	85.7	0	1	2
17	86.7	86.1	2	1	1
18		87.6	0	3	0
19	88.9	87.9	1	0	2
20	90.8	91.4	2	2	0
21	92.8	92.6	1	1	2
22	94.4	94.4	1	3	0
23	96.1	96.5	0	3	1
24	99.9	99.5	0	2	2

Table 5.3: Room resonance frequencies

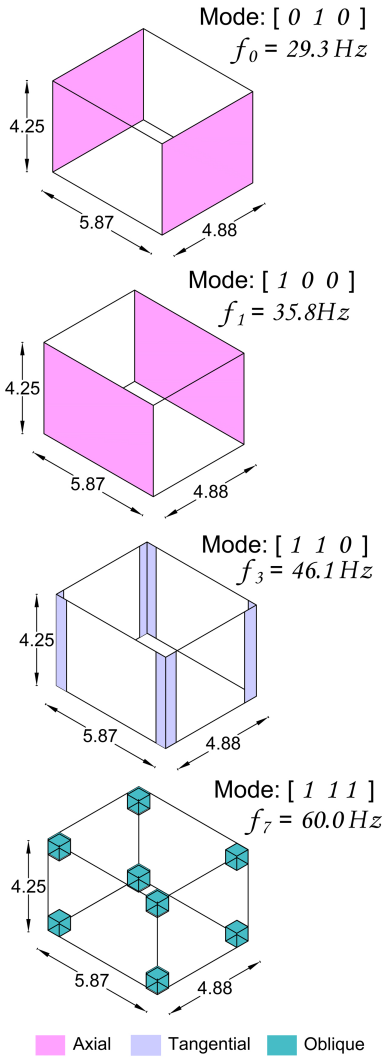

Figure 5.5: Few room modes

Besides, there could also be small error in terms of physical volume of the room considered in the analytical estimate. As the receiving room was not a typical rectangular/shoe-box shaped room (see figure 4.3a), an average height of $4.25m$ was considered in the estimate instead of an absolute height of the room. Likewise, the analytical expression (3.9) to calculate the natural frequencies also depends upon the speed of sound c_0 which is influenced by temperature. For each degree change in temperature, c_0

changes by 0.6 m/s (Kuttruff, 2000, see equation 1.1) Basements tend to be little warmer than outer air temperature. The receiving room was actually located below the basement level. It could have been slightly warmer in the receiving room but the temperature was not recorded during the measurement session.

5.2.1 Damping in the receiving room

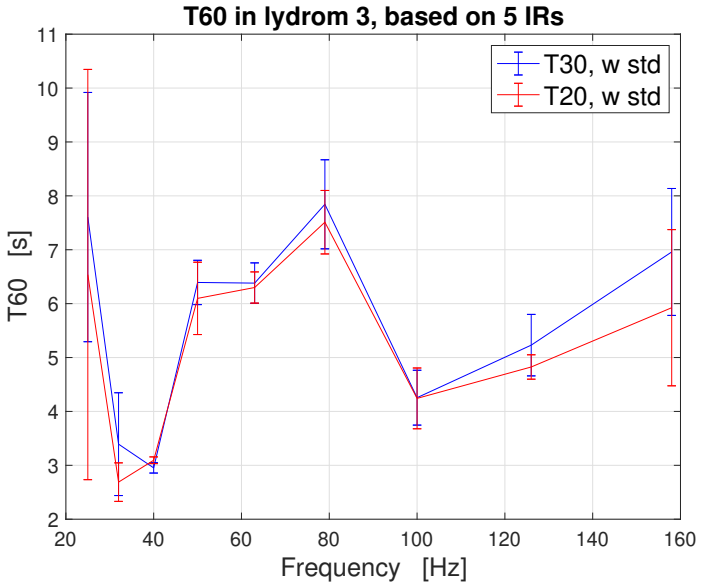

Figure 5.6: Reverberation time in the receiving room

(Courtesy of: P. Svennson)

Table 5.4: Estimated Reverberation time in the receiving room

1/3 octave band (Hz)		25	32	40	50	63	79	100	126	158
T_{60}	mean T20 (s)	6.5	2.7	3.1	6.1	6.3	7.5	4.2	4.8	5.9
	mean T30 (s)	7.6	3.4	3.0	6.4	6.4	7.8	4.3	5.2	7.0

There were very few objects/conditions in the receiving room (as explained in chapter 4.2.1) that could highly influence the damping in the room. Thus, the reverberation time T_{60} must have significantly influenced the damping in the room, given by equation (3.10). To understand the damping in the room, the five impulse response measurements were used to estimate the T_{60} of the room as shown in figure (5.6, calculated by P.Svennson) and table (5.4). From the calculations, the T_{60} for 32 & $40Hz$ were found to be very low compared to other frequencies in the third octave band. The signal

to noise ratio in the measurements of IR was very high, so the measurements as well as the estimate of the T_{60} can be considered convincing.

5.3 Sound Pressure Spectrum

5.3.1 Analytical estimate

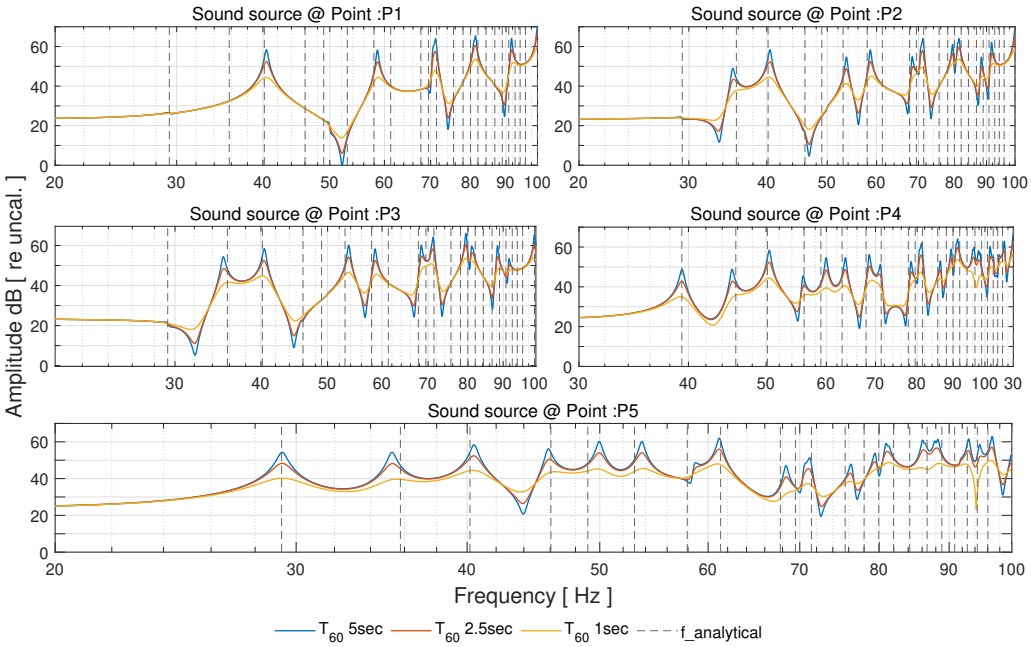

Figure 5.7: Analytical Sound Pressure Spectrum

The analytical estimate of the sound pressure spectrum for three reverberation time (T_{60}) values with the chosen source position and listening position in the receiving room is shown in figure (5.7). As expected, very well separated peaks are seen in the curves that represent the room resonance frequencies denoted by (f_analytical) in the figure. It can be noticed that the number of modes are increasing with decrease in distance between the sound source and the receiver positions. Further, different modes appear with varying amplitudes at the different source points due to the influence of the room modes on the source and receiver positions. Besides, changes in the (T_{60}) introduced new modal damping in the room given by equation (3.10). As the modal damping is inversely proportional to the (T_{60}), the modal amplitudes decreased with decrease in (T_{60}), as seen in figure (5.7).

5.3.2 Impact sound transmission measurements

As shown in figure (5.8), the Schröeder frequency is estimated roughly around 128 Hz at T_{60} of 0.5 s. The peaks are very well separated from 20-100Hz and from 100-128Hz they start to get closer while beyond 128Hz, the peaks are quite condensed.

Figures (5.9a), (5.9b) and (5.9c) show the measured sound pressure spectrum in the receiving room induced by the excitation with medisin ball, footstep with shoes and footstep without shoes respectively between $20 - 100Hz$. As seen in the analytical estimate, the measured sound pressure spectrum also featured well separated modes in the frequency range. Some peaks were also visible at the natural frequencies of the floor(see table 5.1) with a fairly combined room and floor resonance frequencies around $29Hz, 56Hz \ \& \ 78Hz$.

The acoustic energy induced in the receiving room from all sound sources on both the floors were mostly concentrated around $f2 = 40 \ Hz$. About 10dB less energy compared to the maximum were found around $29Hz \ \& \ 35Hz$. Similarly, the energy dissipated above $50Hz$ with some peaks at the floor and room resonance frequencies with roughly about 20 dB less energy compared to the maximum. Refer annex (A.3) to see the measured data for medisin ball excitation on both main floor and floating floor for all repetition also showing the signal to noise ratio.

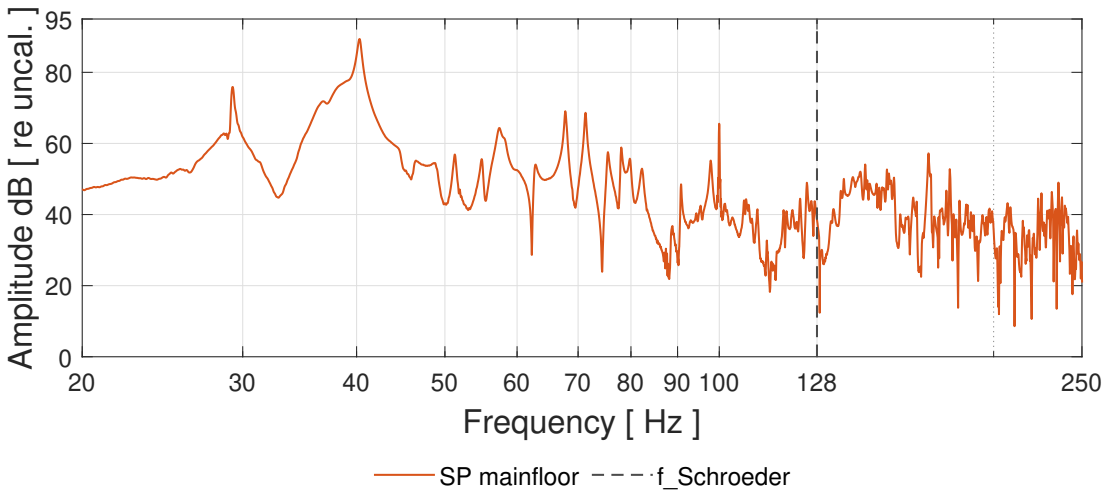

Figure 5.8: Estimated Schröeder frequency

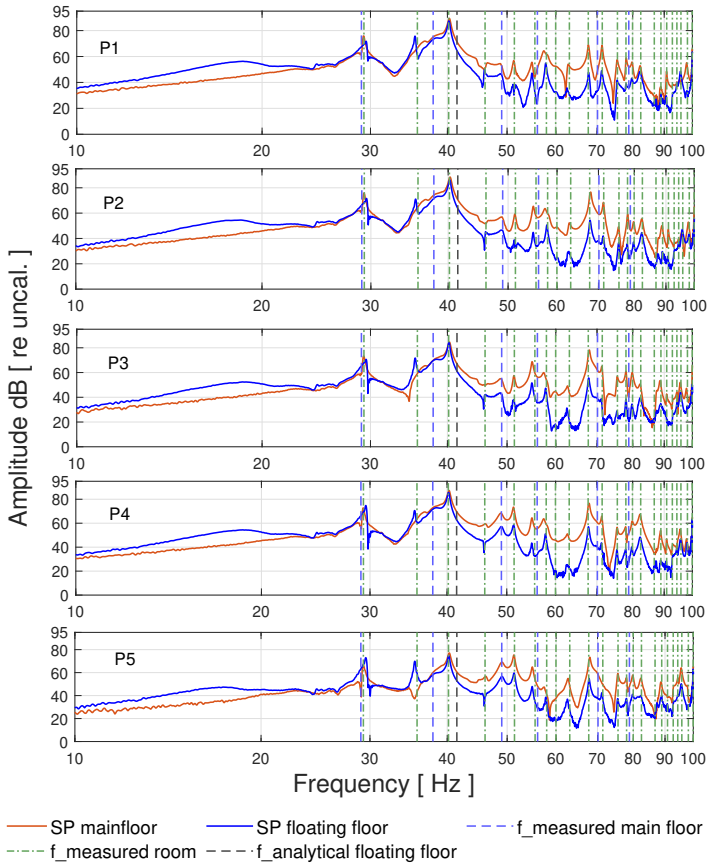

(a) Medisin ball excitation at points (P1-P5)

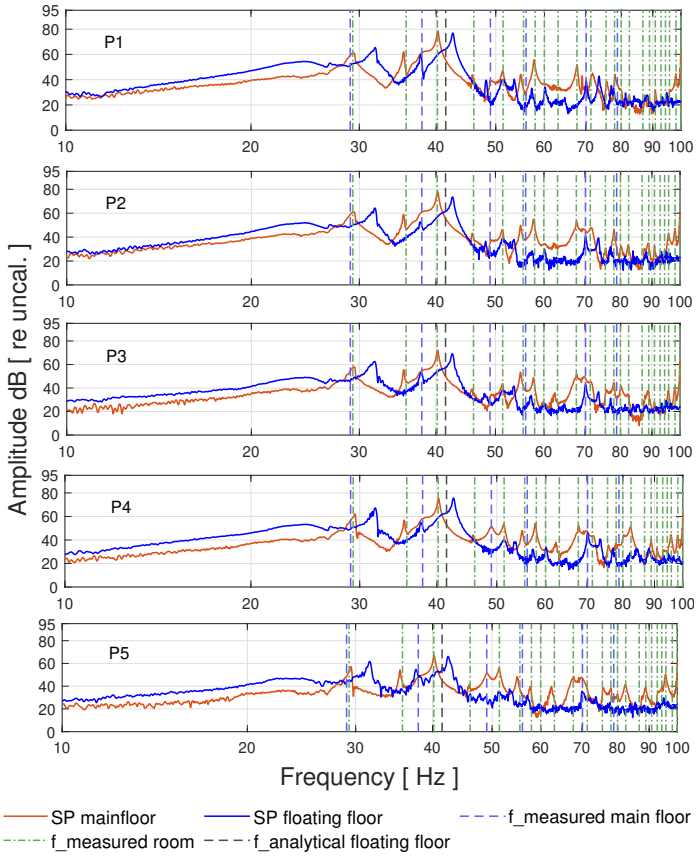

(b) Footstep excitation with shoes at points (P1-P5)

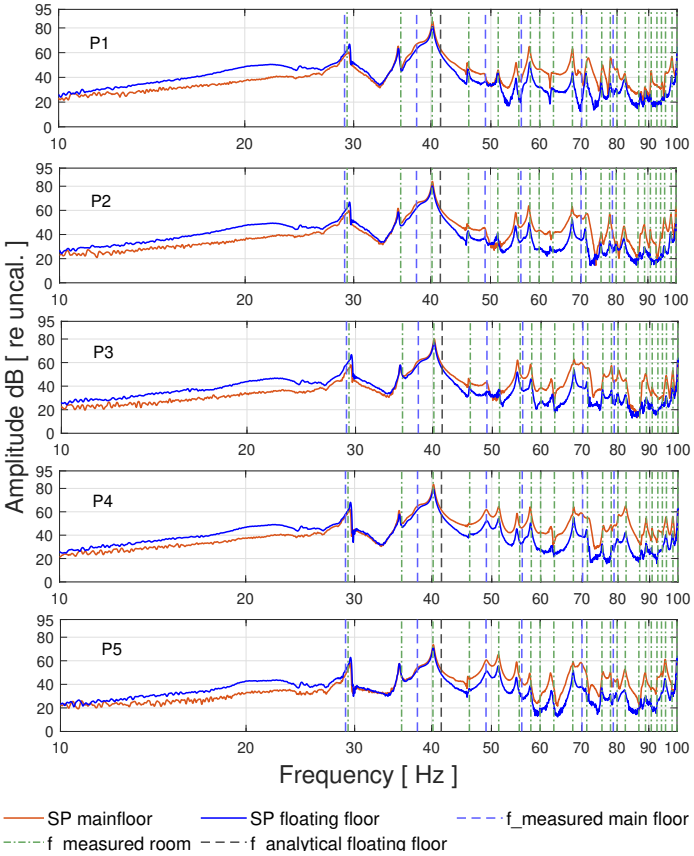

(c) Footstep excitation without shoes at points (P1-P5)

Figure 5.9: Sound pressure spectrum measured with various sound sources

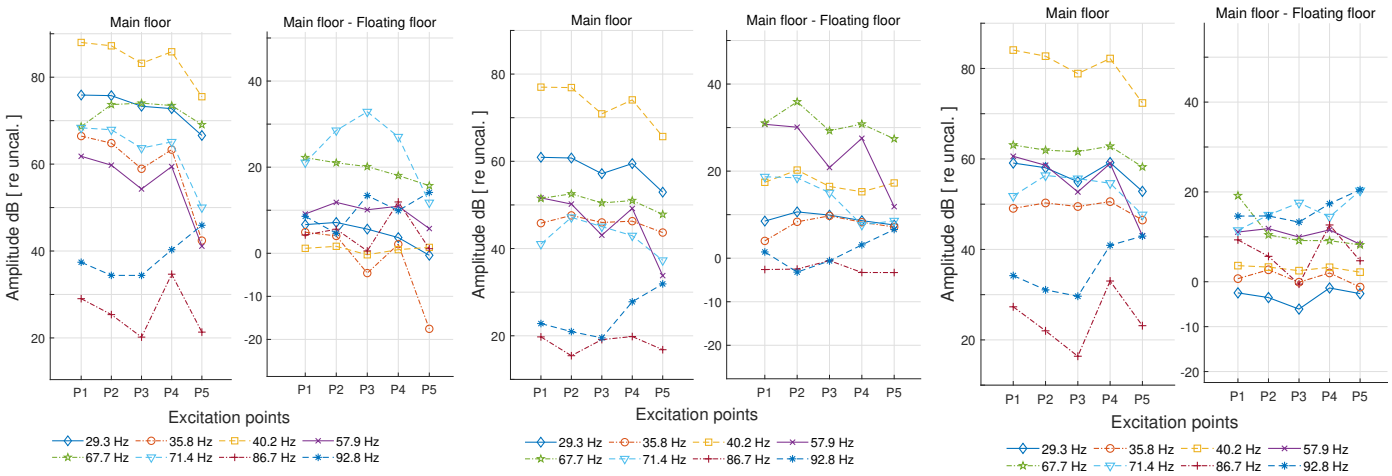

(a) Medisin ball excitation

(b) Footstep excitation with shoes

(c) Footstep excitation without shoes

Figure 5.10: Measured sound pressure spectrum amplitude Vs Excitation points

The measurements reflect the improvement of sound insulation from the floating floor (figure 5.10). As expected, the attenuation was more with the footstep excitation with the soft shoes. However, the relation of attenuation was different for different sources. In the case of footstep without shoes, the floating floor amplified the noise at $\boldsymbol{29.3Hz}$ while for the other two sources, the noise at $\boldsymbol{29.3Hz}$ was reduced at all points except for medisin ball at P5 where the difference in the noise level was almost 0dB and so on.

The precise reason behind the observed behaviour of the floating floor was not known. It could have been influenced by the added weight of the subject who stepped on the floating floor during the measurements with footsteps. In addition, the combination of floating floor and the main floor could have some influence on the modes of vibration of the floating floor. Moreover, the unknown factor of boundary condition of the main floor added another challenge to find the difference between the measured and the analytical natural frequencies of the floors.

While focusing the medisin ball excitation on the main floor, as shown in figure (5.10a), sensitivity at the selected listening position in the measurement decreased from source positions P1-P3, which increased from P3-P4 and dropped down from P4-P5 at all frequencies except $\boldsymbol{67.7Hz}$ and $\boldsymbol{92.8Hz}$. Similarly, at $\boldsymbol{67.7Hz}$, P2-P4 are at very similar levels while the levels at P1 and P5 drop about 5-6dB from the levels at P2-P4. Likewise, at $\boldsymbol{92.8Hz}$, the level at P1 decreases by about 2,3dB to P2 where the levels

remain same at P3 which again rises at a rate of about 5-6 dB from P3-P5. A more or less similar pattern can be seen in the acceleration spectrum amplitude induced by the excitation of the medisin ball (figure (5.11b). Although the acceleration of the floor was measured only at the two points *a1 & a2*, it was still possible to see the influence of the dynamic response of the floor on the measured sound pressure spectrum to some extent. The estimated sound pressure spectrum for the medisin ball excitation as shown in figure (5.11a) was calculated by simple property of proportionality between sound pressure amplitude and acceleration amplitude at the corresponding resonance frequencies as follows;

$$\boldsymbol{P_i}(\omega) = \boldsymbol{Acc_i}(\omega) \times \frac{\boldsymbol{P_1}(\omega)}{\boldsymbol{Acc_1}(\omega)} \tag{5.1}$$

where $\boldsymbol{i}$ is the five excitation points, $\boldsymbol{\omega}$ is the resonance frequencies as shown in figure (5.11), $\boldsymbol{P}$ is the sound pressure amplitude and $\boldsymbol{Acc}$ is the acceleration amplitude.

When the vibration pattern on the floor is dominated by a single mode, which happens around single resonance frequency, then the acceleration amplitude at that frequency, measured in a single point, should go up and down when changing the excitation position. This would then make the sound pressure amplitude in the room to go up and down in proportion. This phenomenon of proportionality between the sound pressure and the vibration of the floor fits very well as seen in figure (5.11). The shape of the acceleration spectrum are more or less identical/ in proportion with the curves of the sound pressure amplitude. This signifies that the model is working quite well.

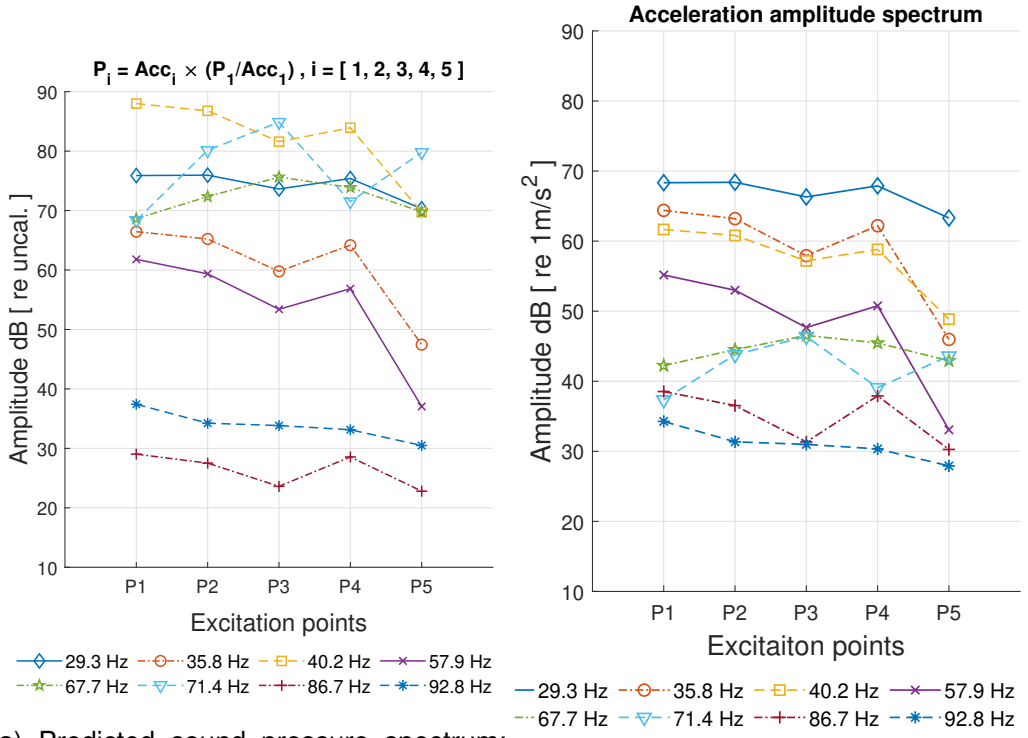

(a) Predicted sound pressure spectrum: Medisin ball

(b) Acceleration amplitude spectrum at a1

Figure 5.11: Predicting sound pressure in the receiving room

5.4 Auralization

5.4.1 Objective analysis

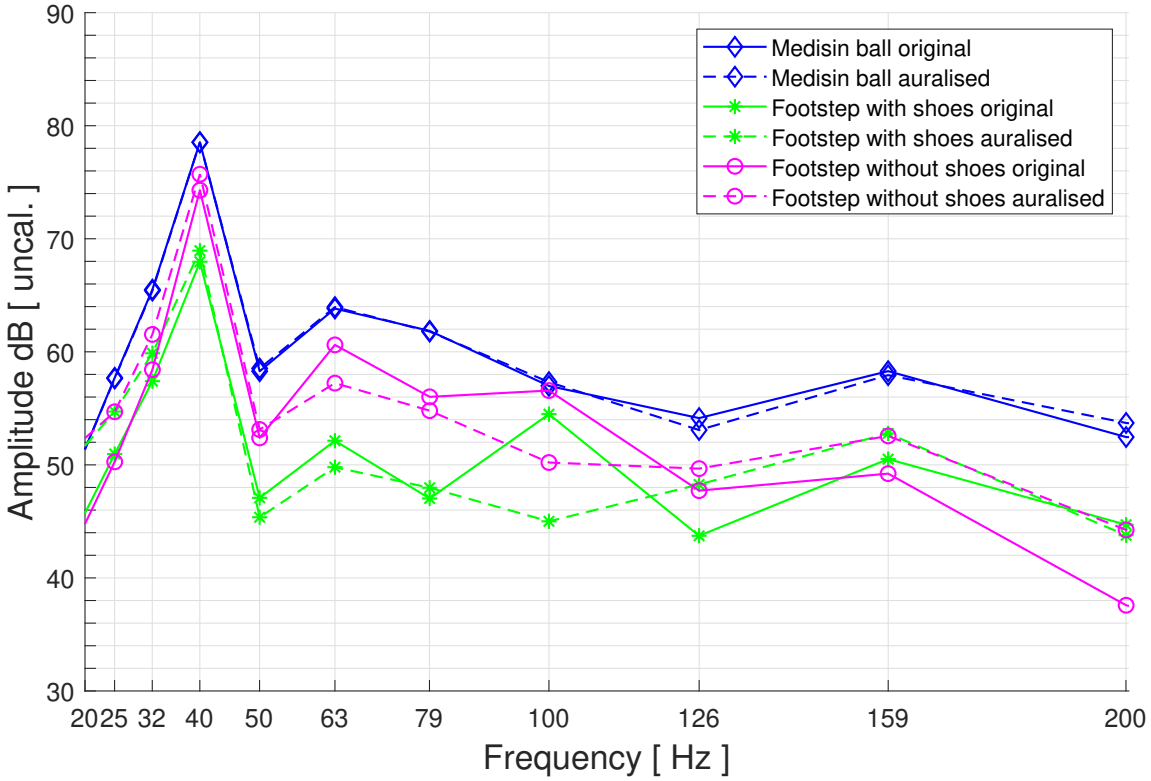

Figure 5.12: Sound Pressure Spectrum at P1: Auralised Vs Original

Figure (5.12) shows the sound pressure spectrum of the auralized and original signals for all the three sound sources in 1/3 octave band for excitation on the main floor at point P1. As the force of the medisin ball was used as the reference force for designing the equilization filter (figure A.9), auralization of the medisin matched to its original signal to a significant extent. This shows that the auralization model has significantly less error. Refer annex (A.5) for design of the equilazation filter to create the auralization.

However, the original and auralized signals of footstep with shoes were within a difference of $2dB$ at $40, 50, 63, 79, 159$ & $200Hz$ and they were at a difference of $4dB$ & $9dB$ at 126 &$100Hz$ respectively. Similarly, difference between the auralized and original signals of footstep without shoes were about $2dB$ at $40, 50, 79,$ & $126Hz$, about 3dB at $63Hz$ and 6dB at $63, 100$ &$200Hz$. The resulting auralized signals did not seem to be significantly different from the corresponding original sig-

nals. However, the outcomes were not accurate either. Two important factors have been identified behind such limitations, which are; force signals and estimation of impulse response of the coupled system.

The force signals measured with the vernier force plate were upsampled with a rate of 48khz in the post-processing where the unrecorded real characteristics of the original signals were filled in with *alian* data through interpolation. Measuring the fore signals at higher sampling rate can contribute to improved accuracy in the auralization. Refer annex (A.4) for a sample of the original and upsampled force signal data from the measurements.

Similarly, accuracy of auralization will also highly depend on the IR of the coupled system simply because IR characterizes the system itself. Again to calculate the IR of the coupled system using equation (3.11), a measured reference sound pressure in the receiving room with high signal to noise ratio should be convolved with inverse filter of force signal of the reference sound source. So, the quality of IR will then depend on the quality of the inverse filter. Creating a quality inverse filter could be challenging depending upon the nature of the recorded force signals and desired level of accuracy. The higher the demand of accuracy, more resources will be required interms of tools, equipment, available technology, time, skill and patience to gather high quality input data to acquire the desired IR and output signals.

5.4.2 Subjective analysis

The original sound pressure signals recorded in the receiving room induced by the medisin ball excitation were perceived as the loudest among all the recorded sound pressure signals. However, the signals induced by the footstep without shoes were judged as slightly more boomier than the medisin ball and highly boomier than the footstep with shoes. The soft sole shoes used in the measurements perhaps altered/reduced the force of the impact on the main floor which resulted in inducing less acoustic energy in the receiving room. Besides, a ringing tone was noticed in all of the original signals but it was more dominant and more or less equally present in the signals induced by the medisin ball and footstep without shoes. The ringing of the signals may

have caused due to amplitude modulation or frequency modulation or a combination of the two. However the precise reason for the ringing sound was unknown.

On the other hand, all three auralized signals were perceived as more boomier, more louder and found to be influenced by more ringing sounds compared to their corresponding original signals. It was challenging to maintain similar amplitude between the original signal and the exported auralized signals as the latter were scaled down when exported. But the challenge was tried to resolve by using *Reaper*[(xii)] to listen to the sounds by balancing the gains between the original and the recorded signals.

Besides, all the auralized signals also introduced a new broad band noise. Perhaps these kind of impurities perceived in the auralized singals were reflected in sound pressure spectrum of the auralized signals. A little bit of broadband noise was already present in the original signals but the noise heard in the auralized signals had slightly different timbre.

The formulated hypothesis to create auralization signals seemed to be working well as the methodology applied revealed significantly less error for the reference aulalization of the medisin ball. However, the factors influencing the accuracy/quality of the auralization as described earlier may have caused the highlighted issues. Thus, quality recordings of the force signals, sound pressure signals and precise inverser filter are required to calculate a more accurate impulse response of the coupled system to get more accurate auralization results while applying the current method used in this study.

5.5 Future works

One of the future works could be to study the vibration pattern of the floor more in detail and do a modal analysis to understand what are the causes of the resonance frequencies and the vibration patterns.

Similarly, acceleration of the floor can be measured at many points on the floor so that maximum vibrating modes of the floor could be captured in the measurement. This can

[(xii)] a type of digital audio workstation

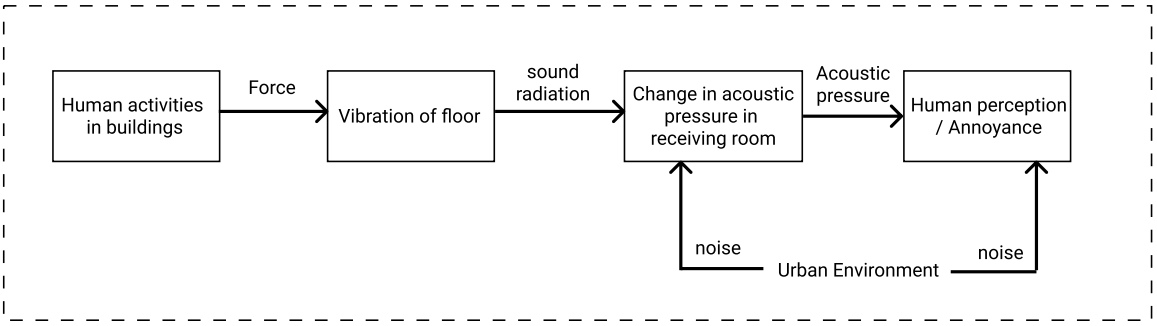

Figure 5.13: Annoyane from noise exposure in buildings in an urban environment

further enhance the study of dynamic response of the floor together with information of structural properties and boundary condition of the floor.

The impact sound transmission can be measured at several listening positions in the receiving room. The amplitude of the sounds generated in a room are affected by the room modes and this could be compared/studied well if measurements are taken at several listening positions. Similalry, a more accurate impulse response of the system can be calculated in two ways which are; 1) Designing a more precise inverse filter 2) Using a new equipment like shakers for example which can directly measure the impulse response of the coupled system. This setup will work almost in the same way like the method used to calculate the IR of the receiving room in this study.

Besides, auralization could also be performed at a higher level by addressing directionality of the sounds in the receiving room either working with binaural approach or multi-channel spatial audio techniques.

Moreover, on a broader level, for the study of low frequency impact sound transmission in multi-unit dwellings in an urban environment, the ImSoTra model, introduced in chapter (4.2.5), can be extended as shown in figure (5.13). As such, the extended model can also be incorporated with the assessment of annoyance and risk assessments by linking the methods from EEA (European Environment Agency, 2010).

6 Conclusion

The simplified approach of studying the dynamic response of the main floor by measuring the acceleration of the floor at two fixed positions for all excitations did not seem to be enough. The method did not reveal many modes of vibration. It did not provide enough information on amplitude of vibration which did not allow to perform an accurate estimation of sound pressure level in the receiving room. If many acceleration amplitudes were known, then more accurate estimation of the sound pressure level could have been achieved by using the modal sum method.

Six natural frequencies of the main floor were identified from the measurements, which are; $28.9, 37.9, 49, 56, 70.1$ & $78.8Hz$. To calculate a similar values, the theoretical expression assuming a simply supported boundary condition however had to be tweaked by considering $E = 2.77GPa$ which gave the following set of natural frequencies; $12.7, 29.0, 34.5, 50.8, 56.2, 70.9, 78.0$ & $87.2Hz$. So there seemed to be a great discrepancy between the observed and the analytical estimates of the natural frequency of the floor. Moreover, in the absence of actual information regarding the structural properties and boundary condition of the main floor, a random calculation by considering the main floor as a floating floor was calculated that gave a natural frequency of $29.2Hz$. Similarly, mode shapes of the vibration of the main floor were just speculated based on the measured natural frequencies of the main floor.

Likewise, natural frequency of the floating floor was analytically estimated to be $41.2Hz$. But the behaviour of the floating floor was not clearly known for the three sound sources. The improvement with the floating floor about 1.5 times f_0 did not seem to match the observed relation between the three sound sources. Moreover, the repeatability of excitation with both footstep with shoes and without shoes were found to be very poor in comparison to that of the medisin ball. Thus it was concluded that both of the footsteps measurements could have influenced the measurements with the floating floor in addition to unknown behaviour of both the main floor and the floating

floor.

Further, the frequency response of the receiving room calculated from the impulse response of the room revealed 23 room resonance frequencies between $20 - 100Hz$. The analytical modal sum method however estimated a total of 24 room resonances with 7 axial modes, 13 tangential modes and 4 oblique modes. 21 of the measured room resonances were found to be within a difference of 1Hz from the analytical estimate while two modes were measured within a difference of 1.5Hz. Similarly, T_{60} values in the receiving room were found to be very low between $2.7 - 3.7s$ at $32 \ \& \ 40Hz$ while in the range of $25 - 158Hz$, T_{60} value spread out from $4.2to7.6s$.

Similarly, both the analytical estimate and the measurement of the sound pressure spectrum in the receiving room revealed very well separated modes in the range of $20 - 100Hz$. The measured room resonances complied very well to the measured and estimated sound pressure spectrum in the receiving room. Some peaks were also seen at the floor resonances but the overall measured sound pressure spectrum were dominated by the room resonances. Thus, it was concluded that the modal sum method can estimate the sound pressure spectrum at low frequency resolution for the impact sound transmission between two vertically adjacent rooms.

Finally, the formulated hypothesis to create auralization signals was found to be affirmative based on the precision of the auralization of medisin ball excitation from $20 - 200Hz$ in 1/3 octave band. The auralization for the other two sound sources were found to be relatively close to the corresponding original sounds. Besides, the subjective analysis of the aurlalized signals revealed that all of the auralized signals were more boomier, more louder and contained more ringing sounds compared to their corresponding original signals. The auralized signals introduced broad band noise different from the original signals.

Force signals and estimation of impulse response of the coupled system have been identified as two major influencing factor for such inaccuracies. The force signals in this study were measured at 1kHz sampling rate and upsampled to 48kHz in post processing. In addition, a modal of force signal was used to design the inverse filter to calculate the impulse response of the system. Thus, it is highly likely that these

consequences added impurities in the post processing causing the inaccuracies in the outcome of the auralization. Quality recordings of the force signals with high sampling rate, sound pressure signals with high signal to noise ratio and precise inverser filter can contribute in calculating a more accurate impulse response of the coupled system to get more accurate auralization results while applying the current method.

Bibliography

Babisch, Wolfgang (July 1, 2002). “The noise/stress concept, risk assessment and research needs”. In: *Noise and Health* 4.16. Publisher: Medknow Publications, p. 1. ISSN: 1463-1741. URL: https://www.noiseandhealth.org/article.asp?issn=1463-1741;year=2002;volume=4;issue=16;spage=1;epage=11;aulast=Babisch;type=0 (visited on 04/30/2021).

Berglund, Birgitta, Peter Hassmén, and Raymond Soames Job (June 1, 1996). “Sources and effects of low-frequency noise”. In: *The Journal of the Acoustical Society of America* 99, pp. 2985–3002. DOI: 10.1121/1.414863.

Berglund, Birgitta, Thomas Lindvall, et al. (1999). “Guidelines for community noise”. In: Publisher: World Health Organization. URL: https://apps.who.int/iris/handle/10665/66217 (visited on 05/03/2021).

Burkhart, C and M Wolf (2016). “Strategies to avoid boomy screeds”. In: p. 5.

Cremer, Lothar and Helmut A. Muller (1982). *Principles and Applications of Room Acoustics*. English. Trans. by Theodore J. Schultz. Vol. 2. Applied Schence Publishers.

Direktoratet for byggkvalitet (2016). *Lydforhold i boliger. Evaluering av byggtekniske krav til lydforhold*. Tech. rep. 127762-RIA-RAP-001. Oslo. URL: https://dibk.no/globalassets/byggeregler/tek10-til-tek17/rapporter/lydforhold-i-boliger_samlerapport_sintef_toi_multiconsult_mars-2016.pdf.

European Environment Agency (Nov. 2010). *Good practice guide on noise exposure and potential health effects — European Environment Agency*. 1725-2237. 140 pp. ISBN: 978-92-9213-140-1. URL: https://www.eea.europa.eu/publications/good-practice-guide-on-noise (visited on 04/30/2021).

Fletcher, Harvey and W A Munson (1933). "Loudness, Its Definition, Measurement and Calculation". In: *The Journal of the Acoustical Society of America*, p. 28.

Goldsmith, Mike (n.d). *History of noise*. en. URL: https://mikegoldsmith.weebly.com/history-of-noise.html (visited on 05/04/2021).

Homb, Anders (Aug. 2006). "Low frequency sound and vibrations from impacts on timber floor constructions". PhD thesis.

Hongisto, Valtteri et al. (Oct. 2020). "Impact sound insulation of floating floors: A psychoacoustic experiment linking standard objective rating and subjective perception". In: *Building and Environment* 184, p. 107225. ISSN: 03601323. DOI: 10.1016/j.buildenv.2020.107225. URL: https://linkinghub.elsevier.com/retrieve/pii/S0360132320305965 (visited on 01/17/2021).

Inukai, Yukio et al. (Sept. 1, 1986). "A Multidimensional Evaluation Method for the Psychological Effects of Pure Tones at Low and Infrasonic Frequencies". In: *Journal of Low Frequency Noise, Vibration and Active Control* 5.3. Publisher: SAGE Publications Ltd STM, pp. 104–112. ISSN: 1461-3484. DOI: 10.1177/026309238600500303. URL: https://doi.org/10.1177/026309238600500303 (visited on 04/30/2021).

ISO (1989). *ISO 9052-1:1989*. en. URL: https://www.iso.org/cms/render/live/en/sites/isoorg/contents/data/standard/01/66/16620.html (visited on 05/20/2021).

– (2003). *Acoustics — Normal equal-loudness-level contours*. en. URL: https://www.iso.org/cms/render/live/en/sites/isoorg/contents/data/standard/03/42/34222.html (visited on 05/16/2021).

ISO (2020a). *Acoustics — Field measurement of sound insulation in buildings and of building elements — Part 2: Impact sound insulation*. ISO. URL: https://www.iso.org/cms/render/live/en/sites/isoorg/contents/data/standard/07/74/77436.html (visited on 01/17/2021).

– (2020b). *ISO 717-2:2020(en), Acoustics — Rating of sound insulation in buildings and of building elements — Part 2: Impact sound insulation*. URL: https://www.iso.org/obp/ui/#iso:std:iso:717:-2:ed-4:v1:en (visited on 05/10/2021).

– (2021). *ISO 10140-3:2021*. en. URL: https://www.iso.org/cms/render/live/en/sites/isoorg/contents/data/standard/07/94/79483.html (visited on 05/05/2021).

Japanese Standard Association (2000). *JIS A 1418-2:2000 Acoustics - Measurement Of Floor Impact Sound I*. URL: https://infostore.saiglobal.com/en-gb/standards/jis-a-1418-2-2000-625497_SAIG_JSA_JSA_1436250/ (visited on 05/06/2021).

Kuttruff, Heinrich (2000). *Room acoustics*. 4th ed. London, [England] ; New York, NY: Spon Press. ISBN: 978-0-419-24580-3. URL: https://danylastchild07.files.wordpress.com/2016/05/room-acoustics-kuttruff.pdf.

Leventhall, H. G. (Apr. 1, 2004). "Low frequency noise and annoyance". In: *Noise and Health* 6.23. Publisher: Medknow Publications, p. 59. ISSN: 1463-1741. URL: https://www.noiseandhealth.org/article.asp?issn=1463-1741;year=2004;volume=6;issue=23;spage=59;epage=72;aulast=Levent;type=0 (visited on 05/03/2021).

Løvstad, Anders et al. (June 2017). "Perceived sound quality in dwellings in Norway". In:

Martins, Carlos et al. (Dec. 2015). "Acoustic performance of timber and timber-concrete floors". en. In: *Construction and Building Materials* 101, pp. 684–691. ISSN: 0950-

0618. DOI: 10.1016/j.conbuildmat.2015.10.142. URL: https://www.sciencedirect.com/science/article/pii/S0950061815305626 (visited on 05/18/2021).

Møller, Henrik and Morten Lydolf (Sept. 2002). "A Questionnaire Survey of Complaints of Infrasound and Low-Frequency Noise". en. In: *Journal of Low Frequency Noise, Vibration and Active Control* 21.2. Publisher: SAGE Publications Ltd STM, pp. 53–63. ISSN: 1461-3484. DOI: 10.1260/026309202761019507. URL: https://doi.org/10.1260/026309202761019507 (visited on 05/05/2021).

Na, Seunguk et al. (Jan. 2019). "Evaluation of the Floor Impact Sound Insulation Performance of a Voided Slab System Applied to a High-Rise Commercial Residential-Complex Building". In: *International Journal of Concrete Structures and Materials* 13.1, p. 3. ISSN: 2234-1315. DOI: 10.1186/s40069-018-0315-y. URL: https://doi.org/10.1186/s40069-018-0315-y (visited on 05/06/2021).

Norwegian Standard (2019). *NS 8175:2019*. URL: https://www.standard.no/no/Nettbutikk/produktkatalogen/Produktpresentasjon/?ProductID=1045700 (visited on 05/11/2021).

– (2020). *Norwegian Standard for acoustic classification of buildings now available in English | standard.no*. URL: https://www.standard.no/en/nyheter/news-in-english/2020-news/norwegian-standard-for-acoustic-classification-of-buildings-now-available-in-english/ (visited on 05/16/2021).

Park, Sang Hee and Pyoung Jik Lee (May 1, 2017). "Effects of floor impact noise on psychophysiological responses". In: *Building and Environment* 116, pp. 173–181. ISSN: 0360-1323. DOI: 10.1016/j.buildenv.2017.02.005. URL: http://www.sciencedirect.com/science/article/pii/S0360132317300586 (visited on 01/16/2021).

Park, Sang Hee, Pyoung Jik Lee, and Kwan Seop Yang (Sept. 1, 2016). "Perception and Reaction to Floor Impact Noise in Apartment Buildings: A Qualitative Approach".

In: *Acta Acustica united with Acustica* 102.5, pp. 902–911. DOI: 10.3813/AAA.919004.

Park, Sang Hee, Pyoung Jik Lee, Kwan Seop Yang, and Kyoung Woo Kim (Mar. 1, 2016). "Relationships between non-acoustic factors and subjective reactions to floor impact noise in apartment buildings". In: *The Journal of the Acoustical Society of America* 139.3. Publisher: Acoustical Society of America, pp. 1158–1167. ISSN: 0001-4966. DOI: 10.1121/1.4944034. URL: https://asa.scitation.org/doi/10.1121/1.4944034 (visited on 01/16/2021).

Persson Waye, Kerstin (Dec. 31, 2011). "Noise and Health - Effects of Low Frequency Noise and Vibrations: Environmental and Occupational Perspectives". In: *Encyclopedia of Environmental Health*. Vol. 4. Journal Abbreviation: Encyclopedia of Environmental Health, pp. 240–253. DOI: 10.1016/B978-0-444-52272-6.00245-2.

Samarasinghe, Prasanga, Thushara D. Abhayapala, and Walter Kellermann (Oct. 2017). "Acoustic reciprocity: An extension to spherical harmonics domain". en. In: *The Journal of the Acoustical Society of America* 142.4, EL337–EL343. ISSN: 0001-4966. DOI: 10.1121/1.5002078. URL: http://asa.scitation.org/doi/10.1121/1.5002078 (visited on 06/19/2021).

Schneider, Martin and Heinz-Martin Fischer (2013). "Complaints about low frequency noise with floating floors". In: p. 6.

Schroeder, Manfred R. (May 1996). "The "Schroeder frequency" revisited". en. In: *The Journal of the Acoustical Society of America* 99.5, pp. 3240–3241. ISSN: 0001-4966. DOI: 10.1121/1.414868. URL: http://asa.scitation.org/doi/10.1121/1.414868 (visited on 05/07/2021).

Shi, Wanqing (1995). "Assessing and Modelling Impact Sound Insulation of Wooden Joist Constructions". PhD thesis.

Sjösten, Per et al. (June 2016). “The effect of Helmholtz resonators on the acoustic room response”. In: *Proc. of BNAM 2016*. Stockholm.

Smith, Steven W. (Jan. 1997). *The Scientist & Engineer's Guide to Digital Signal Processing*. English. 1st edition. San Diego, Calif: California Technical Pub. ISBN: 978-0-9660176-3-2.

SSB, Statistics Norway (2016). *Growing number of Norwegians are exposed to noise*. en. URL: https://www.ssb.no/en/natur-og-miljo/artikler-og-publikasjoner/growing-number-of-norwegians-are-exposed-to-noise (visited on 05/07/2021).

Svennson, Peter (2020). *Transfer function/Impulse response measurements. TTT4170 - Audio technology*. en. Lecture notes. Norwegian University of Science and Technology (NTNU). Delivered on 9 January 2020.

Tackett, Jeff (2021). *ISO 226 Equal-Loudness-Level Contour Signal*. en. URL: https://se.mathworks.com/matlabcentral/fileexchange/7028-iso-226-equal-loudness-level-contour-signal (visited on 05/18/2021).

Takahashi, Yukio (Mar. 1, 2013). “Vibratory Sensation Induced by Low-Frequency Noise: The Threshold for “Vibration Perceived in the Head” in Normal-Hearing Subjects”. In: *Journal of Low Frequency Noise, Vibration and Active Control* 32.1. Publisher: SAGE Publications Ltd STM, pp. 1–9. ISSN: 1461-3484. DOI: 10.1260/0263-0923.32.1-2.1. URL: https://doi.org/10.1260/0263-0923.32.1-2.1 (visited on 04/30/2021).

UN (2019). “World Urbanization Prospects The 2018 Revision”. en. In: p. 126.

Vigran, Tor Erik (2008). *Building acoustics*. en. OCLC: ocn173480513. London ; New York: Taylor & Francis. ISBN: 978-0-415-42853-8 978-0-203-93131-8.

Vorländer, Michael (2008). *Auralization: Fundamentals of Acoustics, Modelling, Simulation, Algorithms and Acoustic Virtual Reality*. en. RWTHedition. Berlin Heidelberg:

Springer-Verlag. ISBN: 978-3-540-48829-3. DOI: 10.1007/978-3-540-48830-9. URL: https://www.springer.com/gp/book/9783540488293 (visited on 05/06/2021).

WHO (June 1946). *Preamble to the Constitution of the World Health Organization as adopted by the International Health Conference, New York, 19–22 June 1946; signed on 22 July 1946 by the representatives of 61 States (Official Records of the World Health Organization, no. 2, p. 100) and entered into force on 7 April 1948.* Publisher: BMJ Publishing Group Ltd Section: Speakers' corner. New York. URL: https://jech.bmj.com/content/63/6/419 (visited on 04/30/2021).

– (1980). *Noise. Environmental Health Criteria Document, 12*. Tech. rep. Geneva, Switzerland: World Health Organization. URL: http://www.inchem.org/documents/ehc/ehc/ehc012.htm (visited on 05/04/2021).

Yamada, S. et al. (Sept. 1, 1983). "Body Sensation of Low Frequency Noise of Ordinary Persons and Profoundly Deaf Persons". In: *Journal of Low Frequency Noise, Vibration and Active Control* 2.3. Publisher: SAGE Publications Ltd STM, pp. 32–36. ISSN: 1461-3484. DOI: 10.1177/026309238300200302. URL: https://doi.org/10.1177/026309238300200302 (visited on 04/30/2021).

A Various

A.1 Original Lab drawings

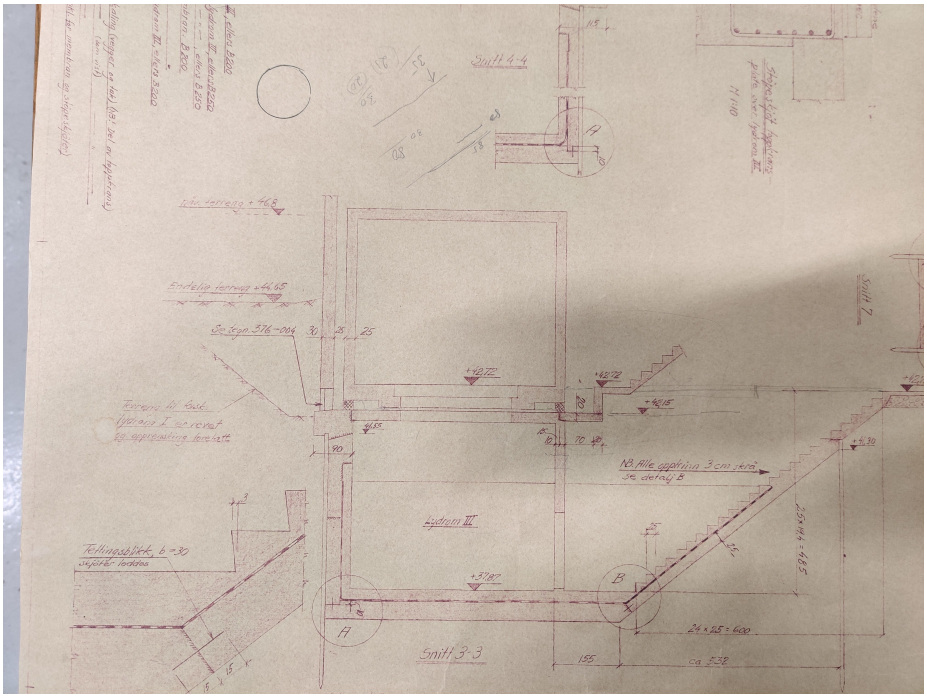

Figure A.1: Section of Lydrom 2 and Lydrom 3

A.2 Reviewing natural frequency - data

				Plate	Sorrounding		Pivoting 1	Pivoting 2
	t [m]	L [m]	B [m]	m [kg]	M [kg]	f0 [Hz]	f1 [Hz]	f2 [Hz]
	0.145	3.61	3.12	4001	10035	28.9	35	41
Rim	0.2	5.87	4.88	10035				
Gasket	100	MN/m3	94.22	MN/m3	8.4			
	1	MN/m2	0.9422	MN/m2				
Area fe	0.07	0.51	0.4368	0.94	m2			

Figure A.2: Calculation for reviewing natural frequency

A.3 Microphone signals data

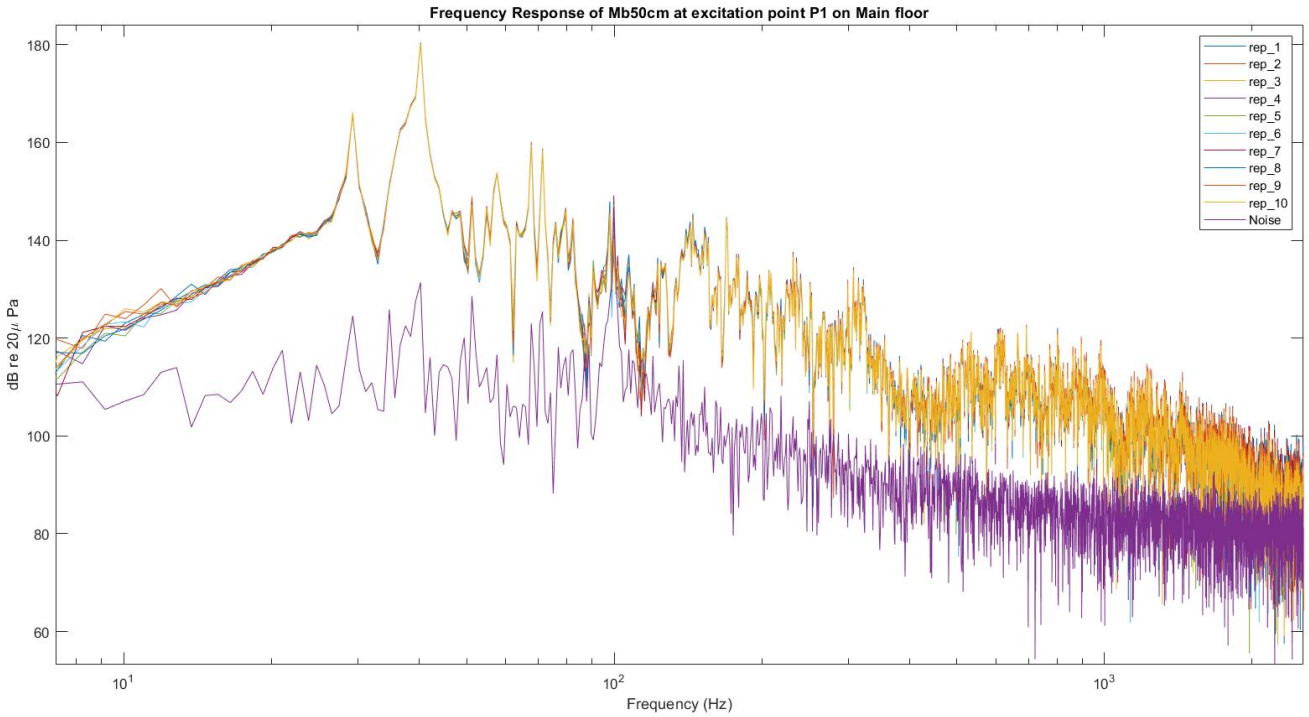

Figure A.3: Signal to noise ration Medisin ball main floor

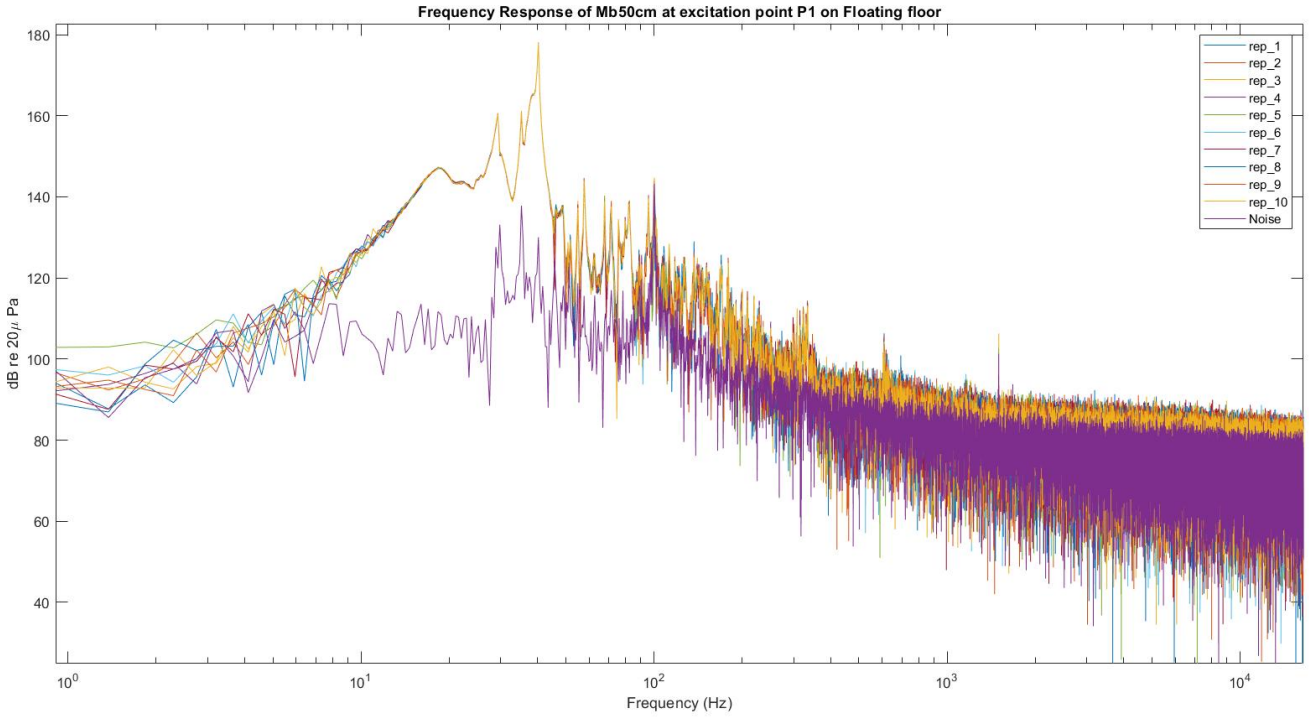

Figure A.4: Signal to noise ration Medisin ball floating floor

A.4 Force signals data

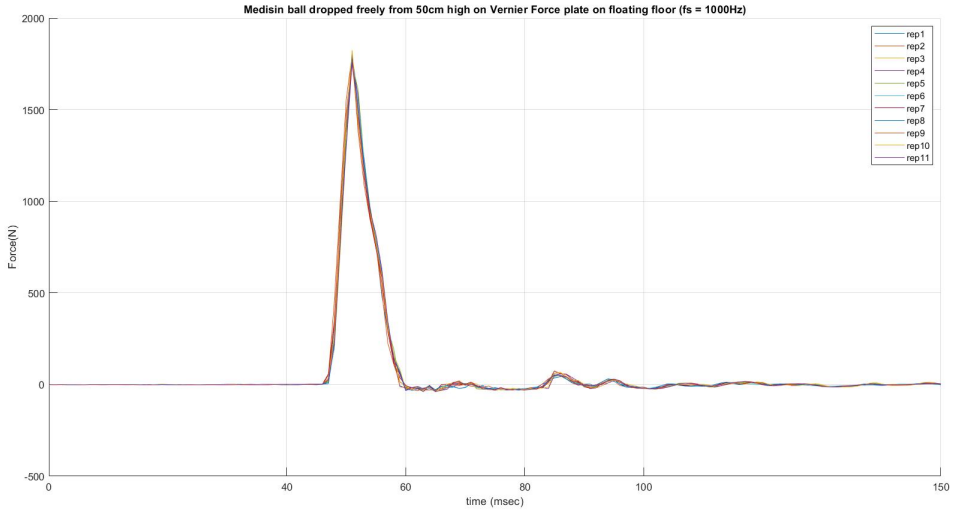

Figure A.5: Force signal medisin ball 1kHz

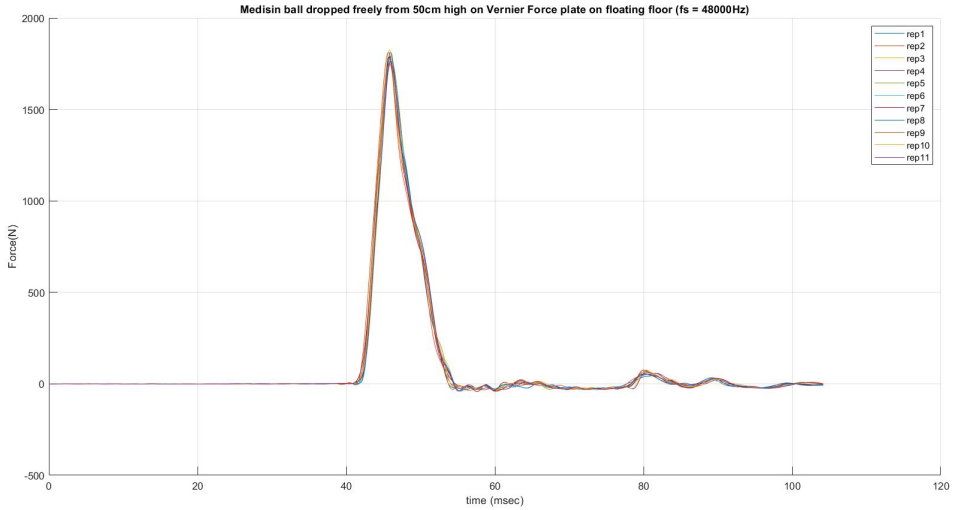

Figure A.6: Force signal medisin ball 48kHz

A.5 Equilization filter design for Auralization

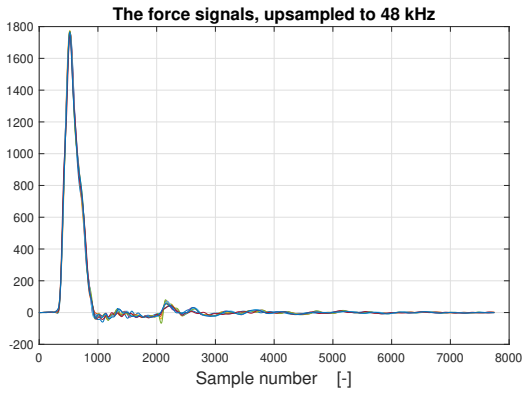

(a) Force signal upsampled to 48kHz

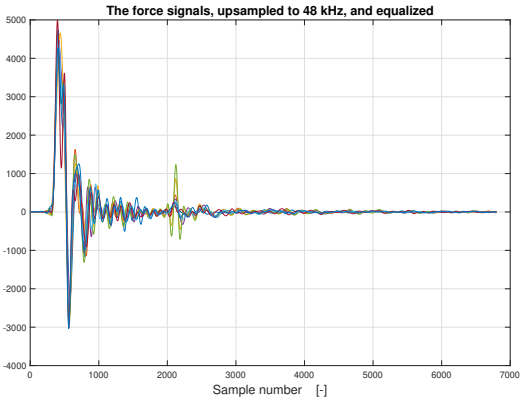

(b) Upsampled and equalized forcesignal

Figure A.7: Upsampling and equallizing forcesignal: Medisin ball

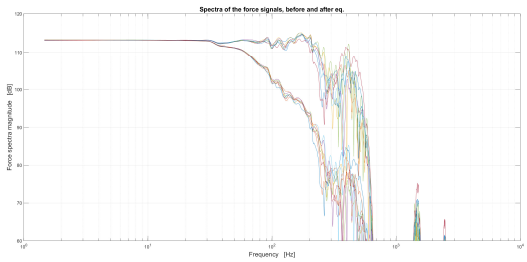

(a) Spectra of force signal upsampled to 48kHz

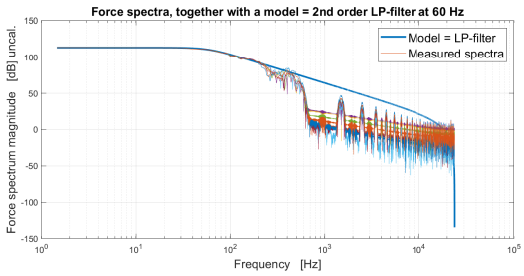

(b) Spectra of model and measured spectra

Figure A.8: Spectra of modeled and measured force signal:Medisin ball

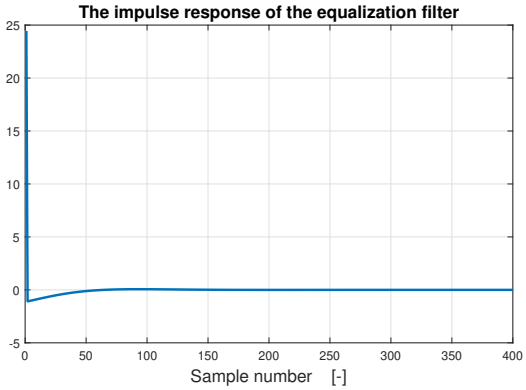

(a) IR of equilization filter

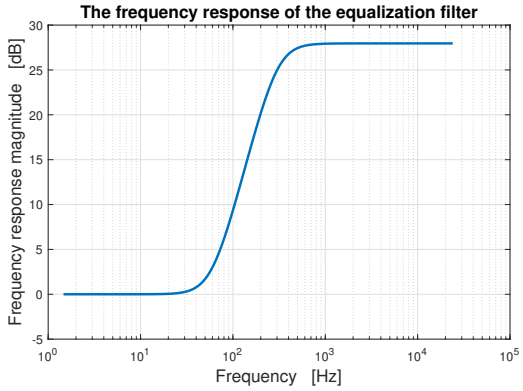

(b) FR of equilization filter

Figure A.9: IR and FR of equilization filter

B Matlab Scripts

B.1 Acceleration signals: Medisin ball

```
%% Program to read and proccess acceleration signals from medisin ball
% Created Feb-May 2021
% Author: shreejay
% shreejayshrestha@gmail.com

%% Stay in the root folder: Medisinball_clean, to run this script
clc
clear variables
%% Part1: Reading wave files with decay signals and loading decaystarttime matrix
tic
source_title = cell(1,4);
source_title{1,1} = ['Medisinball on Main Floor Ch1'];
source_title{1,2} = ['Medisinball on Main Floor Ch2'];
source_title{1,3} = ['Medisinball on Floating Floor Ch1'];
source_title{1,4} = ['Medisinball on Floating Floor Ch2'];

reload = 0;
if reload == 1
    path_audiofiles = 'D:\NTNU\MCT2018_2020\MasterThesis2021\LABMeasurements\
        Clean_measurement_set_for_Analysis\Medisinball_clean\data_acceleration';
    audiofiles = dir(fullfile(path_audiofiles,'*.wav'));
    filenames = natsort({audiofiles.name}');

    % associating the decaysignals of main floor and floating floor
    rawacc_mf = cell(1,6);
    rawacc_ff = cell(1,6);
    for i = 1:numel(filenames)/2
        rawacc_mf{1,i} = audioread(fullfile(path_audiofiles,filenames{i,1}));
        rawacc_ff{1,i} = audioread(fullfile(path_audiofiles,filenames{i+6,1}));
    end

    % Decaystarttime matrix
    struct_decaytimes = load(strcat(path_audiofiles,'\acc_decaystarttimes_mb.mat'));
    decaystarttimes = struct_decaytimes.decaystarttimes_mfff;

    %% Acceleration signals Calibration
    % Main floor
    acc_scaled = cell(1,4);
    calibrationfactor = 10; % ref signal from VOC calibrator = 10mv RMS eqv 10m/s^2
    [acc_scaled{1,1},check_rms_precal_ch1_mf,check_rms_postcal_ch1_mf] =
        calibrate_acceleration(rawacc_mf{1,1},rawacc_mf{1,3},rawacc_mf{1,5},
        calibrationfactor);
    [acc_scaled{1,2},check_rms_precal_ch2_mf,check_rms_postcal_ch2_mf] =
        calibrate_acceleration(rawacc_mf{1,2},rawacc_mf{1,4},rawacc_mf{1,6},
        calibrationfactor);

    % Floating floor
    [acc_scaled{1,3},check_rms_precal_ch1_ff,check_rms_postcal_ch1_ff] =
        calibrate_acceleration(rawacc_ff{1,1},rawacc_ff{1,3},rawacc_ff{1,5},
        calibrationfactor);
    [acc_scaled{1,4},check_rms_precal_ch2_ff,check_rms_postcal_ch2_ff] =
        calibrate_acceleration(rawacc_ff{1,2},rawacc_ff{1,4},rawacc_ff{1,6},
        calibrationfactor);

    %% Calculating decay, delay and aligned signals in time domain
    %Note: The delay time between each signals will allow to identify the early
    %and the most lagging signals which are helpful to align all the signals.
    decay = cell(1,4);
    delay = cell(1,4);
```

```
51      sigalignrefnum = cell(1,2);
52      decay_aligned = cell(1,2);
53
54      fs = 48000;
55      decaylength = 3;
56
57      % Decay Main floor
58  %       function [decay,delay,sigalignrefnum,sig_align_full,sig_align_trim] =
        func_decaydelayalignsig(fs,longsigwithdecays,decaystarttime,decaylen)
59
60      [~,~,~,~,decay{1,1}] = func_decaydelayalignsig(fs,acc_scaled{1,1},
            decaystarttimes{1,1},decaylength);
61      [~,~,~,~,decay{1,2}] = func_decaydelayalignsig(fs,acc_scaled{1,2},
            decaystarttimes{1,1},decaylength);
62
63      % Decay Floating floor
64      decay{1,3} = func_chopdecay(fs,acc_scaled{1,3},decaystarttimes{1,2},decaylength)
            ;
65      decay{1,4} = func_chopdecay(fs,acc_scaled{1,4},decaystarttimes{1,2},decaylength)
            ;
66
67       % check decay
68      indx = 2;
69      ch1_mf = func_plot_allrep_allp(decay{1,indx},source_title{1,indx});
70
71      noiseselecttvec = cell(1,4);
72      noisesamp = cell(1,4);
73
74      % Noise selection Main floor
75      noiseselecttvec{1,1}    =(round(51.5*fs):round(53.5*fs));
76      noisesamp{1,1}          = acc_scaled{1,1}(noiseselecttvec{1,1});
77      noiseselecttvec{1,2}    =(round(51.5*fs):round(53.5*fs));
78      noisesamp{1,2}          = acc_scaled{1,2}(noiseselecttvec{1,2});
79
80      % Noise selection Floating floor
81      noiseselecttvec{1,3}   =(round(53*fs):round(56*fs));
82      noisesamp{1,3}         = acc_scaled{1,3}(noiseselecttvec{1,3});
83      noiseselecttvec{1,4}   =(round(53*fs):round(56*fs));
84      noisesamp{1,4}         = acc_scaled{1,4}(noiseselecttvec{1,4});
85
86      %% Exporting
87  %       save data_acceleration\acc_sig_aligned_mb.mat decay_aligned
88  %       save data_acceleration\chopped_decay_mb.mat decay
89  %       save data_acceleration\acc_noiseselection_mb.mat noisesamp
90  %       save data_acceleration\acc_decaystarttimes_mb.mat decaystarttimes
91  end
92
93  %% Part 2: This part can be run without running Part 1.
94  path_audiofiles = 'D:\NTNU\MCT2018_2020\MasterThesis2021\LABMeasurements\
        Clean_measurement_set_for_Analysis\Medisinball_clean\data_acceleration';
95  % Reset/Load following parameters/matrices
96  fs = 48000;
97  % struct_decay = load(strcat(path_audiofiles,'\chopped_decay_mb_48000Hz.mat'));
98  struct_sigaligned = load(strcat(path_audiofiles,'\acc_sig_aligned_mb.mat'));
99  struct_noise = load(strcat(path_audiofiles,'\acc_noiseselection_mb.mat'));
100
101 %% Assign individual decay signals
102 % acc_sig = struct_decay.decay;
103 acc_sig = struct_sigaligned.decay_aligned;
104 noise_sig = struct_noise.noisesamp;
105
106 %% Filtering wit Lp filter
107 %% Filtering at 200 Hz (previously tried with 100. While no filtering at all,
        signals are very noisy)
108 [Blp,Alp]= butter(4,200/(fs/2));
109 % acc_temp_f = filter(Blp,Alp,acc_temp);
110 acc_filt = cell(1,4);
111 for k = 1:4
112     for i = 1:5
113         for j = 1:10
114             acc_filt{1,k}{i,j}= filter(Blp,Alp,acc_sig{1,k}{i,j});
115         end
116     end
```

```
117 end
118 % % check
119 % % ch1_mf = func_acc_plot_allrep_allp(acc_filt{1,1},source_title{1,1});
120 % % acc_filt_temp = acc_filt{1,1};
121 % % plot(acc_filt_temp{1,1})
122
123 %% Final Cut: cuttiing the acc decay
124 acc_finalcut = cell(1,4);
125 acc_cut_win = cell(1,4);
126 % acc_filt = acc_sig;
127 nwin = 70000;
128 hanwin = hanning(nwin*2);
129 halfhanwin = hanwin(nwin+1:end);
130 figure()
131 plot(halfhanwin)
132
133 %% Filtering at 100 Hz
134 % for k = 1:4
135 %     for i = 1:5
136 %         for j = 1:10
137 %             if k ==1 && i==5
138 %             [npeak,ninit] = findinit(acc_filt{1,k}{i,j}.^2,0.03);
139 %             else
140 %             [npeak,ninit] = findinit(acc_filt{1,k}{i,j}.^2,0.006);
141 %             end
142 %             acc_finalcut{1,k}{i,j}= [0;acc_filt{1,k}{i,j}(ninit:end)];
143 %             acc_cut_win{1,k}{i,j}  = acc_finalcut{1,k}{i,j};
144 %             acc_cut_win{1,k}{i,j}(end-nwin+1:end) = acc_cut_win{1,k}{i,j}(end-nwin
    +1:end).*halfhanwin;
145 %         end
146 %     end
147 % end
148
149 %% use this while filtering at 200 Hz
150
151 for k = 1:4
152     for i = 1:5
153         for j = 1:10
154             if k ==1 && i==5
155             [npeak,ninit] = findinit(acc_filt{1,k}{i,j}.^2,0.03);
156             elseif k==1 && i == 3 && j==4
157             [npeak,ninit] = findinit(acc_filt{1,k}{i,j}.^2,0.008);
158             elseif k==1 && i == 4 && j==5
159             [npeak,ninit] = findinit(acc_filt{1,k}{i,j}.^2,0.008);
160             elseif k==2 && i == 5 && j==10
161             [npeak,ninit] = findinit(acc_filt{1,k}{i,j}.^2,0.008);
162             else
163             [npeak,ninit] = findinit(acc_filt{1,k}{i,j}.^2,0.006);
164             end
165             acc_finalcut{1,k}{i,j}= [0;acc_filt{1,k}{i,j}(ninit:end)];
166             acc_cut_win{1,k}{i,j}  = acc_finalcut{1,k}{i,j};
167             acc_cut_win{1,k}{i,j}(end-nwin+1:end) = acc_cut_win{1,k}{i,j}(end-nwin
                +1:end).*halfhanwin;
168         end
169     end
170 end
171 %% Export acceleration of the floor in time domain
172 acc_floor_mb = acc_cut_win;
173 % save Final_Output_from_allscripts_23_04_2021\medisinball\acc_floor_mb.mat
    acc_floor_mb % cell1 is mf and cel2 is ff.
174 % save Final_Output_from_allscripts_23_04_2021\medisinball\acc_filtered_at_200Hz\
    acc_floor_mb.mat acc_floor_mb % cell1 is mf and cel2 is ff.
175
176 %% checking Final cut
177 checkfinalcut = 0;
178 if checkfinalcut ==1
179     ind =1;
180     p = 4;  % ind1,p3 r4. p4 rep 5, r7 to be excluded. ind2 only p5 r 10
181     for k = 1:10
182         subplot(2,5,k)
183     %     plot(acc_sig{1,ind}{p,k})
184         plot(acc_cut_win{1,ind}{p,k})
185         title (['P\_',int2str(p),'rep\_',int2str(k)])
```

```
186     %       xlim([0 5000])
187     %     ylim([0 0.3])
188     end
189 end
190
191 %% PLOT:
192 plotthissection = 0;
193 if plotthissection ==1
194     %% CHECK  all reps at all points for
195     % function tvec = func_acc_plot_allrep_allp(decaysig,sigtitle)
196     ch1_mf = func_plot_allrep_allp(acc_cut_win{1,1},source_title{1,1});
197     ch2_mf = func_plot_allrep_allp(acc_cut_win{1,2},source_title{1,2});
198     ch1_ff = func_plot_allrep_allp(acc_cut_win{1,3},source_title{1,3});
199     ch2_ff = func_plot_allrep_allp(acc_cut_win{1,4},source_title{1,4});
200
201     %% Check all rep overlappiing at one selected point.
202     % function tvec = func_acc_plot_allrep_onep(decaysig,selectp,sigtitle)
203     p = 1; % select point
204     ch1_mf = func_plot_allrep_onep(acc_filt{1,1},p,source_title{1,1});
205     ch2_mf = func_plot_allrep_onep(acc_filt{1,2},p,source_title{1,2});
206     ch1_ff = func_plot_allrep_onep(acc_filt{1,3},p,source_title{1,3});
207     ch2_ff = func_plot_allrep_onep(acc_filt{1,4},p,source_title{1,4});
208 end
209
210 %% Frequency Domain
211 fs=48000;
212 nfft = cell(1,4);
213 ivf = cell (1,4);
214 fvec = cell (1,4);
215 % decaylength = zeros(5,10,4); % to define nfft
216 %
217 % for i = 1:4
218 %     for j = 1:5
219 %         for k = 1:10
220 %             decaylength(j,k,i)= length(acc_cut_win{1,i}{j,k});
221 %         end
222 %     end
223 % end
224 %
225 % maxdecaylength = max(max(max(decaylength)));
226
227 for i = 1:4
228 %     nfft{1,i} = 2^(nextpow2(maxdecaylength)+2);
229 %     nfft{1,i} = 8388608;% previous nfft of microphone
230     nfft{1,i} = 2097152;% updated nfft of microphone 20.04.2021
231     ivf{1,i} = [1:nfft{1,i}/20];
232     fvec{1,i}= fs/nfft{1,i}*[0:nfft{1,i}/2-1];
233 end
234
235 Fbig_acc = cell(1,4);
236 Fbig_acc{1,1} = func_freqdom(acc_cut_win{1,1},nfft{1,1});
237 Fbig_acc{1,2} = func_freqdom(acc_cut_win{1,2},nfft{1,2});
238 Fbig_acc{1,3} = func_freqdom(acc_cut_win{1,3},nfft{1,3});
239 Fbig_acc{1,4} = func_freqdom(acc_cut_win{1,4},nfft{1,4});
240
241 %% CHECK  all reps at all points
242 % function fvec = func_acc_plotfreq_allrep_allp(decaysig,noiseselection,nfft,
        sigtitle)
243 check_freqplot =0;
244 if check_freqplot ==1
245     fvec_ch1mf = func_plotfreq_allrep_allp(Fbig_acc{1,1},nfft{1,1},source_title
            {1,1});
246     fvec_ch2mf = func_plotfreq_allrep_allp(Fbig_acc{1,2},nfft{1,2},source_title
            {1,2});
247     fvec_ch1ff = func_plotfreq_allrep_allp(Fbig_acc{1,3},nfft{1,3},source_title
            {1,3});
248     fvec_ch2ff = func_plotfreq_allrep_allp(Fbig_acc{1,4},nfft{1,4},source_title
            {1,4});
249
250     %% CHECK  all reps at one selected point
251     p = 1;
252     % function fvec = func_acc_plotfreq_allrep_onep(decaysig,nfft,sigtitle,selectp)
253     fvec_ch1mf = func_plotfreq_allrep_onep(Fbig_acc{1,1},nfft{1,1},source_title
```

```
        {1,1},p);
254     fvec_ch2mf = func_plotfreq_allrep_onep(Fbig_acc{1,2},nfft{1,2},source_title
        {1,2},p);
255     fvec_ch1ff = func_plotfreq_allrep_onep(Fbig_acc{1,3},nfft{1,3},source_title
        {1,3},p);
256     fvec_ch2ff = func_plotfreq_allrep_onep(Fbig_acc{1,4},nfft{1,4},source_title
        {1,4},p);
257 end
258
259 %% Averaging signals
260 Favgcomp = cell(1,4);
261 Favgreal_acc = cell(1,4);
262
263 for i = 1:4
264     for j = 1:5
265         Favgcomp{1,i}= squeeze(Fbig_acc{1,i}(:,:,j));
266         if i==1 && j==4
267            Favgcomp{1,i}(:,7)= [];
268         end
269         Favgreal_acc{1,i}(:,j)=  mean(abs(Favgcomp{1,i}).' ).';
270     end
271 end
272
273 %% Export average acceleration spectrum in frequency domain
274 acc_Spectrum_Avg_mb = Favgreal_acc;
275 % save Final_Output_from_allscripts_23_04_2021\medisinball\acc_filtered_at_200Hz\
    acc_Spectrum_Avg_mb.mat acc_Spectrum_Avg_mb % cell1 is mf and cel2 is ff.
276
277 %% Plotting avg acc with observed and analytical natural freq of the conc floor
278 checkavg =1;
279 if checkavg==1
280 %     plot(Favgreal{1,1}(ivf{1,1},1))
281     % plotavg = 0;
282     % if plotavg ==1
283     f0_analyt = [12.80 29.22 34.79 51.21 56.59 71.43 78.58 87.85 115.22];
284     f0_observed = [29 38 49 56 70 79];
285
286    figure()
287    for i = 1:2
288         subplot (1,2,i)
289         h(1:5) = semilogx(fvec{1,i}(ivf{1,i}),20*log10(Favgreal_acc{1,i}(ivf{1,i},:)
            ));
290         c=6;
291         for k = 1:length(f0_observed)
292             h(c) = xline(f0_observed(k),'-.r');
293             c=c+1;
294         end
295         dd=c+1;
296          for k = 1:length(f0_analyt)
297             h(dd) = xline(f0_analyt(k),'-.b');
298             dd=dd+1;
299          end
300         xlim([20 100])
301         ylim([30 75])
302         xlabel('Frequency(Hz)')
303         grid on
304         title(['Avg of acc spectrum around P1: Mb main floor Ch:',int2str(i),' (
            using LP filter)']);
305    end
306         legend(h([1,2,3,4,5,6,21]),{'P1','P2','P3','P4','P5','f_0 measurement','f_0
            analytical'});
307         legend('boxoff')
308         legend('Location','EastOutside')
309         ylabel('dB re 1m/s^2')
310 end
311
312 %% Finding relation between acce. spektrum amplitude vs different positions
313 figure()
314 semilogx(fvec{1,1}(ivf{1,1}),20*log10(Favgreal_acc{1,1}(ivf{1,1},1)))
315 xlim([20 100])
316 xlabel('Frequency (Hz)')
317 ylabel('dB (re 1m/s^2)')
318 legend('P1','P2','P3','P4','P5');
```

```
319 title('Average of acceleration spectrum CH1 at each excitation Point: Mb main floor'
    );
320
321 %% Finding Peaks, locs in each excitation point within 20-100 Hz
322 pks = cell(2,5);
323 lcs = cell(2,5);
324 Favgrealdb = cell(1,2);
325
326 for k = 1:2
327     for j = 1:5
328         Favgrealdb{1,k}(:,j) = 20*log10(Favgreal_acc{1,k}(:,j));
329     end
330 end
331
332 for k = 1:2
333         for j = 1:5
334             target = 20*log10(Favgreal_acc{1,k}((round(20*nfft{1,1}/fs):round(100*
                    nfft{1,1}/fs)),j));
335              [p,l] = findpeaks(target,'MinPeakDistance',65);
336 %             [p,l] = findpeaks(target,'MinPeakDistance',1000); % old value 65
337             pks{k,j} = p;
338             lcs{k,j}= l;
339             clear p l
340         end
341 end
342
343 seg = cell(1,2);
344 ll = 20;
345 ul = 300;
346 % seg{1,1} = (round(ll*nfft{1,1}/fs):round(ul*nfft{1,1}/fs))';
347 % seg{1,2} = (round(ll*nfft{1,2}/fs):round(ul*nfft{1,2}/fs))';
348
349 seg{1,1} = (round(ll*nfft{1,1}/fs):round(ul*nfft{1,1}/fs))';
350 seg{1,2} = (round(ll*nfft{1,2}/fs):round(ul*nfft{1,2}/fs))';
351 figure()
352 ch = 1; % input 1 for channel 1 and 2 for channel 2
353 for j = 1:5
354     subplot (3,2,j)
355 %     semilogx(fvec{1,ch}(ivf{1,ch}(lim{1,1})),20*log10(Favgreal{1,ch}(ivf{1,ch}(lim
    {1,1}),j)),fvec{1,ch}(ivf{1,ch}(lcs{1,j}+218-1)),pks{1,j},'or')
356     semilogx(fvec{1,ch}(seg{1,ch}),20*log10(Favgreal_acc{1,ch}(seg{1,ch},j)),fvec{1,
            ch}(lcs{ch,j}+(seg{1,ch}(1))-1),pks{ch,j},'or')
357     xlim([20 300])
358     legend('Ch1 mf')
359     title(['Average of acceleration spectrum for excitation Point1\_',int2str(j),'
            Mb main floor Ch:',int2str(ch)])
360     grid on
361 %     pause
362 end
363
364 %% locating pks and lcs
365 lcslength = zeros(2,5);
366 for ch = 1:2
367     for j = 1:5
368         lcslength(ch,j)= length(lcs{ch,j});
369     end
370 end
371
372 maxlcslength = max(max(lcslength));
373 lcs_Hz = cell(2,5);
374 lcs_Hz2 = cell(2,5);
375 lcs_adj = cell(2,5);
376 lcs_Hz_adj_acc = zeros(maxlcslength,5,2);
377 lcs_adj_acc = zeros(maxlcslength,5,2);
378 %
379
380 for ch = 1:2
381     for j = 1:5
382        lcs_Hz{ch,j}= (lcs{ch,j}+(seg{1,ch}(1))-1)*(fs/nfft{1,ch});
383        lcs_Hz2{ch,j} =  lcs_Hz{ch,j};
384        lcs_adj{ch,j} = lcs{ch,j};
385
386        if length(lcs_Hz2{ch,j}) <maxlcslength
```

```
            lcs_Hz2{ch,j}(end+1:maxlcslength)=0;
             lcs_adj{ch,j}(end+1:maxlcslength)=0;
%             lcs_Hz_adj(:,j,ch)=  round(lcs_Hz2{ch,j});
            lcs_Hz_adj_acc(:,j,ch)=  (lcs_Hz2{ch,j});
            lcs_adj_acc(:,j,ch)=  lcs_adj{ch,j};

        elseif length(lcs_Hz2{ch,j})== maxlcslength
%             lcs_Hz_adj(:,j,ch)=  round(lcs_Hz2{ch,j});
            lcs_Hz_adj_acc(:,j,ch)=  (lcs_Hz2{ch,j});
            lcs_adj_acc(:,j,ch)=  lcs_adj{ch,j};
        end
    end
end

%% Export peakindex
acc_Peakindex_Hz_mb = lcs_Hz_adj_acc;
% save Final_Output_from_allscripts_23_04_2021\medisinball\acc_filtered_at_200Hz\
    acc_Peakindex_Hz_mb.mat acc_Peakindex_Hz_mb % cell1 is mf and cel2 is ff.

% this matrix contains the index of peak of avg acc in Hz
%  save data_acceleration\peakindexin_Hz_accavg.mat lcs_Hz_adj_acc; %

%% locating f0 observed
% It is important to obtain amplitude of mic at each point at the same
% natural freqneucy. So define a fixed natural freq. for all points.

f0pk_Hzloc = zeros(5,7,2);
f0pk_indloc = zeros(5,7,2);
f0pk = zeros(5,7,2);
lookupf0 = [29 37 40 49 56 71 79]; % <28-29>,<37-38>,
for j = 1:2
    for c = 1:7
        for r = 1:5
            [row,~] = find(lcs_Hz_adj_acc(:,r,j)>lookupf0(c) & lcs_Hz_adj_acc(:,r,j)
                <lookupf0(c)+1);
%             if  r ==1 && isempty(row)
%                 row = 0;
%             elseif isempty(row)
%                 row = f0pk_Hzloc(r-1,c,j);
%             end
            if  isempty(row)
               [~,closest_index] = min(abs(lcs_Hz_adj_acc(:,r,j)-lookupf0(c)));
               f0pk_Hzloc(r,c,j) = closest_index;
            else
                f0pk_Hzloc(r,c,j) = row;
            end
            f0pk_indloc(r,c,j) = lcs_adj_acc(f0pk_Hzloc(r,c,j),r,j);
%
        end
    end
end

% [~,closest_index] = min(abs(lcs_Hz_adj_acc(:,3,1)-lookupf0(7)));

%% Defining fixed natural frequency
f0fix = zeros(4,7);
for ii = 1:7
    f0fix(2,ii) = median(f0pk_indloc(:,ii,1)); % freq index ch 1
    f0fix(1,ii) = fvec{1,1}(f0fix(2,ii)+(seg{1,1}(1))-1); % freq in Hz ch 1
    f0fix(4,ii) = median(f0pk_indloc(:,ii,2)); % freq index ch 2
    f0fix(3,ii) = fvec{1,1}(f0fix(4,ii)+(seg{1,1}(1))-1); % freq in Hz ch 2
end

%% Export fixed observed natural frequency of the floor
acc_floor_Observed_Resfreq_mb = f0fix;
% save Final_Output_from_allscripts_23_04_2021\medisinball\acc_filtered_at_200Hz\
    acc_floor_Observed_Resfreq_mb.mat acc_floor_Observed_Resfreq_mb % cell1 is mf
    and cel2 is ff.

%% creating matrix with amplitude for fixed f0 at all 5 points
%% This is the latest version for this part.

%% f0fix(4,:) is chosen as the f0 for the floor which is acc from ch 2
```

```
amp_acc_vs_pts = zeros(5,7,2);
for p = 1:5
    for ii = 1:7
        amp_acc_vs_pts(p,ii,1) = Favgrealdb{1,1}((f0fix(4,ii)+(seg{1,1}(1))-1),p);
        amp_acc_vs_pts(p,ii,2) = Favgrealdb{1,2}((f0fix(4,ii)+(seg{1,1}(1))-1),p);

    end
end
%% Export average amplitude at observed resonance frequency
acc_amp_at_Obs_Resfreq_vs_pts_mb = amp_acc_vs_pts ;
% save Final_Output_from_allscripts_23_04_2021\medisinball\acc_filtered_at_200Hz\
    acc_amp_at_Obs_Resfreq_vs_pts_mb.mat acc_amp_at_Obs_Resfreq_vs_pts_mb % cell1 is
     mf and cel2 is ff.
toc
```

B.2 Microphone signals: Medisin ball

```
%% Program to read and process microphone signals for medisin ball
%% This version is revised with reduced nfft size from 8388608 to 2097152
% revesion is also done for mic amplitude vs excitation points.

% Created Feb-May 2021
% Author: shreejay
% shreejayshrestha@gmail.com

clc
clear variables
tic
fs = 48000;
source_title_time = cell(1,2);
source_title_freq = cell(1,2);
source_title_time{1,1} = ['Medisinball on Main Floor'];
source_title_time{1,2} = ['Medisinball on Floating Floor'];
source_title_freq{1,1} = ['Sound pressure spectrum: Medisinball on Main Floor'];
source_title_freq{1,2} = ['Sound pressure spectrum: Medisinball on Floating Floor'];

reload =0 ;
if reload == 1
    path_audiofiles = 'D:\NTNU\MCT2018_2020\MasterThesis2021\LABMeasurements\
        Clean_measurement_set_for_Analysis\Medisinball_clean\data_microphone';
    audiofiles = dir(fullfile(path_audiofiles,'*.wav'));
    filenames = natsort({audiofiles.name}');

    rawmic_mf = cell(1,3);
    rawmic_ff = cell(1,3);
    for ii = 1:numel(filenames)/2
        rawmic_mf{1,ii} = audioread(fullfile(path_audiofiles,filenames{ii,1}));
        rawmic_ff{1,ii} = audioread(fullfile(path_audiofiles,filenames{ii+3,1}));
    end

    %% Decaystarttime matrix
    struct_decaytimes = load(strcat(path_audiofiles,'\mic_decaystarttimes_mb.mat'));
    decaystarttimes = struct_decaytimes.decaystarttimes_mfff;

    %% Microphone Calibration
    [micscaled_mf,xprecal_db_mf,xpostcal_db_mf] = func_miccalibration(rawmic_mf
        {1,1},rawmic_mf{1,2},rawmic_mf{1,3});
    [micscaled_ff,xprecal_db_ff,xpostcal_db_ff] = func_miccalibration(rawmic_ff
        {1,1},rawmic_ff{1,2},rawmic_ff{1,3});

    micscaled = cell(1,2);
    micscaled{1,1} = micscaled_mf;
    micscaled{1,2} = micscaled_ff;

    %% Calculating decay, delay and aligned signals in time domain
    %Note: The delay time between each signals will allow to identify the early
    %and the most lagging signals which are helpful to align all the signals.
    decay = cell(1,2);
    delay = cell(1,2);
    noisesamp = cell(1,2);
```

```
51
52      sigalignrefnum = cell(1,2);
53      decay_aligned = cell(1,2);
54      fs = 48000;
55      decaylength = 7;
56
57      % function [decay,delay,sigalignrefnum,sig_align_full,sig_align_trim] =
            func_decaydelayalignsig(fs,longsigwithdecays,decaystarttime,decaylen)
58      [decay{1,1},delay{1,1},sigalignrefnum{1,1},~,decay_aligned{1,1}] =
            func_decaydelayalignsig(fs,micscaled{1,1},decaystarttimes{1,1},decaylength);
59      [decay{1,2},delay{1,2},sigalignrefnum{1,2},~,decay_aligned{1,2}] =
            func_decaydelayalignsig(fs,micscaled{1,2},decaystarttimes{1,2},decaylength);
60
61      noiseselect_mf =(round(63.03*fs):round(69.65*fs));
62      noisesamp{1,1} = micscaled{1,1}(noiseselect_mf);
63
64      noiseselect_ff =(round((15*60+48)*fs):round((15*60+54)*fs));
65      noisesamp{1,2} = micscaled{1,2}(noiseselect_ff);
66
67      %% Export decay aligned
68      decay_aligned_mb = decay_aligned;
69  %     save Medisinball_clean\data_microphone\decay_aligned_mb.mat decay_aligned_mb
70  end
71
72  load 'D:\NTNU\MCT2018_2020\MasterThesis2021\LABMeasurements\
        Clean_measurement_set_for_Analysis\Medisinball_clean\data_microphone\
        decay_aligned_mb.mat';
73
74  %% Filtering wit Lp filter
75  %% Not Filtering this time
76
77  % [Blp,Alp]= butter(4,100/(fs/2));
78  % mic_filt = cell(1,2);
79  % for k = 1:2
80  %     for ii = 1:5
81  %         for j = 1:10
82  %             mic_filt{1,k}{ii,j}= filter(Blp,Alp,decay_aligned_mb{1,k}{ii,j});
83  %         end
84  %     end
85  % end
86
87  %% Using findit function to cut the signal and windowing to slightly fade the signal
        towards the end
88  mic_finalcut = cell(1,2);
89  mic_cut_win = cell(1,2);
90  nwin = 70000;
91  hanwin = hanning(nwin*2);
92  halfhanwin = hanwin(nwin+1:end);
93  reltrig = 0.001;
94
95  mic_filt = decay_aligned_mb;
96
97  for k = 1:2
98      for ii = 1:5
99          for j = 1:10
100             if k ==2 && ii==5
101                 reltrig = 0.003;
102                 [npeak,ninit] = findinit(mic_filt{1,k}{ii,j}.^2,reltrig);
103             else
104             [npeak,ninit] = findinit(mic_filt{1,k}{ii,j}.^2,reltrig);
105             end
106             mic_finalcut{1,k}{ii,j}= [0;mic_filt{1,k}{ii,j}(ninit:end)];
107             mic_cut_win{1,k}{ii,j}  = mic_finalcut{1,k}{ii,j};
108             mic_cut_win{1,k}{ii,j}(end-nwin+1:end) = mic_cut_win{1,k}{ii,j}(end-nwin
                    +1:end).*halfhanwin;
109         end
110     end
111 end
112
113 soundpressure_mb = mic_cut_win;
114
115 %% Export total sound pressure signals in time domain
116 %  save Final_Output_from_allscripts_23_04_2021\medisinball\signals_not_filtered\
```

```
    soundpressure_mb.mat soundpressure_mb % cell1 is mf and cel2 is ff.

%% Checking
plotthissection = 0;
if plotthissection ==1
    %% CHECK  all reps at all points for
    % function tvec = func_acc_plot_allrep_allp(decaysig,sigtitle)
    mic_mf = func_plot_allrep_allp(mic_cut_win{1,1},source_title_time{1,1});
    mic_ff = func_plot_allrep_allp(mic_cut_win{1,2},source_title_time{1,2});
    %% Check all rep overlappiing at one selected point.
    % function tvec = func_acc_plot_allrep_onep(decaysig,selectp,sigtitle)
    figure()
    p = 5; % select point
%     mic_mf = func_acc_plot_allrep_onep(mic_cut_win{1,1},p,source_title{1,1});
    mic_ff = func_acc_plot_allrep_onep(mic_cut_win{1,2},p,source_title{1,2});
end

%% Frequency Domain
fs=48000;
nfft = cell(1,2);
ivf = cell (1,2);
fvec = cell (1,2);

for ii = 1:2
    maxdecaylength = length(mic_cut_win{1,ii}{1});
%     nfft{1,ii} = 2^(nextpow2(maxdecaylength)+4); % it is slightly more
    nfft{1,ii} = 2^(nextpow2(maxdecaylength)+2);
    ivf{1,ii} = [1:nfft{1,ii}/20];
    fvec{1,ii}= fs/nfft{1,ii}*[0:nfft{1,ii}/2-1];
end

fvec_2097152_nfft_mb = fvec;

%% Exporting frequency vector
% save Final_Output_from_allscripts_23_04_2021\medisinball\fvec_2097152_nfft_mb.mat
    fvec_2097152_nfft_mb % cell1 is mf and cel2 is ff.

Fbig_mic = cell(1,2);
Fbig_mic{1,1} = func_freqdom(mic_cut_win{1,1},nfft{1,1});
Fbig_mic{1,2} = func_freqdom(mic_cut_win{1,2},nfft{1,2});

%% CHECK  all reps at all points
% function fvec = func_acc_plotfreq_allrep_allp(decaysig,noiseselection,nfft,
    sigtitle)
checkplot =0;
if checkplot ==1
    fvec_mf = func_plotfreq_allrep_allp(Fbig_mic{1,1},nfft{1,1},source_title_freq
        {1,1});
    fvec_ff = func_plotfreq_allrep_allp(Fbig_mic{1,2},nfft{1,2},source_title_freq
        {1,2});
 %% CHECK  all reps at one selected point
    p = 1;
    % function fvec = func_acc_plotfreq_allrep_onep(decaysig,nfft,sigtitle,selectp)
    fvec_mf = func_plotfreq_allrep_onep(Fbig_mic{1,1},nfft{1,1},source_title_freq
        {1,1},p);
    fvec_ff = func_plotfreq_allrep_onep(Fbig_mic{1,2},nfft{1,2},source_title_freq
        {1,2},p);
end

%% Averaging signals
Favgcomp = cell(1,2);
Favgreal_mic = cell(1,2);

for ii = 1:2
    for j = 1:5
        Favgcomp{1,ii}= squeeze(Fbig_mic{1,ii}(:,:,j));
        Favgreal_mic{1,ii}(:,j)=  mean(abs(Favgcomp{1,ii}).' ).';
    end
end

SoundPressureAvg_mb = Favgreal_mic;

%% Export average sound pressure spectrum in frequency domain
```

```
%  save Final_Output_from_allscripts_23_04_2021\medisinball\signals_not_filtered\SoundPressureAvg_mb.mat SoundPressureAvg_mb % cell1 is mf and cel2 is ff.

%% Plotting all 5 average in one plot
% fvec = fs/nfft{1,1}*[0:nfft{1,1}/2-1];
% ivf = [1:nfft{1,1}/20];
p0 = 2e-5;
ch = 2;
plotavg = 0;
    figure()
    semilogx(fvec{1,ch}(ivf{1,ch}),20*log10((Favgreal_mic{1,ch}(ivf{1,ch},:))))
%     xlim([20 100])
%     ylim([10 95])

%     xl = xline(55.54,'--r');
%     xl.LabelVerticalAlignment = 'bottom';
%     xl.LabelHorizontalAlignment = 'right';
%     for ii = 1:26
%         xl2 = xline(f0room_theo(ii),'--');
%     end
%     set(xl2,'linewidth',1);
    g = xlabel('Frequency [ Hz ]');
    set(g,'FontSize',14);
    g = ylabel('Amplitude dB [ uncal. ]');
    set(g,'FontSize',14);
    g = legend('P1','P2','P3','P4','P5','Natural freq.floor','Natural freq.room','Location','NorthWest');
    set(g,'FontSize',12);
    legend show
    legend('boxoff')
    legend('Location','SouthOutside','Orientation','Horizontal')
%     title('Sound pressure spectrum for exciat each excitation Point: Mb main floor');
    ax = gca;
    ax.FontSize = 12;
%     g = subtitle();
%     set(g,'FontSize',14);
    grid on
%% Finding peaks and location of the average
pks = cell(1,2);
lcs = cell(1,2);
Favgrealdb = cell(1,2);
for k = 1:2
    for j = 1:5
        Favgrealdb{1,k}(:,j) = 20*log10(Favgreal_mic{1,k}(:,j));
    end
end

for k = 1:2
        for j = 1:5
            target = 20*log10(Favgreal_mic{1,k}((round(20*nfft{1,k}/fs):round(100*nfft{1,k}/fs)),j));
%             [p,l] = findpeaks(target,'MinPeakDistance',70);
%             [p,l] = findpeaks(target,'MinPeakDistance',300); % old value 65
            [p,l] = findpeaks(target,'MinPeakDistance',70); % This works good for nfft = 2097152.00

            pks{k,j} = p;
            lcs{k,j}= l;
            clear p l
        end
end
seg = cell(1,2);
seg{1,1} = (round(20*nfft{1,1}/fs):round(100*nfft{1,1}/fs))';
seg{1,2} = (round(20*nfft{1,2}/fs):round(100*nfft{1,2}/fs))';

figure()
ch = 2; % input 1 for channel 1 and 2 for channel 2
for j = 1:5
    subplot (3,2,j)
%     semilogx(fvec{1,ch}(ivf{1,ch}(lim{1,1})),20*log10(Favgreal{1,ch}(ivf{1,ch}(lim{1,1}),j)),fvec{1,ch}(ivf{1,ch}(lcs{1,j}+218-1)),pks{1,j},'or')
    semilogx(fvec{1,ch}(seg{1,ch}),20*log10(Favgreal_mic{1,ch}(seg{1,ch},j)),fvec{1,
```

```
        ch}(lcs{ch,j}+(seg{1,ch}(1))-1),pks{ch,j},'or')
%     for ii = 1:26
%          xl2 = xline(f0room_theo(ii),'--');
%     end
    xlim([20 100])
    legend('Ch1 mf')
    title(['Average of Measured SPL spectrum for excitation Point1\_',int2str(j),'
        Mb main floor',int2str(ch)])
    grid on
%     pause
end

%% locating pks and lcs
lcslength = zeros(2,5);
for ch = 1:2
    for j = 1:5
        lcslength(ch,j)= length(lcs{ch,j});
    end
end

maxlcslength = max(max(lcslength));
lcs_Hz = cell(2,5);
lcs_Hz2 = cell(2,5);
lcs_adj = cell(2,5);
lcs_Hz_adj_mic = zeros(maxlcslength,5,2);
lcs_adj_mic = zeros(maxlcslength,5,2);
%

for ch = 1:2
    for j = 1:5
       lcs_Hz{ch,j}= (lcs{ch,j}+(seg{1,ch}(1))-1)*(fs/nfft{1,ch});
       lcs_Hz2{ch,j} =  lcs_Hz{ch,j};
       lcs_adj{ch,j} = lcs{ch,j};

       if length(lcs_Hz2{ch,j}) <maxlcslength
            lcs_Hz2{ch,j}(end+1:maxlcslength)=0;
             lcs_adj{ch,j}(end+1:maxlcslength)=0;
%              lcs_Hz_adj(:,j,ch)=  round(lcs_Hz2{ch,j});
            lcs_Hz_adj_mic(:,j,ch)=  (lcs_Hz2{ch,j});
            lcs_adj_mic(:,j,ch)=  lcs_adj{ch,j};

       elseif length(lcs_Hz2{ch,j})== maxlcslength
%              lcs_Hz_adj(:,j,ch)=  round(lcs_Hz2{ch,j});
            lcs_Hz_adj_mic(:,j,ch)=  (lcs_Hz2{ch,j});
            lcs_adj_mic(:,j,ch)=  lcs_adj{ch,j};
       end
    end
end

% maxlcslength = max(max(lcslength));
% lcs_Hz = cell(2,5);
% lcs_Hz2 = cell(2,5);
% lcs_Hz_adj_mic = zeros(maxlcslength,5,2);
% lcs_ajd = cell(1,2);
%
% for ch = 1:2
%     for j = 1:5
%        lcs_ajd {1,ch}(:,j)= lcs_ajd {1,ch}(:,j);
%     end
% end
% save data_microphone\peakindexin_Hz_micavg.mat lcs_Hz_adj_mic

%% locating f0 observed
% It is important to obtain amplitude of mic at each point at the same
% natural freqneucy. So define a fixed natural freq. for all points.

% f0pk_Hzloc = zeros(5,8,2);
% f0pk_indloc = zeros(5,8,2);
% f0pk = zeros(5,8,2);
% lookupf0 = [29 40 51 54 67 71 79 82];
% %  lookupf0 = [29 37 40 49 56 70 79]; % <28-29>,<37-38>, This is for
% %  acceleration
% for j = 1:2
```

```
%     for c = 1:8
%         for r = 1:5
%             [row,~] = find(lcs_Hz_adj_mic(:,r,j)>lookupf0(c) & lcs_Hz_adj_mic(:,r,
    j)<lookupf0(c)+1);
%             if  isempty(row)
%                [~,closest_index] = min(abs(lcs_Hz_adj_mic(:,r,j)-lookupf0(c)));
%                f0pk_Hzloc(r,c,j) = closest_index;
%             else
%                 f0pk_Hzloc(r,c,j) = row;
%             end
%             f0pk_indloc(r,c,j) = lcs_adj_mic(f0pk_Hzloc(r,c,j),r,j);
%         end
%     end
% end

% for j = 1:2
%     for c = 1:8
%         for r = 1:5
%             [row,~] = find(lcs_Hz_adj_mic(:,r,j)>lookupf0(c) & lcs_Hz_adj_mic(:,r,
    j)<lookupf0(c)+1);
%             if isempty(row)
%                 row = f0pk_Hzloc(r-1,c,j);
%             end
%             f0pk_Hzloc(r,c,j) = row;
%             f0pk_indloc(r,c,j) = lcs_adj_mic(f0pk_Hzloc(r,c,j),r,j);
%         end
%     end
% end

%% locating f0 observed
% It is important to obtain amplitude of mic at each point at the same
% natural freqneucy. So define a fixed natural freq. for all points.

f0pk_Hzloc_full = zeros(5,25,2);
f0pk_indloc_full = zeros(5,25,2);
f0pk_full = zeros(5,25,2);
lookupf0_full = resfreqs_analytical(1:25);
% valvec = lookupf0_full ./(fs/nfft{1});
% valvec = zeros(25,1);
% for i = 1:25
%     valvec(i) = find(fvec,lookupf0_full(i));
% end


% lookupf0_full = [29
% 35
% 40
% 46
% 50
% 53
% 58
% 61
% 68
% 70
% 71
% 76
% 79
% 81
% 81
% 86
% 86
% 88
% 88
% 91
% 93
% 94
% 96
% 100
% 100];
%  lookupf0 = [29 37 40 49 56 70 79]; % <28-29>,<37-38>, This is for
%  acceleration
for j = 1:2
    for c = 1:25
```

```
        for r = 1:5
            [row,~] = find(lcs_Hz_adj_mic(:,r,j)>lookupf0_full(c) & lcs_Hz_adj_mic
                (:,r,j)<lookupf0_full(c)+1);
            if  isempty(row)
               [~,closest_index] = min(abs(lcs_Hz_adj_mic(:,r,j)-lookupf0_full(c)));
               f0pk_Hzloc_full(r,c,j) = closest_index;
            else
                f0pk_Hzloc_full(r,c,j) = row;
            end
            f0pk_indloc_full(r,c,j) = lcs_adj_mic(f0pk_Hzloc_full(r,c,j),r,j);
        end
    end
end
%% Defining fixed natural frequency
% f0fix = zeros(2,8);
% for j = 1:2
%     for ii = 1:8
%         f0fix(2,ii) = median(f0pk_indloc_full(:,ii,1));% freq index
%         f0fix(1,ii) = fvec{1,1}(f0fix(2,ii)+(seg{1,1}(1))-1); % freq in Hz.
%     end
% end
%
% room_Observed_Resfreq_mb = f0fix;
%% Defining fixed natural frequeny: full
f0fix_full = zeros(2,25);
for j = 1:2
    for ii = 1:25
        f0fix_full(2,ii) = median(f0pk_indloc_full(:,ii,1));% freq index
        f0fix_full(1,ii) = fvec{1,1}(f0fix_full(2,ii)+(seg{1,1}(1))-1); % freq in Hz
            .
    end
end
resfreq_mb_obs = cell(1,2);
resfreq_mb_obs{1} = unique(f0fix_full(1,:));
resfreq_mb_obs{2} = unique(f0fix_full(2,:));

room_Observed_Resfreq_mb_full = f0fix_full;


%% Export the observed resonance frequency of the sound pressure from the
    measurements
%  save Final_Output_from_allscripts_23_04_2021\medisinball\signals_not_filtered\
    room_Observed_Resfreq_mb.mat room_Observed_Resfreq_mb % cell1 is mf and cel2 is
    ff.

%% Creating matrix with sound pressure amplitude at the observed resonance frequency
     at all 5 excitation points
%% with floor natura freq
load('D:\NTNU\MCT2018_2020\MasterThesis2021\LABMeasurements\
    Clean_measurement_set_for_Analysis\Final_Output_from_allscripts_08_05_2021\acc\
    floor_f0fix_mb.mat')

%% with room natura freq

% amp_mic_vs_pts_f0floor = zeros(5,6);
amp_mic_vs_pts_f0room = zeros(5,8,2);

% for p = 1:5
%     for ii = 1:6
%         amp_mic_vs_pts_f0floor(p,ii) = Favgrealdb{1,1}((floor_f0fix_mb(4,ii)+(seg
    {1,1}(1))-1),p);
%     end
% end
for ch = 1:2
    for p = 1:5
        for ii = 1:8
            amp_mic_vs_pts_f0room(p,ii,ch) = Favgrealdb{1,ch}((f0fix_full(2,ii)+(seg
                {1,ch}(1))-1),p);
        end
    end
end
% for p = 1:5
%     for ii = 1:8
```

```
%          amp_mic_vs_pts(p,ii) = Favgrealdb{1,1}((f0fix(2,ii)+(seg{1,1}(1))-1),p);
%      end
% end

%% Export
%% updated 09-05-2021
% save Final_Output_from_allscripts_23_04_2021\medisinball\signals_not_filtered\
    amp_mic_vs_pts_f0room.mat amp_mic_vs_pts_f0room % cell1 is mf and cel2 is ff.
% save Final_Output_from_allscripts_23_04_2021\medisinball\signals_not_filtered\
    amp_mic_vs_pts_f0floor.mat amp_mic_vs_pts_f0floor % cell1 is mf and cel2 is ff.

toc
```

B.3 Modal sum main

```
%% Program to calculate analytical sound pressure in the receiving room
% while using modal sum theory applying the function modalsum_rigidroom.m
% by Peter Svennson

% Created Feb-May 2021
% Author: shreejay
% shreejayshrestha@gmail.com
clc
clear variables
%% Setting up input values
source = zeros(5,3);
source(1,:)= [2.44 2.94 4.25]; %P1
source(2,:)= [1.92 2.94 4.25]; %P2
source(3,:)= [1.4  2.94 4.25]; %P3
source(4,:)= [1.92 3.56 4.25]; %P4
source(5,:)= [1.4  4.19 4.25]; %P5

receiver = [0.2 0.24 0.25]; % corner mic position
roomsize = [4.88 5.87 4.25];


%% Calculating shortest distance between source and receiver position
base_PR = [3.5 3.2 2.95 2.69 1.88];
height_PR = 4.25 -0.25 ;
short_dist_PR = zeros (1,5);
for i = 1:5
    short_dist_PR(i) = sqrt((base_PR(i))^2 + (height_PR)^2);
end
%%
T60 = [5.2 2.5 1];

safetyfactor = 1.1;
rhoair = 1.2;
cair = 344;
nfft = 2097152;% corresponding to the medisinball microphone nfft
fs = 48000;
fvec= fs/nfft*[0:nfft/2-1];
seg = (round(20*nfft/fs):round(120*nfft/fs))';

freqvec = fvec(seg);

room_analytical_soundpres = cell(3,5); %% cell(a,b) where a1 = T60_5sec, a2= T60_2.5
    sec, a3= T60_1sec andb = excitation points P1:P5
nmodes_modsum = cell(3,5);
room_analytical_resfreq = cell(3,5);
room_analytical_resfreq_sorted = cell(3,5);
modeamp_modsum = cell(3,5);

%% Using the modal sum function from Peter. S.
for t = 1:3
    for ii = 1:5
        [room_analytical_soundpres{t,ii},nmodes_modsum{t,ii},room_analytical_resfreq
            {t,ii},modeamp_modsum{t,ii}] = modalsum_rigidroom(source(ii,:),receiver,
            freqvec,roomsize,T60(t),safetyfactor,rhoair,cair);
        room_analytical_resfreq_sorted{t,ii} = sort(room_analytical_resfreq{t,ii});
        %     pressureadj = pressure;
```

```
    %     pressureadj(isnan(pressureadj)) = 0;
    end
end
 room_analytical_resfreq_cut = room_analytical_resfreq_sorted{1,1}(2:26);

%% Export
% save Final_Output_from_allscripts_23_04_2021\room_modal_analysis_modsum\
    room_analytical_soundpres.mat room_analytical_soundpres;
% save Final_Output_from_allscripts_23_04_2021\room_modal_analysis_modsum\
    nmodes_modsum.mat nmodes_modsum;
% save Final_Output_from_allscripts_23_04_2021\room_modal_analysis_modsum\
    room_analytical_resfreq.mat room_analytical_resfreq;
% save Final_Output_from_allscripts_23_04_2021\room_modal_analysis_modsum\
    room_analytical_resfreq_sorted.mat room_analytical_resfreq_sorted;
% save Final_Output_from_allscripts_23_04_2021\room_modal_analysis_modsum\
    room_analytical_resfreq_cut.mat room_analytical_resfreq_cut;
% save Final_Output_from_allscripts_23_04_2021\room_modal_analysis_modsum\
    modeamp_modsum.mat modeamp_modsum;

%% Check Plots
check = 0;
if check ==1
    prs = 20*log10(abs(room_analytical_soundpres{1,1}));
    figure(2)
    semilogx(fvec(seg),prs);
end

check2 = 0;
if check2 ==1
    RT= 1; % select 1,2 or3
    figure()
    for ii = 1:5
        y1 = 20*log10(abs(room_analytical_soundpres{1,ii}));
        y2 = 20*log10(abs(room_analytical_soundpres{2,ii}));
        y3 = 20*log10(abs(room_analytical_soundpres{3,ii}));
        subplot (3,2,ii)
        semilogx(fvec(seg),y1,fvec(seg),y2,fvec(seg),y3)
        for j = 1:24
            xl2 = xline(resfreqs(j),'--');
        end
        xlim([20 100])
        ylim([0 70])
    %     set(xl2,'linewidth',1)
%         ylabel('dB (arbritrary)')
%         xlabel('Frequency (Hz)')
        g = title(['Sound source @ Point :P',int2str(ii)]);
        set(g,'FontSize',12);
        grid on
        ax = gca;
        ax.FontSize = 12;
    end
  g = legend( 'RT 5sec','RT 2.5sec','RT 1sec','f\_analytical');
% g = legend(h([1,2,3,18]),{'RT 5sec','RT 2.5sec','RT 1sec','f_0 analytical'});
 set(g,'FontSize',12);
legend('boxoff')
legend('Location','SouthOutside')
end

%% Calculating room modes
% [resfreqs,modenumbers] = calcroommodefreqs(roomsize,maxmodenumber,cair);
 maxmodenumber = [30,30,30];
[resfreqs,room_modes_lydrom3] = calcroommodefreqs(roomsize,maxmodenumber,cair);
%% Rough
% Plotting mode amplitude
% figure()
% plot(20*log10(abs(modeamp_modsum{1,5}(1,:))))

%% Converting complex into real dB values
FrealdB = cell(1,3);

for ii = 1:3
    for j = 1:5
        FrealdB{ii}(:,j)=  20*log10(abs(room_analytical_soundpres{ii,j}));
```

```
    end
end

modsum_SP_dB = FrealdB ;
% save Final_Output_from_allscripts_23_04_2021\room_modal_analysis_modsum\
    modsum_SP_dB.mat modsum_SP_dB;


xx1 = 20*log10(abs(room_analytical_soundpres{1,1}(1,:)));
xx11 = 20*log10(abs(room_analytical_soundpres{1,1}));
xx2 = 20*log10(abs(room_analytical_soundpres{1,2}(1,:)));


nfft = 2097152;
fvec = fs/nfft*[0:nfft/2-1];
ivf = find(fvec>= 20 & fvec<=100);
RT = 1;
figure()
    semilogx(fvec(seg),FrealdB{1}(:,3))
    xlim([20 100])
    ylim([10 95])
%% Finding peaks and location
pks = cell(1,3);
lcs = cell(1,3);
for k = 1:3
        for j = 1:5
            target = FrealdB{1,k}(:,j);
            [p,l] = findpeaks(target,'MinPeakDistance',70); % Working good for all
                now
% %              [p,l] = findpeaks(target,'MinPeakDistance',300); % old value 65
%              if k==1
%                  [p,l] = findpeaks(target,'MinPeakDistance',70);
%              else
%                  [p,l] = findpeaks(target,'MinPeakDistance',70);
%              end
            pks{k,j} = p;
            lcs{k,j}= l;
            clear p l
        end
end
figure()
RT = 1;
for j = 1:5
    subplot (3,2,j)
%     semilogx(fvec{1,ch}(ivf{1,ch}(lim{1,1})),20*log10(Favgreal{1,ch}(ivf{1,ch}(lim
    {1,1}),j)),fvec{1,ch}(ivf{1,ch}(lcs{1,j}+218-1)),pks{1,j},'or')
    semilogx(fvec(seg),(FrealdB{RT}(:,j)),fvec(lcs{RT,j}+(seg(1)-1)),pks{RT,j},'or')
%     for ii = 1:26
%          xl2 = xline(f0room_theo(ii),'--');
%     end
    xlim([20 100])
%     legend('Ch1 mf')
    title(['Average of Measured SPL spectrum for excitation Point1\_',int2str(j),'
        Mb main floor',int2str(RT)])
    grid on
%     pause
end
%% locating pks and lcs
lcslength = zeros(3,5);
for ch = 1:3
    for j = 1:5
        lcslength(ch,j)= length(lcs{ch,j});
    end
end

maxlcslength = max(max(lcslength));
lcs_Hz = cell(3,5);
lcs_Hz2 = cell(3,5);
lcs_adj = cell(3,5);
lcs_Hz_adj_mic = zeros(maxlcslength,5,3);
lcs_adj_mic = zeros(maxlcslength,5,3);
%

```

```
for ch = 1:3
    for j = 1:5
        lcs_Hz{ch,j}= (lcs{ch,j}+(seg(1)-1))*(fs/nfft);
        lcs_Hz2{ch,j} =  lcs_Hz{ch,j};
        lcs_adj{ch,j} = lcs{ch,j};

        if length(lcs_Hz2{ch,j}) <maxlcslength
             lcs_Hz2{ch,j}(end+1:maxlcslength)=0;
              lcs_adj{ch,j}(end+1:maxlcslength)=0;
%              lcs_Hz_adj(:,j,ch)=  round(lcs_Hz2{ch,j});
             lcs_Hz_adj_mic(:,j,ch)=  (lcs_Hz2{ch,j});
             lcs_adj_mic(:,j,ch)=  lcs_adj{ch,j};

        elseif length(lcs_Hz2{ch,j})== maxlcslength
%              lcs_Hz_adj(:,j,ch)=  round(lcs_Hz2{ch,j});
             lcs_Hz_adj_mic(:,j,ch)=  (lcs_Hz2{ch,j});
             lcs_adj_mic(:,j,ch)=  lcs_adj{ch,j};
        end
    end
end

%% SPS vs Points
lookup_freq = [29.3;35.2;40.4;49.9;58.6;68.3;76.3;81.2];
ind = zeros(1,8);
for i = 1:8
    ind(i) = find(ceil(resfreqs(1:24))==ceil(lookup_freq(i)));
end

ss = find(ceil(resfreqs(1:24))==ceil(lookup_freq(8)));
indfvec_resfreqs = round(resfreqs(1:24).*(nfft/fs));
SP_modsum_pts = zeros(8,5,3);
for i = 1:3
    for j = 1:5
        for k = 1:8
            SP_modsum_pts(k,j,i) = FrealdB{1,i}(indfvec_resfreqs(ind(k))-seg(1),j);
        end
    end
end

sp_pts_fig = plot_SP_vs_pts_modsum(SP_modsum_pts,lookup_freq);

ll = FrealdB{1,1}(indfvec_resfreqs(1)-seg(1),5);
```

B.4 Equilization filter

```
% analyze_forcesig_PS.m

load forcesigtimedom_mb_48000Hz_mf_ff.mat

nsigs = 12;

%%%%%%%%%%%%%%%%%%%%%%%%%%%%%%%%%%%%%%%%%%%%%%%%%%%%%%%%
% We "clean up" the force signals as we load them:
% There seems to be a tiny little DC offset, which can be observed
% in the first 6700 samples, before the main pulse, so we do this:
% 1. FInd the average signal value in the initial part, and subtract it.
% 2. Remove the 6700 first samples.
% 3. Apply a short half-Hanning window, which means a gentle "fade-in"
%    during the first 150 samples, to avoid clicks at the onset of the
%    signal.


ivinitial = [1:6700];
startwin = hanning(300);
startwin = startwin(1:150);

ivfinal = [1:6800];


for ii = 1:nsigs
```

```
26      oneforcesig = upsampalign{1,1}{ii};
27      oneforcesig = oneforcesig - mean(oneforcesig(ivinitial));
28      oneforcesig = oneforcesig(ivinitial(end)+1:end);
29      oneforcesig(1:length(startwin)) = oneforcesig(1:length(startwin)).*startwin;
30      if ii == 1
31          forcesigs_mf = zeros(length(oneforcesig),nsigs);
32      end
33      forcesigs_mf(:,ii) = oneforcesig;
34  end
35
36  % Plot the loaded, and cleaned, force signals
37
38  figure(1)
39  h = plot(forcesigs_mf);
40  g = xlabel(['Sample number    [-]']);
41  set(g,'FontSize',14);
42  g = title('The force signals, upsampled to 48 kHz');
43  set(g,'FontSize',14);
44  grid
45
46  %%%%%%%%%%%%%%%%%%%%%%%%%%%%%%%%%%%%%%%%%%%%%%%%%%%%
47  % Calculate the spectra and plot together with a simplified model of the
48  % force signal, which is generated with an IIR low-pass filter.
49  % Find the low-frequency amplitude.
50
51  fLPmodel = 60;
52
53  fs = 48000;
54  nfft = 32768;
55  F = fft(forcesigs_mf,nfft);
56  fvec = fs/nfft*[0:nfft/2-1];
57
58  LFamp = mean(mean(abs(F(2:10,:))));
59
60  [Bmodel,Amodel] = butter(2,fLPmodel/(fs/2));
61  irmodel = zeros(nfft/8,1);
62  irmodel(1) = LFamp;
63  irmodel = filter(Bmodel,Amodel,irmodel);
64
65  Fmodel = fft(irmodel,nfft);
66
67  figure(2)
68  h = semilogx(fvec,20*log10(abs(Fmodel(1:nfft/2,:))),fvec,20*log10(abs(F(1:nfft/2,:))
        ));
69  set(h(1),'LineWidth',2)
70  g = xlabel(['Frequency    [Hz]']);
71  set(g,'FontSize',14);
72  g = ylabel(['Force spectrum magnitude    [dB] uncal.']);
73  set(g,'FontSize',14);
74  grid
75  g = title(['Force spectra, together with a model = 2nd order LP-filter at ',num2str(
        fLPmodel),' Hz']);
76  set(g,'FontSize',14);
77  g = legend('Model = LP-filter','Measured spectra');
78  set(g,'FontSize',14);
79
80  %%%%%%%%%%%%%%%%%%%%%%%%%%%%%%%%%%%%%%%%%%%%%%%%%%%%
81  % Construct an equalization filter based on the model.
82  % We add an extra LP filter around 300 Hz since we don't any information
83  % above 300 Hz from the measurements anyway.
84
85  extraLPfrequency = 300;
86
87  [BextraLP,AextraLP] = butter(2,extraLPfrequency/(fs/2));
88
89  % We construct IIR filter coefficients from the inverse of the model,
90  % and the extra LP filter.
91  Beqtot = conv(BextraLP,Amodel);
92  Aeqtot = conv(AextraLP,Bmodel/Bmodel(1));
93
94  % Now we construct an FIR filter from the IIR filter coefficients.
95  % We arbitrarily give it a long length to begin with (nfft/4), and then cut
96  % it to a length where the FIR filter amplitude has died out to very low
```

```
% values, and that seems to happen within 400 samples.

irEQ = zeros(nfft/4,1);
irEQ(1) = 1;
irEQ = filter(Beqtot,Aeqtot,irEQ);
irEQ = irEQ(1:400);

% We enforce the equalization filter to have the response 0 dB for very low
% frequencies

irEQ = irEQ/sum(irEQ);

% Plot the impulse response of the equalization filter

figure(3)
h = plot([irEQ]);
set(h(1),'LineWidth',2)
g = xlabel(['Sample number    [-]']);
set(g,'FontSize',14);
g = title('The impulse response of the equalization filter');
set(g,'FontSize',14);
grid

% Plot the frequency response of the equalization filter

FEQ = fft(irEQ,nfft);
figure(4)
h = semilogx(fvec,20*log10(abs(FEQ(1:nfft/2,:))));
set(h(1),'LineWidth',2)
grid
g = xlabel(['Frequency   [Hz]']);
set(g,'FontSize',14);
g = ylabel(['Frequency response magnitude   [dB]']);
set(g,'FontSize',14);
g = title('The frequency response of the equalization filter');
set(g,'FontSize',14);

%%%%%%%%%%%%%%%%%%%%%%%%%%%%%%%%%%%%%%%%%%%%%%%%%%%%%%%%%%%%%%%%%%%%%%%%%%%
% Now we filter the force signals with the equalization filter, and we
% cut away the end of the equalized force signals since there is some click
% generated by the ending of the measured force signals.

for ii = 1:nsigs
    oneEQsignal = contwo(forcesigs_mf(:,ii),irEQ);
    oneEQsignal = oneEQsignal(ivfinal);
   if ii == 1
       forceEQ = zeros(length(oneEQsignal),nsigs);
   end
   forceEQ(:,ii) = oneEQsignal;
end

% Also convert them to spectra

FforceEQ = fft(forceEQ,nfft);

% Plot the time signals

figure(5)
h = plot(forceEQ);
g = xlabel(['Sample number    [-]']);
set(g,'FontSize',14);
g = title('The force signals, upsampled to 48 kHz, and equalized');
set(g,'FontSize',14);
grid

figure(6)
h = semilogx(fvec,20*log10(abs(FforceEQ(1:nfft/2,:))),...
    fvec,20*log10(abs(F(1:nfft/2,:))));
grid
g = xlabel(['Frequency   [Hz]']);
set(g,'FontSize',14);
g = ylabel(['Force spectra magnitude   [dB]']);
set(g,'FontSize',14);
```

```
g = title('Spectra of the force signals, before and after eq.');
set(g,'FontSize',14);

maxlevel = 20*log10(LFamp);
maxplotlevel = ceil(maxlevel/10)*10;
ylim([maxplotlevel-60 maxplotlevel])
```

B.5 Auralization main

```
%% Program to create and analyze auralization
% Created Feb-May 2021
% Author: shreejay
% shreejayshrestha@gmail.com
%%
clc
clear variables
%Load force signals
load('D:\NTNU\MCT2018_2020\MasterThesis2021\LABMeasurements\
    Clean_measurement_set_for_Analysis\Clean_Output_Good_For_Analysis\
    data_auralization\force_aur.mat')
%Load soundpressure signals
load('D:\NTNU\MCT2018_2020\MasterThesis2021\LABMeasurements\
    Clean_measurement_set_for_Analysis\Clean_Output_Good_For_Analysis\
    data_auralization\sp_aur.mat')
%Load impulse response EQulization filter
load('D:\NTNU\MCT2018_2020\MasterThesis2021\LABMeasurements\
    Clean_measurement_set_for_Analysis\Clean_Output_Good_For_Analysis\
    data_auralization\irEQ.mat')

%% Calculate impulse response of the coupled system
irsys = contwo(irEQ,sp_aur{1}{1,1});

%% selecting force and sound pressure signals
% From footstep_with_shoes, neglect : P1 rep 2, P3-Rep 2,5 and 6
% From footstep_without_shoes, neglect : P2 rep 3
% Reason for neglecting them: They were excluded in the main correcpoiding
% analysis scripts. mic_footstep_without_shoes_nofilt.m and
% mic_footstep_withshoes_nofilt.m
%% For simplicity select Rep # 7 for all signals.
% use the following function to generate auralization in time and freq.
% domain.
% function [p_aur,F_orig,F_aur,F_aur_shift,ecf] = auralise_calc_empfact_v2(irsys,
    forcesig,soundpressure,refp)
% refp = select reference repetition # for estimating the
% auralization.

repnum = 2;
[p_aur,p_aur_concat,F_orig,F_aur,F_aur_shift,ecf] = auralise_calc_empfact_v3(irsys,
    force_aur,sp_aur,repnum);

%% Play auralized sounds
fs = 48000;
% sound(p_aur_concat{1,3},fs);

%% Plot Auralization Spectrum vs original sound pressure spectrum
% function fvec = plot_aura_sps(F_orig,F_aur_shift,refsource); % refsource = [1,2,3]
fig = plot_aura_sps(F_orig,F_aur_shift,1,repnum); % refsource = [1,2,3]

%% Perform Octaveband analysis: using octavebandanalysis.m function from PS.
fs = 48000;
nfft = 2^19;
iv = 1:nfft/2;
fvec= fs/nfft*(0:nfft/2-1);
F_aur_3oct = cell(3,5);
F_orig_3oct = cell(3,5);
fvecout_orig = cell(3,5);
fvecout_shift = cell(3,5);
for i = 1:3
    for j = 1:5
        [F_orig_3oct{i,j},fvecout_orig{i,j}] = octavebandanalysis(fvec,abs(F_orig{i,
            j}(iv)).^2,3,20,500);
```

```
        [F_aur_3oct{i,j},fvecout_shift{i,j}] = octavebandanalysis(fvec,abs(
            F_aur_shift{i,j}(iv)).^2,3,20,500);
    end
end

figure()
plot(fvecout_orig{1},10*log10([F_aur_3oct{1} F_aur_3oct{2} F_aur_3oct{3}]))
% plot(fvecout{1},20*log10([F_aur_spec{1} F_aur_spec{2} F_aur_spec{3}])./p0)
legend('Medisin ball','Footstep with shoes','Footstep without shoes')
xlim([20 200])
xticks([20  25  32  40  50  63  79  100 126 159 200])
xticklabels({'20', '25.1', '31.6', '39.8', '50.1', '63.1', '79.4', '100','125.9','
    158.5','199.5'})
grid on
g = xlabel('Frequency [ Hz ]');
set(g,'FontSize',16)
g = ylabel('Amplitude dB [ re uncal. ]');
set(g,'FontSize',16)
g = title('Auralized Sound Pressure in 1/3rd Octave Band');
set(g,'FontSize',16)
ax = gca;
ax.FontSize = 12;
%5 plot option 2
%% PLOT Uncalibrated auralised Vs original sps
linS = {'-','--','-','--','-','--'};
markS = {'d','*','o','s','x','p'};
col = [{'b'},{'g'},{'m'}];
legentry = [{'Medisin ball original'},{'Medisin ball auralised'},{'Footstep with
    shoes original'},{'Footstep with shoes auralised'},{'Footstep without shoes
    original'},{'Footstep without shoes auralised'}];
ep = 4;
figure()
hold on
for c = 1:3
    plot(fvecout_orig{1},8*log10(F_orig_3oct{c,ep}),'-','Marker',markS{c},'
        MarkerSize',7,'LineWidth',1,'Color',col{c})
    plot(fvecout_orig{1},8*log10(F_aur_3oct{c,ep}),'--','Marker',markS{c},'
        MarkerSize',7,'LineWidth',1,'Color',col{c})

end
grid on
ax = gca;
ax.FontSize = 12;
legend([legentry])
g = xlabel('Frequency [ Hz ]');
set(g,'FontSize',16)
g = ylabel('Amplitude dB [ uncal. ]');
set(g,'FontSize',16)
g = title('Auralized vs original Sound Pressure in 1/3rd Octave Band');
set(g,'FontSize',16)
ylim ([30 90])
xlim([20 200])
xticks([20.0  25.1  31.6  39.8  50.1  63.1  79.4  100.0 125.9 158.5 199.5])
xticklabels({'20', '25', '32', '40', '50', '63', '79', '100','126','159','200'})
yticks ([30 32  34  36  38  40  42  44  46  48  50  52  54  56  58  60  62  64  66
    68  70  72  74  76  78  80  82  84  86  88  90])
yticklabels({'30', '', '', '', '', '40', '', '','','','50', '', '', '','','60', '',
    '', '','','70', '', '', '','','80', '', '', '','','90'})

%% PLOT Calibrated auralised Vs original sps
p0 = 2e5;
linS = {'-','--','-','--','-','--'};
markS = {'d','*','o','s','x','p'};
col = [{'b'},{'g'},{'m'}];
legentry = [{'Medisin ball orig'},{'Medisin ball aur'},{'Footstep with shoes orig'
    },{'Footstep with shoes aur'},{'Footstep without shoes orig'},{'Footstep without
     shoes aur'}];
ep = 1;
figure()
hold on
for c = 1:3
    plot(fvecout_orig{1},10*log10(F_orig_3oct{c,ep}./p0),'-','Marker',markS{c},'
        MarkerSize',7,'LineWidth',1,'Color',col{c})
```

```
    plot(fvecout_orig{1},10*log10(F_aur_3oct{c,ep}./p0),'--','Marker',markS{c},'
        MarkerSize',7,'LineWidth',1,'Color',col{c})

end
grid on
legend([legentry])
g = xlabel('Frequency [ Hz ]');
set(g,'FontSize',14)
g = ylabel('Amplitude dB [ 20 \mu pa. ]');
set(g,'FontSize',14)
g = title('Auralized vs original Sound Pressure in 1/3rd Octave Band');
set(g,'FontSize',16)
xlim([20 200])
xticks([20.0  25.1  31.6  39.8  50.1  63.1  79.4  100.0 125.9 158.5 199.5])
xticklabels({'20', '25.1', '31.6', '39.8', '50.1', '63.1', '79.4', '100','125.9','
    158.5','199.5'})
%


F_aur_3oct{2} F_aur_3oct{3}]))
% plot(fvecout{1},20*log10([F_aur_spec{1} F_aur_spec{2} F_aur_spec{3}])./p0)
legend('Medisin ball','Footstep with shoes','Footstep without shoes')
xlim([20 200])
xticks([20.0  25.1  31.6  39.8  50.1  63.1  79.4  100.0 125.9 158.5 199.5])
xticklabels({'20', '25.1', '31.6', '39.8', '50.1', '63.1', '79.4', '100','125.9','
    158.5','199.5'})
grid on
g = xlabel('Frequency [ Hz ]');
set(g,'FontSize',14)
g = ylabel('Amplitude dB [ uncal. ]');
set(g,'FontSize',14)
g = title('Auralized Sound Pressure in 1/3rd Octave Band');
set(g,'FontSize',16)
```

B.6 Impulse Response main

```

%% Program to read Impulse Response

% Created: 20.03.2021
% updated: 11.04.2021

% Author: shreejay
% shreejayshrestha@gmail.com
%%
tic
clc
clear variables

% path_txtfiles = 'D:\NTNU\MCT2018_2020\MasterThesis2021\LABMeasurements\
    Clean_measurement_set_for_Analysis\ImpulseResponse';
path_txtfiles = 'D:\NTNU\MCT2018_2020\MasterThesis2021\LABMeasurements\
    Clean_measurement_set_for_Analysis\Medisinball_clean\data_ir';
txtfiles = dir(fullfile(path_txtfiles,'*.etx'));
filenames = natsort({txtfiles.name}');
fs = 48000;
Mic_index   = cell(1,numel(filenames));

%% Checking IR signals
reload = 1;
if reload == 1
    impres = cell(1,length(filenames));
    for i = 1:length(filenames)
        fid = fopen(fullfile(path_txtfiles,filenames{i,1}));
        TxtScan = textscan(fid,'%f%f','HeaderLines',22); % skipping first 21 lines
        impres{1,i} = TxtScan{2}; %retreiving force signal data from column 2
        fclose(fid);
        Mic_index{1,i} = extractBefore(filenames{i,1},'.');
    end
end
```

```
33
34 plotir = 0;
35 if plotir ==1
36     tvec = cell(1,length(filenames));
37     for i = 1:length(impres)
38         tvec{1,i} = (0:length(impres{1,i})-1)*1/fs;
39     %      subplot (6,2,i)
40         plot(tvec{1,i},impres{1,i});
41         xlabel('time (s)')
42         ylabel('Amplitude');
43         title(['Impulse Response: Mic @ P\_',int2str(i)]);
44     %      xlim([-0.25 5])
45         ylim ([-0.2 0.2])
46         pause
47     end
48 end
49
50 % plot([impres{1,1},impres{1,2}]) % P1_2 looks good
51 % legend ('P1\_1','P1\_2')
52
53 % plot([impres{1,3},impres{1,4}]) % P2_2 looks good
54 % legend ('P2\_1','P2\_2')% P2_2 looks good
55
56 % plot([impres{1,5},impres{1,6}]) % P3_2 looks good
57 % legend ('P3\_1','P3\_2')% P2_2 looks good
58
59 % plot([impres{1,7},impres{1,8},impres{1,9}]) % P4_1 looks good
60 % legend ('P4\_1','P4\_2','P4\_3')% P2_2 looks good
61
62 % plot([impres{1,10},impres{1,11},impres{1,12}]) % P5_1 looks good
63 % legend ('P5\_1','P5\_2','P5\_3')% P2_2 looks good
64
65 %% Selecting one good signal for each point and saving the matrix for further
       processing
66 impres_good = cell(1,5);
67 impres_good{1,1}= impres{1,2};
68 impres_good{1,2}= impres{1,4};
69 impres_good{1,3}= impres{1,6};
70 impres_good{1,4}= impres{1,7};
71 impres_good{1,5}= impres{1,10};
72 % save data_ir\impulseresponse.mat impres_good
73
74 %% re-check selected impulse response
75 checkir =0;
76 if checkir ==1
77     figure()
78     tvec = cell(1,length(filenames));
79     for i = 1:length(impres_good)
80         tvec{1,i} = (0:length(impres_good{1,i})-1)*1/fs;
81          subplot (3,2,i)
82         plot(tvec{1,i},impres_good{1,i});
83         xlabel('time (s)')
84         ylabel('Amplitude');
85         title(['Impulse Response: Mic @ P\_',int2str(i)]);
86     %      xlim([-0.25 5])
87         %ylim ([-0.2 0.2])
88     %      pause
89     end
90 end
91
92 % semilogy(abs(impres_good{1,1}));
93
94 %% Frequency Domain
95 plotirspect = 0;
96 L = cell(1,5);
97 Fimpres = cell(1,5);
98 Frealir = cell(1,1);
99 for k = 1:5
100     ires = impres_good{1,k}(1:3e5);
101     noise = impres_good{1,k}(1e6:1.5e6);
102 %      nfft = 2^nextpow2(length(ires));
103 %      nfft = 8388608; % nfft of microphone signals
104      nfft = 2097152; % nfft of microphone and acc signals readjusted
```

```
105
106     fs = 48000;
107     fvec = fs/nfft*([0:nfft/2-1]);
108     figure(1)
109     Fimpres{1,k} = fft(ires,nfft);
110     Frealir{1,1}(:,k) = abs(Fimpres{1,k}(1:nfft/2));
111     L{1,k} = 20*log10(abs(Fimpres{1,k}(1:nfft/2)));
112     Fn = fft(noise,nfft);
113     Ln = 20*log10(abs(Fn(1:nfft/2)));
114     if plotirspect ==1
115         subplot(3,2,k)
116         semilogx(fvec,L{1,k},fvec,Ln);
117         grid on
118         xlim([20 200])
119         title(['Impulse Response of the room on mainfloor at P:',int2str(k)])
120     end
121 end
122 legend ('signal','noise','Location','EastOutside')
123 % save data_ir\Frealir.mat Frealir
124
125 pks = cell(1,5);
126 lcs = cell(1,5);
127 seg = (round(20*nfft/fs):round(120*nfft/fs))';
128
129 for j = 1:5
130     [p,l] = findpeaks(L{1,j}(seg),'MinPeakDistance',75);
131     pks{1,j} = p;
132     lcs{1,j}= l;
133     clear p l
134 end
135 pkslcs = 1;
136 if pkslcs ==1
137 figure()
138     for j = 1:5
139         subplot (3,2,j)
140     %     semilogx(fvec{1,ch}(ivf{1,ch}(lim{1,1})),20*log10(Favgreal{1,ch}(ivf{1,ch
        }(lim{1,1}),j)),fvec{1,ch}(ivf{1,ch}(lcs{1,j}+218-1)),pks{1,j},'or')
141         semilogx(fvec(seg),L{1,j}(seg),fvec(lcs{1,j}+seg(1)-1),pks{1,j},'or')
142     %     for k = 1:length(f0_observed)
143     %         xline(f0_observed(k),'-.o');
144     %     end
145     %     semilogx(fvec(seg),L{1,j}(seg),fvec(lcs{1,j}),pks{1,j},'or')
146         xlim([20 100])
147     %     legend('Ch1 mf')
148         title(['Resonance Frequency of the room for excitation Point1\_',int2str(j)
            ])
149         grid on
150     %     pause
151     end
152 end
153 roomsize = [4.88 5.87 4.25];
154 maxmodenumber = [10,10,10];
155 cair = 344;
156 [f0room_theo,f0room_modenumbers] = calcroommodefreqs(roomsize,maxmodenumber,cair);
157 % save data_ir\f0room_theo.mat f0room_theo
158 % save data_ir\f0room_modenumbers.mat f0room_modenumbers
159
160 lcslength = zeros(1,5);
161     for j = 1:5
162         lcslength(1,j)= length(lcs{1,j});
163     end
164
165 maxlcslength = max(max(lcslength));
166 lcs_Hz = cell(1,5);
167 lcs_Hz2 = cell(1,5);
168 lcs_adj = cell(1,5);
169 lcs_Hz_adj_ir = zeros(maxlcslength,5);
170 lcs_adj_ir = zeros(maxlcslength,5);
171
172     for j = 1:5
173        lcs_Hz{1,j}= (lcs{1,j}+seg(1)-1)*(fs/nfft);
174        lcs_Hz2{1,j} =  lcs_Hz{1,j};
175        lcs_adj {1,j}= (lcs{1,j}+seg(1)-1);
```

```
176
177         if length(lcs_Hz2{1,j}) <maxlcslength
178              lcs_Hz2{1,j}(end+1:maxlcslength)=0;
179              lcs_adj{1,j}(end+1:maxlcslength)=0;
180              lcs_Hz_adj_ir(:,j)= (lcs_Hz2{1,j});
181              lcs_adj_ir(:,j)= (lcs_adj{1,j});
182
183         elseif length(lcs_Hz2{1,j})== maxlcslength
184              lcs_Hz_adj_ir(:,j)= (lcs_Hz2{1,j});
185              lcs_adj_ir(:,j)= (lcs_adj{1,j});
186
187         end
188     end
189
190
191 sorted_lcs_Hz_adj_ir = sort(lcs_Hz_adj_ir);
192 lcs_Hz_adj_ir_floor = floor(lcs_Hz_adj_ir );
193
194 freq_order = zeros(100,5);
195
196 for i = 1:43
197     for j = 1:5
198          val = floor(lcs_Hz_adj_ir(i,j));
199          if val == 0
200              val = 1;
201          end
202          freq_order(val,j) = lcs_Hz_adj_ir(i,j);
203 %          min_val = floor(min(lcs_Hz_adj_ir(i,:)));
204 %          if floor(lcs_Hz_adj_ir(i,j)) == min_val
205 %              freq_order(min_val,j) = lcs_Hz_adj_ir(i,j);
206 %          else
207 %              diff = floor(lcs_Hz_adj_ir(i,j)) - min_val;
208 %              freq_order(i+diff,j) = lcs_Hz_adj_ir(i,j);
209 %          end
210     end
211 end
212 freq_order_median3 = zeros(length(freq_order),1);
213 for i = 1:length(freq_order)
214     freq_order_median3(i) = median(freq_order(i,:));
215     if freq_order_median3(i)==0
216          freq_order_median3(i) = max(freq_order(i,:));
217     end
218 end
219
220 freq_order_median = nonzeros(freq_order_median3);
221 freq_order_median_orig = freq_order_median;
222 freq_order_median(1:8) = [];
223 freq_order_median(49:end) = [];
224 freq_order_median(2:4) = [];
225 freq_order_median(3:4) = [];
226 freq_order_median(4:6) = [];
227 freq_order_median(5:6) = [];
228 freq_order_median(6:8) = [];
229 freq_order_median(7) = [];
230 freq_order_median(8) = [];
231 freq_order_median(8) = [];
232 freq_order_median(9:10) = [];
233 freq_order_median(12:13) = [];
234 freq_order_median(13) = [];
235 freq_order_median(16:17) = [];
236 freq_order_median(22) = [];
237 freq_order_median(23) = [];
238
239 freq_order_median(11) = [];
240 freq_order_median(15) = [];
241
242 room_measured_Resfreq_from_ir_updated = freq_order_median;
243 % save Final_Output_from_allscripts_23_04_2021\room_impulse_response\
      room_measured_Resfreq_from_ir_updated.mat room_measured_Resfreq_from_ir_updated
244
245 % toc
```